Title

Polar bear (Ursus maritimus) behavior and energetics: New metrics for examining the physiological impact of a changing Arctic environment

Author

Pagano, Anthony Michael

Publication Date

2018

UNIVERSITY OF CALIFORNIA
SANTA CRUZ

POLAR BEAR (*URSUS MARITIMUS*) BEHAVIOR AND ENERGETICS: NEW METRICS FOR EXAMINING THE PHYSIOLOGICAL IMPACT OF A CHANGING ARCTIC ENVIRONMENT

A dissertation submitted in partial
satisfaction of the requirements for the
degree of

DOCTOR OF PHILOSOPHY

in

ECOLOGY AND EVOLUTIONARY
BIOLOGY

By

Anthony Michael Pagano

June 2018

The Dissertation of Anthony M. Pagano
is approved:

Professor Terrie M. Williams, Chair

Professor Daniel P. Costa

Elizabeth Peacock, Ph.D.

Karyn D. Rode, Ph.D.

Tyrus Miller
Vice Provost and Dean of Graduate Studies

TABLE OF CONTENTS

List of Tables vii

List of Figures ix

Abstract xvi

Acknowledgements xviii

Introduction 1

Dissertation outline 4

1 Using tri-axial accelerometers to identify wild polar bear behaviors 7

Abstract 7

Introduction 8

Methods 11

Accelerometer recordings on captive bears 11

Accelerometer recordings on free-ranging polar bears 12

Behaviors 13

Modeling 13

Analyses 15

Results 17

Behaviors on the sea ice 18

Behaviors on land 20

Sampling frequency 21
Discussion 22
Habitat effects 23
Use of captive animals and surrogate species 24
Accelerometer attachment 25
Video calibration 26
Conclusions 27
Tables 29
Figures 37

2 Energetic costs of locomotion in bears: Is plantigrade locomotion energetically economical? 44

Abstract 44
Introduction 45
Materials and methods 48
Experimental design 48
Animals 49
Metabolic measurements 50
Gait kinematics 51
Overall dynamic body acceleration 51
Body composition 52
Preferred locomotor speeds 53
Analyses 54
Results 55

Metabolic rates 55
Gait kinematics 57
Overall dynamic body acceleration 57
Body composition 58
Preferred locomotor speeds 58
Discussion 58
Tables 65
Figures 66

3 Energetic costs of aquatic locomotion in a subadult polar bear 74

Abstract 74
Introduction 74
Materials and methods 76
Results 78
Discussion 79
Figures 83

4 High-energy, high-fat lifestyle challenges an Arctic apex predator, the polar bear 86

Abstract 86
Introduction 86
Materials and methods 88
Study design 88
Captures 89

Doubly-labeled water 89
Urea/creatinine ratios 92
Video collars and archival loggers.. 92
Analyses 94
Resting metabolic rates.. 95
Results and Discussion 97
Tables.. 105
Figures 107

5 Estimating the energy expenditure of free-ranging mammals using tri-axial accelerometers: A validation with doubly-labeled water 115

Abstract... 115
Introduction... 116
Methods 120
Analyses 124
Results... 124
Discussion... 125
Tables.. 131
Figures 133

Synthesis 136

Bibliography 139

LIST OF TABLES

Table 1.1 Polar bears and grizzly bears wearing collars with tri-axial accelerometers that were video recorded (captive bears) or that wore video-equipped collars (wild bears) **29**

Table 1.2 Video recording schedules used by GPS-equipped video camera collars deployed on polar bears on the sea ice of the southern Beaufort Sea and on land on Akimiski Island, Nunavut **29**

Table 1.3 Parameters extracted from tri-axial accelerometer and conductivity data and used in random forest models to predict wild polar bear behaviors. Respective acceleration measures from the surge (X), heave (Y), sway (Z), and magnitude (Q) axes **30**

Table 1.4 Number of 2 s long behaviors used in random forest training datasets for predicting behaviors of wild polar bears. Ice bears: polar bears on the sea ice of the southern Beaufort Sea. Land bears: polar bears on Akimiski Island, Nunavut **31**

Table 1.5 Performance of a random forest model testing the effect of sampling distributions on the predictive ability of accelerometer data in discriminating the behaviors of bears on the sea ice as verified by video data. MCC: Matthews' correlation coefficient **32**

Table 1.6 Performance of a random forest model using accelerometer data from polar bears on the sea ice to predict behaviors from bears on the sea ice as verified by video data. MCC: Matthews' correlation coefficient **33**

Table 1.7 Performance of a random forest model using accelerometer data from captive polar bears to predict behaviors from bears on the sea ice as verified by video data. MCC: Matthews' correlation coefficient **33**

Table 1.8 Cross-validation comparing predicted behaviors (rows) from accelerometer analyses of polar bears on the sea ice to actual behaviors (columns) confirmed by video recordings. Correct classifications are denoted in bold. See Table 1.6 for performance statistics in predicting behaviors **34**

Table 1.9 Performance of a random forest model using accelerometer data from captive grizzly bears to predict behaviors from bears on the sea ice as verified by video data **34**

Table 1.10 Mean (standard deviation) static acceleration (*g*) in the surge (X), heave (Y), and sway (Z) directions, and overall dynamic acceleration (ODBA (*g*)) derived from accelerometers deployed on 3 captive polar bears, 2 captive grizzly bears, 5 polar bears on the sea ice, and 2 polar bears on land **35**

Table 1.11 Performance of a random forest model using accelerometer data from polar bears on land to predict behaviors from bears on land as verified by video data **36**

Table 2.1 Summary of animals used in this study **65**

Table 4.1 Video recording schedules. GPS-equipped video camera collars deployed on female polar bears on the spring sea ice of the Beaufort Sea **105**

Table 4.2 Polar bear field metabolic rates (FMRs) and changes in body mass, body composition, and blood biochemistry **106**

Table 5.1 Polar bear age, duration studied, mean body mass, field metabolic rates (FMRs) derived from doubly-labeled water (DLW), FMRs derived from accelerometer-based relationships (ACC), and mean measures of overall dynamic body acceleration (ODBA) **131**

Table 5.2 Model comparisons of mean movement rate (Rate), mean body mass (Mass), daily energy expenditure estimates derived from tri-axial accelerometer data (AccelerometerEnergy), mean overall dynamic body acceleration (ODBA), and mean activity rate (Activity) to explain the daily energy expenditure of free-ranging female polar bears based on measurements from DLW. Results are presented for all models with AIC_c weight > 0 ..... **132**

LIST OF FIGURES

Figure 1.1 Orientation of an archival logger containing a tri-axial accelerometer attached to a collar for use on polar and grizzly bears **37**

Figure 1.2 Ability (*F-measure*) of the random forest model to predict 10 behaviors of polar bears on the sea ice from 3 different training datasets of accelerometer data. Ice bears: polar bears on the sea ice of the southern Beaufort Sea... **38**

Figure 1.3 Variable importance plot from the random forest model of accelerometer data from polar bears on the sea ice. The importance plot provides a relative ranking of parameters in which higher values indicate parameters that contributed more toward classification accuracy. Mean decrease in accuracy is normalized by dividing by the standard errors of the parameters (i.e., *z*-score). See Table 1.3 for description of parameters.. **39**

Figure 1.4 Accelerometer signatures of static acceleration in the surge (X), heave (Y), and sway (Z) directions and overall dynamic acceleration (ODBA) while walking, swimming, standing, and eating a seal from an adult female polar bear on the sea ice of the southern Beaufort Sea............... **40**

Figure 1.5 Accelerometer signatures of static acceleration in the surge (X), heave (Y), and sway (Z) directions and overall dynamic acceleration (ODBA) while walking from a captive adult female polar bear (left) compared to a captive adult female grizzly bear (right)... **41**

Figure 1.6 Ability (*F-measure*) of a random forest model to predict behaviors of polar bears on land from 4 different training datasets. Ice bears: polar bears on the sea ice of the southern Beaufort Sea. Land bears: polar bears on Akimiski Island, Nunavut.. **42**

Figure 1.7 Ability (*F-measure*) of a random forest model to predict behaviors of polar bears on the sea ice using 3 different accelerometer sampling frequencies.. **43**

Figure 2.1 Relationship between oxygen consumption, gait kinematics, and locomotor speed in polar bears and grizzly bears. **A.** Least-squares regression (solid line) of mass-specific oxygen consumption in relation to locomotor speed for polar bears and grizzly bears on a treadmill. Points represent individual steady-state measurements for polar bears (yellow circles, present study; orange circles, (Hurst et al. 1982*a*); dark-orange circles, (Øritsland et al. 1976); orange-red circles, (Watts et al. 1991)) and grizzly bears (black circles) (see text for regression statistics). **B.** Least-squares regression (solid line) between stride frequency and speed in polar bears (yellow circles) and grizzly bears (black circles) (see text for regression statistics). **C.** Least-squares regression (solid line) between stride length and speed in polar bears (yellow circles) and grizzly bears (black circles)... **66**

Figure 2.2 Relationship between oxygen consumption and locomotor speed for bears moving on a treadmill and locomotor speeds of wild polar bears while walking and running on the sea ice. **A.** Mass-specific oxygen consumption in relation to locomotor speed. Points represent individual steady-state measurements for polar bears (orange circles, (Hurst et al. 1982*a*); yellow circles, (Hurst et al. 1982*b*); dark-orange circles, (Øritsland et al. 1976); orange-red circles, (Watts et al. 1991)). The solid line is the least-squares regression from polar bears and grizzly bears at < 5.4 km h^{-1} (Figure 2.1A) and the dotted line is the least-squares regression from polar bears at ≥ 5.4 km h^{-1} (see text for regression statistics). The dashed line is the predicted relationship derived from other terrestrial carnivores (Taylor et al. 1982). **B.** Frequency distribution of walking and running speeds over 10 minute intervals from 6 female polar bears on the sea ice of the Beaufort Sea in April 2015 and 2016 ($n = 533$) **67**

Figure 2.3 Net minimum cost of transport (COT_{MIN}) in digitigrade carnivores and plantigrade mammals. Digitigrade carnivores: canids (grey squares, (Taylor et al. 1982, Bryce and Williams 2017)) and felids (green triangles, (Taylor et al. 1982, Williams et al. 2014)). Plantigrade mammals: primates (blue diamonds, (Taylor et al. 1982, Cunningham et al. 2010)) and ursids (yellow circles, present study). The solid line is the predicted relationship for COT_{MIN} of quadrupedal mammals (Taylor et al. 1982)... **68**

Figure 2.4 Mass-specific total cost of transport (COT_{TOT}) in relation to locomotor speed in polar bears and grizzly bears. Polar bears and grizzly bears while walking at < 1.5 m s^{-1} (grey circles) and polar bears at ≥ 1.5 m s^{-1} (yellow circles). The equation describing the second-order polynomial relationship between COT_{TOT} and walking speed at < 1.5 m s^{-1} is $COT_{TOT} = 0.40\times speed^2 - 0.96\times speed + 0.80$, ($r^2 = 0.83$). The equation describing the second-order polynomial relationship between COT_{TOT} and speed at ≥ 1.5 m s^{-1} is $COT_{TOT} = 0.44 \times speed^2 - 1.64 \times speed + 1.78$, ($r^2 = 0.22$)..... **69**

Figure 2.5 Plantigrade walking gait of the grizzly bear and polar bear. **A.** Single walking stride of an adult female grizzly bear moving on a treadmill at 2.8 km h^{-1} over 1.75 seconds. **B.** Single walking stride of an adult female polar bear moving on a treadmill at 2 km h^{-1} over 2 seconds................. **70**

Figure 2.6 Relationship between oxygen consumption and dynamic body acceleration (dba) in polar bears and grizzly bears. Least-squares regression of mass-specific oxygen consumption and mean absolute dba in the surge (X; **A.**), heave (Y; **B.**), and sway (Z; **C.**) dimension from 2 adult female polar bears (yellow circles, solid line) and 3 adult female grizzly bears (black circles, dashed line) resting and walking on a treadmill. Points are mean steady-state measurements........................... **71**

Figure 2.7 Relationship between oxygen consumption and overall dynamic body acceleration (ODBA) in polar bears and grizzly bears. **A.** Least-squares regression of mass-specific oxygen consumption and mean ODBA from 2 adult female polar bears (Polar Bears 1-2 (yellow and orange circles, respectively)) resting and walking on a treadmill. Points are mean (± SE) steady-state measurements (see text for regression statistics). **B.** Least-squares regression of mass-specific oxygen consumption and mean ODBA from 3 adult female grizzly bears (Grizzly Bears 3-5 (red, blue, and black circles, respectively)) resting and walking on a treadmill. Points are mean (± SE) steady-state measurements (see text for regression statistics) **72**

Figure 2.8 Body composition of 7 grizzly bears based on deuterium oxide injection. Percent total body fat and total body water (median, 1st and 3rd quartiles, maximum, and minimum) **73**

Figure 3.1 Resting and swimming behaviors of a subadult polar bear. **A.** Subadult female polar bear resting in the water in the metabolic chamber while bracing itself against the walls at the water surface; **B.** subadult female polar bear resting in the water in the metabolic chamber while standing on its hindlegs; and **C.** subadult female polar bear swimming against a current in the flume.. **83**

Figure 3.2 Swimming pattern of a subadult polar bear. The first image shows the left forelimb at the beginning of the power phase of the stroke cycle. In the recovery phase (fourth and fifth images), the limb is brought close to the body and moved forward to return to the power phase (last image) **84**

Figure 3.3 Mean stroke costs in a polar bear, semi-aquatic, and marine mammals. Polar bear (green triangle). Semi-aquatic mammals (yellow circles): muskrats (*Ondatra zibethicus*) (Fish 1982, 1984), mink (Williams 1983), ferrets (Fish and Baudinette 2008), platypus (*Ornithorhynchus anatinus*) (Fish et al. 1997), Australian water rats (Fish and Baudinette 1999), sea otters (*Enhydra lutris*) surface swimming and submerged swimming (Williams 1989), and elite front-crawl swimming in humans (Morris et al. 2017). Marine mammals (orange squares): bottlenose dolphins (*Tursiops truncatus*) (Williams et al. 2017), harbor porpoises (*Phocoena phocoena*) (Williams et al. 2017), beluga whales (*Delphinapterus leucas*) (Williams et al. .2017), and killer whales (*Orcinus orca*) (Williams et al. 2017). The solid line is the least squares linear regression for marine mammals (Williams et al. 2017) **85**

Figure 4.1 Field movements and accelerometer signatures of polar bears in April 2014 to 2016. **A.** Capture and recapture locations and GPS movement paths of nine female polar bears dosed with DLW and equipped with GPS-equipped video camera collars and archival loggers with tri-axial accelerometers and conductivity sensors. Gray area denotes land; white area shows sea ice cover. (Inset) Orientation of the accelerometer while attached to the video collar. **B.** Accelerometer signatures of static acceleration in the surge (x), heave (y), and sway (z) directions and overall dynamic body acceleration (ODBA) while walking, swimming, and standing. Images show the corresponding behaviors derived from the animal-borne video camera.. **107**

Figure 4.2 Relationship between body mass and RMR in polar bears and other ursids. RMR of an adult female polar bear (orange triangle, this study), compared with mean RMRs of subadult polar bears (orange circle), hibernating adult female polar bears (orange square), hibernating adult male grizzly bears (blue square), black bears (black circle), hibernating black bears (black square), adult and subadult panda bears (green circle), and female sloth bears (purple circle). Sources are available in the methods. The dashed line is the allometric regression for RMR in vertebrate-eating carnivores (McNab 1988). The solid line is the allometric regression for RMR in eutherian mammals (Kleiber 1975).

(Inset) The adult female bear resting in the metabolic chamber from the present study **108**

Figure 4.3 FMR and overall FMR in relation to body mass, movement, and activity rate of polar bears. **A.** Mean daily FMRs of female polar bears on the sea ice in relation to body mass. The allometric regression (solid line) is compared with predicted daily FMRs for marine and terrestrial mammalian carnivores (upper dashed line) (Nagy et al. 1999), and predicted daily RMRs (lower dotted line) (Kleiber 1975). **B.** Least squares regression (solid line) of mean daily mass-specific FMR in comparison with mean movement rate. **C.** Least squares regression (solid line) of mean daily mass- specific FMR in comparison with mean activity rate derived from video collars. **D.** Least squares regression (solid line) of overall mass-specific FMR in comparison with total distance moved over 8 to 11 days. Regression statistics are provided in the main text. Each point represents a single value for one bear in A. to D......................... **109**

Figure 4.4 Feeding demands, changes in body mass, and foraging success of polar bears. **A.** Number of ringed seals required for a female polar bear to meet its energy demands over 10 to 12 days on the spring sea ice based on the greatest energy expenditure, mean (±SE) energy expenditure, and lowest energy expenditure. **B.** Changes in body mass, lean body mass, and fat mass of female polar bears on the sea ice over 8 to 11 days. Measures of changes in lean body mass and fat mass were only available for bears five to nine. Bar heights represent data for individual bears. **C.** Image of a polar bear eating a recently killed ringed seal. **D.** Prey type consumed by female polar bears. Bar heights represent data for individual bears..... **110**

Figure 4.5 Polar bear movement, foraging, and activity. **A.** Movements of bear #3 over 9 days. **B.** Movements of bear #8 over 8 days. Figures show locations where bears were captured (green squares), recaptured (white squares), resting (red circles), walking (blue circles), exhibiting mixed behaviors (black circles), kill sites of seals (yellow asterisk), kills sites of seal pups (white crosses), or scavenging sites of seal carcasses (green pluses). **C.** Mean (± SE) activity using accelerometer data from 6 female polar bears over 8 – 11 days. **D.** Mean (± SE) daytime activity using video collar data from 9 female polar bears over 5 – 10 days............. **111**

Figure 4.6 Polar bear diel differences in activity. Proportion of the day active (median, 1st and 3rd quartiles, maximum, and minimum) based on accelerometer data from 7 female polar bears on the spring sea ice of the southern Beaufort Sea over 8 – 13 days. Day was from sunrise to sunset and night was from sunset to sunrise **112**

Figure 4.7 Changes in polar bear activity post-capture. Proportion of the time active (median, 1st and 3rd quartiles, maximum, and minimum) since capture based on accelerometer data from 6 female polar bears on the spring sea ice of the Beaufort Sea **113**

Figure 4.8 Polar bear movement, activity, and foraging locations. **A.** Movements of bear #7 over 11 days. **B.** Movements of bear #5 over 9 days. **C.** Movements of bear #6 over 10 days. **D.** Movements of bear #9 over 9 days. Figures show locations where bears were captured (green squares), recaptured (white squares), resting (red circles), walking (blue circles), exhibiting mixed behaviors (black circles), kill sites of seals (yellow asterisk), kill sites of seal pups (white crosses), scavenging sites of seal carcasses (green pluses), or scavenging sites of whale carcasses (yellow pluses) **114**

Figure 5.1 Least-squares regression of mass-specific oxygen consumption and mean overall dynamic body acceleration (ODBA) from 2 adult female polar bears resting and walking on a treadmill and 3 adult female polar bears resting on exhibit. Regression statistics are provided in the main text. **133**

Figure 5.2 Mass-specific energy expenditure in relation to accelerometer-derived estimates, overall dynamic body acceleration (ODBA), movement, and body mass of polar bears. **A.** Least squares regression (solid line) of mean daily mass-specific energy expenditure of female polar bears on the sea ice measured by DLW in comparison to mean daily mass-specific energy expenditure of the same individuals from accelerometer-derived relationships (Acc). **B.** Least squares regression (solid line) of mean daily mass-specific energy expenditure of female polar bears on the sea ice measured by DLW in comparison to mean ODBA. **C.** Least squares regression (solid line) of mean daily mass-specific energy expenditure of female polar bears on the sea ice measured by DLW in comparison to mean movement rate. **D.** Least squares regression (solid line) of mean daily mass-specific energy expenditure of female polar bears on the sea ice measured by DLW in comparison to mean body mass. Regression statistics are provided in the main text. Each point represents a single value for one bear **134**

Figure 5.3 Conceptual chart showing the energetic pathways that account for an animal's overall metabolizable energy. The DLW method measures potential changes in energy expenditure across all of these pathways. Conversely, the accelerometer method only accounts for potential changes in energy expenditure that result from changes in activity..... **135**

ABSTRACT

Polar bear (*Ursus maritimus*) behavior and energetics:
New metrics for examining the physiological impact of a changing Arctic environment

by

Anthony Michael Pagano

Recent declines in Arctic sea ice have been linked to reductions in body condition, survival, and population size of polar bears (*Ursus maritimus*) in some regions of the Arctic. Reduced foraging opportunity is hypothesized as the primary mechanism of sea-ice linked declines, but increased energy expenditure, as a result of changing sea ice composition and extent may be an additional underlying mechanistic factor. Field metabolic rates of polar bears have been previously unknown and limited information has existed on foraging or other behaviors in polar bears while on the sea ice. Such data are increasingly needed to better understand polar bear habitat use and improve projections of the effects of climate change on global polar bear populations. The primary objectives of this work were to: 1) develop metrics to remotely quantify wild polar bear foraging rates and behaviors; 2) measure the energetic costs of resting, walking, and swimming in captive polar bears, to better estimate the energy demands of free-ranging polar bears; 3) measure the field metabolic rates, behaviors, and foraging rates of free-ranging polar bears on the spring sea ice; and 4) evaluate the ability of tri-axial accelerometers to measure the energy expenditure of free-ranging polar bears. In this dissertation, I develop methods using tri-axial accelerometers to remotely discriminate the behaviors (Chapter 1) and index the energy expenditure (Chapter 5) of free-ranging polar bears. I further find that polar bears have energetic costs of walking that are commensurate with other quadrupedal mammals (Chapter 2), but appear to have high energetic costs of swimming similar to other semi-aquatic mammals (Chapter 3). Additionally, similar to other large carnivores, polar bears have high resting metabolic rates and high field metabolic rates (Chapter 4). Of nine polar bears monitored on the spring sea ice of the Beaufort Sea, five of these bears had energy deficits as a result of their high energy demands and low foraging success (Chapter 4). These findings highlight the physiological constraints of these large apex carnivores and reinforce their reliance on energy-dense pagophilic seal prey. Furthermore, these findings elucidate the implications of increases in the frequency of spring fasting on polar bear body composition. Given their large body size and hypercarnivory, polar bears appear to be poorly suited to cope with rapid environmental change. The metrics developed in this dissertation provide a framework to monitor polar bear behaviors and energy expenditure to aid conservation and management of the species.

ACKNOWLEDGEMENTS

This dissertation[1] would not have been possible without the contributions and support provided by a remarkable number of people. My graduate advisor Dr. Terrie Williams challenged me to think broadly and creatively about my research and expanded my expectations on the feasibility and value of ecophysiology research. I'm thankful for the numerous trips Terrie and I made together to captive facilities doing Science! Terrie's passion and enthusiasm for wildlife and research are infectious and inspiring. Terrie sets a high bar both as a scientist and conservationist and I'm eternally grateful to have had her as a mentor.

Drs. George Durner and Steve Amstrup gave me the opportunity to work with the US Geological Survey (USGS) Polar Bear Research Program despite my having virtually no background with mammals, let alone a large carnivore. Dr. Lily Peacock generously supported my ambition to get a PhD degree and helped me conceive this project. This project would not have been possible without her support and confidence in me. Dr. Todd Atwood willingly took on this responsibility when he

---

[1] The text of this dissertation includes a reprint of the following previously published material: Pagano, A.M., K.D. Rode, A. Cutting, M.A. Owen, S. Jensen, J.V. Ware, C.T. Robbins, G.M. Durner, T.C. Atwood, M.E. Obbard, K.R. Middel, G.W. Thiemann, and T.M. Williams. 2017. Using tri-axial accelerometers to identify wild polar bear behaviors. Endangered Species Research 32:19-33. Pagano, A.M., A.M. Carnahan, C.T. Robbins, M.A. Owen, T. Batson, N. Wagner, A. Cutting, N. Nicassio-Hiskey, A. Hash, and T.M. Williams. 2018. Energetic costs of locomotion in bears: Is plantigrade locomotion energetically economical? Journal of Experimental Biology 221: doi:10.1242/jeb.175372. Pagano, A.M., G.M.Durner, K.D. Rode, T.C. Atwood, S.N. Atkinson, E. Peacock, D.P. Costa, M.A. Owen, and T.M. Williams. 2018. High-energy, high-fat lifestyle challenges an Arctic apex predator, the polar bear. Science 359:568-572.

became project leader. I am grateful to both Todd and George for their constant support and patience throughout this project. Karen Oakley also played a vital role in helping this project become a reality. Dr. Karyn Rode helped me establish dialogues with captive facilities and provided valuable feedback and support throughout the project. Kristin Simac has tirelessly put up with my endless questions and requests from my first days when my job was cleaning polar bear skulls to now. Rose Cunningham provided help managing and storing terabytes worth of data.

I've been honored to have Drs. Terrie Williams, Dan Costa, Lily Peacock, and Karyn Rode serve as my PhD committee. Each was instrumental to the success of this dissertation. Dan Costa provided valuable insight on the use of doubly-labeled water on large mammals that facilitated this research. My lab mates, Dr. Caleb Bryce, Jason John, Dr. Jen Maresh, Dr. Nicole Thometz, Dr. Robin Dunkin, Dr. Shawn Noren, and Jessie Kendall-Bar were huge resources in commiserating, talking science, and surviving life as a graduate student. I was fortunate to share an office with Caleb and Jason who were immensely supportive and shared countless hours discussing accelerometers and animal physiology among other things. Yiwei Wang and Jen Maresh provided help in learning to code accelerometer data in R and Igor Pro. Beau Richter and Traci Kendall provided considerable help with grants, permitting, and logistics. Courtney Amundson and Dan Rizzolo have been great friends and were immensely helpful in the development of this project.

Field work occurred under grueling and inhospitable conditions and I am grateful to Drs. Stephen Atkinson and Maria Spriggs for training me to catheterize bears in the field and dose them with doubly-labeled water. This project wouldn't have been nearly as successful without their help. Mehdi Bakhtiari (Exeye) custom designed the video camera collars that were used in the field. Mehdi and I shared countless harrowing phone conversations, but his ingenuity allowed me to observe the behaviors of these animals in a remote and inhospitable environment. Helicopter Pilot Frank Ross (Soloy Helicopters) managed to keep us "out of a body bag". His skill as a pilot allowed us to focus on the research and enabled all of the field data that was collected in the Beaufort Sea for this study. The data collected from polar bears on land in Chapter 1 was made possible by Martyn Obbard, Kevin Middel, and Greg Thiemann.

Shannon Jensen (Alaska Zoo), Amy Cutting (Oregon Zoo), and Megan Owen (San Diego Zoo) were vital to the captive polar bear data that were collected for this study. In particular, Amy Cutting and Megan Owen made tremendous leaps of faith in order to support this study. Prior to this project, the thought of training a polar bear to voluntarily wear a collar seemed laughable and the thought of building a metabolic treadmill and swim flume that keepers could voluntarily train bears to walk-on and swim-in was a pipe dream. Amid all their other duties and responsibilities they devoted countless hours in making those ideas a reality. Their tireless dedication to wildlife conservation is inspiring. Thanks to Lydia Neill (Oregon Zoo) for her efforts in helping construct the first ever polar bear swim flume! Thanks as well to engineer Ryan Milkowski (KPFF Consulting Engineers) for providing pro bono engineering help in constructing the swim flume. Amy Hash, Nicole Nicassio, Sara Morgan, Jenny DeGroot, and Rob Draughon (Oregon Zoo) and Tammy Batson, Nate Wagner, Pete O'Neill, Becky Wolf, Susan Purtell, Matt Price, Nicki Boyd, Chad Summers, Sam Marino, Julie Anderson, and Rod Owlett (San Diego Zoo) did a remarkable job training polar bears to voluntarily wear a collar, rest and walk on a treadmill, and swim in a flume. Their ingenuity, patience, and dedication are remarkable examples of the commitment of zoo staff to animal conservation. I am extremely grateful for their tireless and unfailing effort.

Dr. Charlie Robbins (Washington State University) was vital to the metabolic treadmill study. Despite numerous challenges prior to installing the treadmill in their facility, Charlie, Brandon Evans Hutzenbiler, and Tony Carnahan were able to train 7 grizzly bears to voluntarily rest and walk on the treadmill in 2 months. I am fortunate to have worked with Charlie and inspired by his commitment to bear research. Thanks to Jasmine Ware in helping to collect the data from 2 grizzly bears at Washington State University and a polar bear at the Alaska Zoo that was used in Chapter 1.

Most importantly, I am indebted to the bears that participated in this study both in the wild and in captivity. My hope is that this research will serve to benefit the long-term persistence of these species. Captive polar bears: Tasul and Nora (Oregon Zoo), Tatqiq (San Diego Zoo), and Ahpun (Alaska Zoo) and captive grizzly bears: John, Frank, Luna, Peeka, Kio, Dodge, Zuri, Oakley, and Cooke (Washington State University) were all tremendous ambassadors for their species. It was a privilege to work with, observe, and collect data from these incredible animals.

Lastly, I need to thank my family for all their support. Amazingly my parents have never questioned my desire to study wildlife, even when it involved hanging out of a helicopter in -20 degree temperatures to dart a large apex carnivore on the Arctic sea ice with the nearest rescue support hundreds of miles away. My wife, Kelly, endured life with an overworked graduate student who disappeared for weeks at a time to collect bear data, including having to leave for the field 3 days after the birth of our daughter. Over the course of this dissertation, we had a long distance relationship, lived together, began raising a child, and got married. I'm thankful for her love and fortunate to have her in my life. My daughter, Scarlett, has given my life new meaning and reframed what's important in it. She amazes me on a daily basis. I hope she will have as many opportunities to pursue her passions and dreams as I've had.

This research was funded by the US Geological Survey's Changing Arctic Ecosystems Initiative. Additional funding was provided by Polar Bears International, the North Pacific Research Board, Washington State University, San Diego Zoo Global, Oregon Zoo, Oregon Zoo Foundation, Alaska Zoo, SeaWorld and Busch Gardens Conservation Fund, Point Defiance Zoo & Aquarium Dr. Holly Reed Conservation Fund, World Wildlife Fund, University of California, Santa Cruz, and the International Association for Bear Research and Management. Special thanks to Krista Wright and Geoff York (Polar Bears International) and Julia Bevins and Frederick Dean (International Association for Bear Research and Management) for their continuous support of this project from its infancy. Research on land in Chapter

1 was additionally funded by the Ontario Ministry of Natural Resources and Forestry, Natural Sciences and Engineering Research Council of Canada, Helen McCrea Peacock Foundation, and the Born Free Foundation. Research at Washington State University in Chapter 2 was additionally funded by the Interagency Grizzly Bear Committee, fRI Research, the Raili Korkka Brown Bear Endowment, the Bear Research and Conservation Endowment, and the Nutritional Ecology Endowment. The analyses in this dissertation used resources of the Core Science Analytics and Synthesis Applied Research Computing program at the US Geological Survey.

The research conducted in this dissertation was approved by the Animal Care and Use Committees of the University of California, Santa Cruz, the US Geological Survey, Alaska Science Center, San Diego Zoo Global, Oregon Zoo, Alaska Zoo, and Washington State University (Protocols 04780 and 04952). Polar bear research was further authorized under US Fish and Wildlife Service Marine Mammal Permits MA77245B and MA690038. Research on land in Chapter 1 was further approved by the Animal Care and Use Committees of the Ontario Ministry of Natural Resources and Forestry and York University and authorized under Nunavut Wildlife Research Permit WL 2015-073.

INTRODUCTION

Animal movement, behaviors, and physiological responses to their environment are intrinsic to their ecology (Brown et al. 2004). Although measures of abundance, survival, body condition, and other metrics can indicate trends within a population, they are often inadequate in identifying the underlying biological mechanisms driving such trends (Wikelski and Cooke 2006, Cooke 2008, Cooke et al. 2014). Quantitative measures of animal behavior and energy expenditure can help identify the physiological mechanisms driving population dynamics making such measures important in guiding species management and conservation decisions (Sutherland 1998, Wikelski and Cooke 2006, Cooke 2008, Cooke et al. 2014). Direct observations can provide a method to document animal behaviors and foraging success that can be linked with environmental conditions. Yet, many species are cryptic, occur in remote locations, or occur in inhospitable environments making direct observation difficult, if not impossible. Recent technological advances have enabled new methods for examining animal behavior, spatial ecology, and energy expenditure, which can be linked to environmental conditions (Ropert-Coudert and Wilson 2005, Moll et al. 2007, Cooke 2008, Wilson et al. 2008, Costa et al. 2010, Williams et al. 2014, Wilmers et al. 2015), but these technologies often require species-specific calibrations (Halsey et al. 2009*b*).

Polar bears (*Ursus maritimus*) are an apex predator of the Arctic. The majority of the circumpolar distribution of polar bears remains on the sea ice throughout the year. On the sea ice, they exhibit vast home ranges and movement patterns (Ferguson et al. 1999) under extreme weather conditions, which makes them difficult, if not impossible, to directly observe for extended durations. Polar bear populations in some regions were in severe decline in the 1960s primarily due to sport hunting and research was initiated to monitor polar bear populations to aid conservation and management of the species (Scott et al. 1959, Harrington 1965, Kolenosky and Standfield 1966, Larsen 1968, Lønø 1970). As a consequence, polar bears in some areas of the Arctic have been extensively studied via mark-recapture and radio-telemetry research (Jonkel 1967, Lentfer 1968, Larsen 1971, Rode et al. 2014*a*, Lunn et al. 2016), which circumvents the challenges involved in directly observing these animals for prolonged durations. Nevertheless, such research relies on a basic understanding of polar bear behavior, physiology, and habitat use. Insight into polar bear behavior and foraging success on the sea ice has primarily been based on observational work led by Ian Stirling in Lancaster Sound (Stirling 1974, Stirling and Latour 1978, Stirling et al. 2016) and local traditional knowledge from Arctic indigenous peoples (e.g., Nelson 1966, Kalxdorff 1997, Voorhees et al. 2014, Laforest et al. 2018). Yet, much remains unknown about polar bear behavior on the sea ice, particularly how polar bear behavior may vary in response to sea ice conditions and whether such variation might have important implications for their energy demands. Such information has added importance given ongoing declines in Arctic sea ice and consequent effects on polar bear abundance, survival, and body condition, in some areas (Stirling et al. 1999, Regehr et al. 2007, 2010, Rode et al.

2010, 2012, Bromaghin et al. 2015, Obbard et al. 2016, 2018) and forecasted declines in global polar bear populations (Amstrup et al. 2008, Atwood et al. 2016*a*, Regehr et al. 2016).

Polar bears are the largest walking carnivore and their large body mass inherently necessitates a large overall energy demand (Schmidt-Nielsen 1984). To meet this demand, they preferentially feed on the blubber of marine mammal prey (Stirling and McEwan 1975), primarily ringed (*Phoca hispida*) and bearded seals (*Erignathus barbatus*) (Stirling and Archibald 1977). In particular, polar bears exhibit extreme hyperphagia in the spring and summer as a result of feeding on recently weaned and naïve seal pups (Stirling et al. 1977, 1999, Stirling and Øritsland 1995) and feeding on adult seals that are using more exposed habitats making them more vulnerable to predation (Pilfold et al. 2012, 2015). As sea ice breakup and retreat are occurring progressively earlier (Stroeve et al. 2006, 2014, Markus et al. 2009, Stern and Laidre 2016) and this trend is predicted to continue (e.g., Douglas 2010, Joly et al. 2011), polar bears are likely to experience reduced feeding opportunities of seals during this period of greatest productivity (Stirling and Derocher 1993, Stirling et al. 1999, Regehr et al. 2007, Durner et al. 2009). Furthermore, polar bear movement and activity rates are likely to increase as a result of declining and increasingly fragmented sea ice (Sahanatien and Derocher 2012), which may increase their energy demands (Durner et al. 2017). As a result of projected declines in Arctic sea ice and the potential effects on polar bear foraging success and movement patterns, the polar bear was listed as a globally threatened species under the US Endangered Species Act in 2008. Yet, limited information exists on the behavioral response of polar bears to changing sea ice conditions and the implications for their energy expenditure to better understand the mechanisms by which polar bears are impacted by climate change.

Dissertation outline

I examined the behaviors, foraging rates, and energy expenditure of female polar bears to better understand the implications of changing sea ice conditions on polar bear energy demands. In doing so, I also sought to develop and evaluate metrics to quantify polar bear behaviors and energy expenditure using tri-axial accelerometers as a means to facilitate future research on the species.

In **Chapter 1**, I developed a method to identify free-ranging polar bear behaviors on the sea ice and on land using tri-axial accelerometers and conductivity sensors. Based on data collected from free-ranging and captive polar bears and captive grizzly bears (*U. arctos*), I showed that tri-axial accelerometers in combination with conductivity sensors can reliably discriminate resting, walking, and swimming in free-ranging polar bears, but other behaviors, including eating, exhibited lower predictability. Furthermore, measures from captive grizzly bears poorly predicted free-ranging polar bear behaviors.

In **Chapter 2**, I examined the oxygen consumption, gait kinematics, and tri-axial acceleration of captive polar bears and grizzly bears while resting and walking to understand baseline metabolic costs in these species. I further evaluated the ability of tri-axial accelerometers attached to collars as a means to measure the energy expenditure of bears and I assessed whether polar bears have unique energy demands relative to other ursids. I found polar bears and grizzly bears exhibited similar costs of locomotion and gait kinematics, but differing measures of tri-axial acceleration. In both species, measures of oxygen consumption strongly correlated with tri-axial acceleration indicating tri-axial accelerometers have potential as a method to quantify energy expenditure in these species. I further found polar bears and grizzly bears have relatively high costs of activity, but walking costs were commensurate with other quadrupedal mammals.

In **Chapter 3**, I examined the oxygen consumption and stroke frequency of a captive subadult female polar bear while resting in the water and swimming and diving in a metabolic flume as a preliminary assessment of the energetic costs of swimming in polar bears. I found subadult polar bears have high stroke costs while swimming and diving, similar to other semi-aquatic mammals, which supports previous modelling work suggesting that polar bears are energetically inefficient swimmers.

In **Chapter 4**, I measured the field metabolic rate, activity rate, body condition, and foraging success of female polar bears on the spring sea ice of the Beaufort Sea. I found female polar bears on the sea ice have greater field metabolic rates than previously assumed. These metabolic rates were similar to predictions for marine and terrestrial carnivores. Metabolic rates were strongly influenced by activity and movement and, in combination with poor foraging success, more than half of the bears in the study exhibited energy deficits over 8 – 11 days during a time of year when polar bears are thought to start recuperating energy stores. These findings reinforce the implications of declining and increasingly fragmented Arctic sea ice in increasing polar bear energy demands and the potential consequences of poor foraging success on body condition.

In **Chapter 5**, I examine the ability of tri-axial accelerometers to measure the energy expenditure of free-ranging polar bears in comparison to measures derived from doubly-labeled water. I found energetic estimates derived from accelerometers underestimated measures derived from doubly-labeled water, but accelerometer measures strongly correlated with measures derived from doubly-labeled water. These results indicate relationships between tri-axial accelerometer data and oxygen consumption from captive polar bears may not be equivalent to measures of free-ranging energy expenditure derived from doubly-labeled water, but tri-axial accelerometers can be used as an index for energy expenditure in free-ranging polar bears.

These chapters provide a framework by which to examine the behavioral and physiological mechanisms driving trends in polar bear populations. Such data are increasingly needed to better understand polar bear responses to rapid environmental change in the Arctic. Finally in the synthesis, I contextualize the findings from all five data chapters to describe the energy demands of polar bears, their implications toward continued declines in Arctic sea ice, and suggest future directions for polar bear ecophysiology research.

Chapter 1[‡]

Using tri-axial accelerometers to identify wild polar bear behaviors

ABSTRACT

Tri-axial accelerometers have been used to remotely identify the behaviors of a wide range of taxa. Assigning behaviors to accelerometer data often involves the use of captive animals or surrogate species, as accelerometer signatures are generally assumed to be similar to those of their wild counterparts. However, this has rarely been tested. Validated accelerometer data are needed for polar bears (*Ursus maritimus*) to understand how habitat conditions may influence behavior and energy demands. I used accelerometer and water conductivity data to remotely distinguish 10 polar bear behaviors. I calibrated accelerometer and conductivity data collected from collars with behaviors from video-recorded captive polar bears and grizzly bears (*U. arctos*), and with video from camera collars deployed on free-ranging polar bears on the sea ice and on land. I used random forest models to predict behaviors and found strong ability to discriminate the most common wild polar bear behaviors using a combination of accelerometer and conductivity sensor data from captive or wild polar bears. In contrast, models using data from captive grizzly bears failed to reliably distinguish most active behaviors in wild polar bears. The ability to discriminate

---

[‡] A version of this chapter has been published as: Pagano, A.M., K.D. Rode, A. Cutting, M.A. Owen, S. Jensen, J.V. Ware, C.T. Robbins, G.M. Durner, T.C. Atwood, M.E. Obbard, K.R. Middel, G.W. Thiemann, and T.M. Williams. 2017. Using tri-axial accelerometers to identify wild polar bear behaviors. Endangered Species Research 32:19-33.

behavior was greatest when species- and habitat-specific data from wild individuals were used to train models. Data from captive individuals may be suitable for calibrating accelerometers, but may provide reduced ability to discriminate some behaviors. The accelerometer calibrations developed here provide a method to quantify polar bear behaviors to evaluate the impacts of declines in Arctic sea ice.

INTRODUCTION

Knowledge of an animal's behavior can inform species conservation and management by revealing how individuals respond to environmental conditions (Sutherland 1998, Caro 1999, Cooke et al. 2014). Although visual observation is the most direct method to study animal behavior, it is impractical for many species. Innovations in electronic logging and tracking devices have provided new methods to study the behavior, movement, physiology, energetic rates, and environmental conditions of wildlife that may otherwise be difficult or impossible to monitor (Ropert-Coudert and Wilson 2005, Cooke 2008, Wilson et al. 2008, Bograd et al. 2010, Costa et al. 2010, Wilmers et al. 2015).

Tri-axial accelerometers, which collect high frequency measures of acceleration in the form of gravitational and inertial velocity (Brown et al. 2013), have provided a means to remotely identify animal behaviors (Yoda et al. 1999, Watanabe et al. 2005). Accelerometers have been particularly useful in studying widely dispersed animals or those occurring in remote habitats such as marine mammals and birds (Brown et al. 2013). Once calibrated, tri-axial accelerometer data from wild animals can be used to remotely identify behaviors such as resting, walking, running, and even feeding events (Yoda et al. 2001, Shepard et al. 2008, Wilson et al. 2008, Watanabe and Takahashi 2013, Williams et al. 2014). Calibration typically involves time-synchronizing behavioral observations with their associated accelerometer readings, which often necessitates the use of captive animals or surrogate species (e.g., Yoda et al. 2001, Shepard et al. 2008, Nathan et al. 2012, Campbell et al. 2013). Alternatively, animal-borne video cameras can be used to directly calibrate accelerometers (e.g., Watanabe and Takahashi 2013, Nakamura et al. 2015, Volpov et al. 2015), but cameras can be expensive and can only collect data over limited durations.

Polar bears (*Ursus maritimus*) typically occupy remote environments and few quantitative data exist on their behaviors or activity budgets. Much of what is known about polar bear behavior on the sea ice comes from coastal indigenous resident knowledge (e.g., Nelson 1966, Kalxdorff 1997, Kochnev et al. 2003, Voorhees et al. 2014) and direct observational research limited to two locations over limited time periods (Stirling 1974, Stirling and Latour 1978, Hansson and Thomassen 1983, Stirling et al. 2016). Satellite telemetry has been used to track polar bears in some subpopulations from the late 1970s (Schweinsburg and Lee 1982, Taylor 1986) and has helped to identify important habitats (Ferguson et al. 2000, Mauritzen et al. 2003*a*, Durner et al. 2009, Wilson et al. 2014). However, detailed behavioral data in association with habitat conditions are lacking. Recent declines in Arctic sea ice has already caused declines in abundance, survival, or body condition of polar bears in some subpopulations (Stirling et al. 1999, Regehr et al. 2007, Rode et al. 2010, 2012, Bromaghin et al. 2015, Obbard et al. 2016, 2018) and models project increasing negative impacts in the 21st century (Amstrup et al. 2008, Hunter et al. 2010, Molnár et al. 2010, Atwood et al. 2016*a*, Regehr et al. 2016). In order to better predict the impacts of projected sea ice loss on polar bears, it will be important to understand the behavioral and physiological mechanisms driving current declines (Vongraven et al. 2012, Atwood et al. 2016*a*). Accelerometers could be used in combination with satellite telemetry to better understand the behavioral consequences of sea ice loss. This mechanistic information would allow for improved assessment of the relationships between habitat loss, individual health, and vital rates in polar bear populations.

In this study, I developed a method to quantify wild polar bear behaviors using accelerometers and conductivity sensor data, validated through animal-borne video camera data. Additionally, I evaluated the effectiveness of using accelerometer data from captive polar and grizzly bears (*U. arctos*) to predict behaviors of wild polar bears. Though it is generally assumed that accelerometer signatures of captives or surrogates are similar to those of their instrumented wild counterparts (Williams et al. 2014, McClune et al. 2015, Wang et al. 2015, Hammond et al. 2016), this has rarely been tested. Captive individuals may exhibit different behaviors and/or kinematics than wild counterparts (Mcphee and Carlstead 2010), which could potentially influence accelerometer signatures. Because polar bears use both sea ice and terrestrial habitats and differences in habitat substrate or gradient could also affect accelerometer signatures (Bidder et al. 2012, Shepard et al. 2013, McClune et al. 2014), I examined data from wild polar bears in both of these habitats. Lastly, because sampling frequency affects the longevity of accelerometers during deployment as well as computational power for analyses, I evaluated the ability of accelerometers to predict wild polar bear behaviors using 3 different sampling frequencies (16, 8, and 4 Hz).

METHODS

Accelerometer recordings on captive bears

I deployed collars with archival loggers (TDR10-X-340D, Wildlife Computers, Inc., Redmond, WA) on three adult female polar bears housed at the Alaska Zoo, Oregon Zoo, and San Diego Zoo, as well as two adult female grizzly bears housed at the Bear Research, Education, and Conservation Center at Washington State University (WSU; Table 1.1). Archival loggers recorded tri-axial acceleration ($m \cdot s^{-2}$) at 16 Hz (range ±20 $m \cdot s^{-2}$), time-of-day, and wet/dry conductions (via an on-board conductivity sensor; Figure 1.1). Conductivity data were sampled at 1 Hz. Bears at the Oregon and San Diego Zoos were trained to voluntarily place their heads into crates in which collars would be applied or removed and wore collars for 1–4 hour sessions. Bears at the Alaska Zoo and WSU were anesthetized for collaring with a combination of tiletamine HCl and zolazepam HCl (Telazol®, Pfizer Animal Health, New York, NY) and dexmedetomidine HCl (Dexdomitor®, Pfizer Animal Health) (Teisberg et al. 2014). Following collar placement, anesthetized bears were reversed with atipamezole HCl (Antisedan®, Pfizer Animal Health). Release mechanisms (Lotek Wireless, Inc., Newmarket, ON) were used to remove collars from bears at the Alaska Zoo and WSU. I matched accelerometer recordings to the behaviors of captive bears while they moved freely around enclosures based on visual examination of time-stamped video recordings (camcorder Sony model DCR-TRV280, Sony Corp. or OpenEye Digital Video Security Solutions, Spokane, WA).

Accelerometer recordings on free-ranging polar bears

GPS-equipped video camera collars (Exeye, LLC., Bristow, VA) and archival loggers (TDR10-X-340D, Wildlife Computers, Inc.) were deployed on four adult female polar bears and one subadult female polar bear captured on the sea ice of the southern Beaufort Sea in April 2014 and 2015 (hereafter "ice bears") and two subadult polar bears (1 male and 1 female) captured on land on Akimiski Island, Nunavut in September 2015 (hereafter "land bears"; Table 1.1). Video collars including archival loggers and release mechanisms weighed 1.6 – 2.1 kg (0.8% – 1.5% of body mass of bears in this study). Polar bears were captured by injecting them with immobilizing drugs through projectile syringes fired from a helicopter. On the sea ice, bears were anesthetized using a combination of tiletamine HCl and zolazepam HCl (Telazol®) with no reversal (Stirling et al. 1989). On land, bears were anesthetized with a combination of medetomidine (Domitor®, Pfizer Animal Health) and tiletamine HCl and zolazepam HCl (Telazol®) and reversed with atipamezole HCl (Antisedan®) (Cattet et al. 1997). Archival loggers were attached to collars in the same location and orientation as captive deployments (Figure 1.1) and similarly recorded tri-axial acceleration at 16 Hz (range ±20 $m \cdot s^{-2}$), time-of-day, and wet/dry conductions (via an on-board conductivity sensor). Conductivity data were sampled at

1 Hz. Video cameras were programmed to record at varying frequencies during daylight periods (Table 1.2) and programmed to turn off if the temperature of the collar was ≤ -17 °C to protect video equipment. Collars deployed on ice and land bears were recovered 4 – 23 days following deployment, either by recapture of the individual or by remote activation of the collar release and retrieval of the dropped collar by the field crew. I matched accelerometer data to behavior of ice and land bears based on visual examination of the time-stamped video recordings from the collar.

Behaviors

Behaviors were annotated based on the video data on a per second basis. For bears that were anesthetized, I excluded behaviors on the day of capture and during retrieval of the collar. Resting behaviors included standing, sitting, and lying down. Head movements while standing, sitting, or lying down were included as resting behaviors, but limb movements were treated as transitionary behaviors (Knudsen 1978, Williams 1983). Swimming included surface swimming and diving. I excluded from analyses any behaviors that were not indicative of natural movements in captive bears (e.g., stereotypic behaviors), were rare (e.g., fighting, breeding, drinking), were transitionary, or were non-descript.

Modeling

I derived summary statistics from the accelerometer data and linked the accelerometer data with corresponding behaviors of interest (SAS version 9.3, SAS Institute Inc., Cary, NC). I converted accelerometer measures from $m \cdot s^{-2}$ to *g* (1 *g* =

9.81 m·s^{-2}). I calculated magnitude (Q) as a fourth dimension, where $Q = \sqrt{heave^2 + surge^2 + sway^2}$ (Nathan et al. 2012). I used a 2-second running mean of the raw acceleration data to calculate static acceleration (gravitational acceleration) and subtracted the static acceleration from the raw acceleration data to calculate dynamic acceleration (Wilson et al. 2006, Shepard et al. 2008). I calculated overall dynamic body acceleration (ODBA) as the absolute sum of dynamic acceleration across the 3 axes (Wilson et al. 2006). I used a Fast Fourier Transform to calculate the dominant power spectrum (dps) and frequency (fdps) for each axis (Watanabe et al. 2005, Shamoun-Baranes et al. 2012). In total, I derived 25 predictor variables based on previous accelerometer studies (e.g., Watanabe et al. 2005, Nathan et al. 2012, Shamoun-Baranes et al. 2012, Wang et al. 2015). Predictor variables were extracted from the accelerometer data over 2-second intervals; mean conductivity data (wet/dry) was also extracted over 2-second intervals using program R (R Core Team 2014) (Table 1.3). Video-linked behaviors that lasted less than 2 seconds were excluded from analyses. I used a random forest supervised machine learning algorithm (Breiman 2001) in R (RandomForest package) to predict polar bear behaviors. Random forest models use multiple classification trees from a random subset of predictor variables and then replicate this process over multiple iterations using a subset of the data for each iteration to determine the best variables for making predictions (Breiman 2001). An estimate of error is derived by using the remaining data not used in each iteration to test the predictive ability of the model, which is termed the “out-of-bag” (OOB) error rate (Breiman 2001, Liaw and Wiener 2002).

The random forest algorithm has previously shown high accuracy (>80%) for predicting animal behaviors from accelerometer data (Nathan et al. 2012, Resheff et al. 2014, Graf et al. 2015, Rekvik 2015, Wang et al. 2015, Alvarenga et al. 2016, Lush et al. 2016). I fit 500 classification trees to each training dataset and used a random subset of 5 predictor variables for each split in the tree.

Analyses

Unbalanced datasets can bias the predictive ability of classification algorithms toward the most dominant classes (Chen et al. 2004). Therefore, I performed 3 initial analyses to test the effect of uneven distributions on predictive ability. The first analysis used an uneven distribution in which for ice and land bears, I randomly selected 70% of each behavior for the training dataset and used the remaining 30% to test the predictive ability of the random forest algorithm (e.g., Nathan et al. 2012, Alvarenga et al. 2016). For captive polar bears and grizzly bears I used the entire datasets to train the random forest algorithm. The second analysis used a subsampling approach in which I attempted to reduce the uneven distribution of more frequent behaviors (e.g., resting) in the training dataset. To reduce the uneven distribution of behaviors in the dataset from ice bears, I randomly selected 5% of the resting behaviors, 30% of the walking behaviors, and 70% of each of the remaining behaviors for training the random forest algorithm. I used the remaining data from ice bears for testing predictions. To reduce the uneven distribution of the dataset from land bears, I randomly selected 5% of the resting behaviors and 70% of each of the remaining behaviors for training and used the remaining data to test predictions. To reduce the uneven distribution of the datasets from captive polar bears and grizzly bears, I randomly selected 10% of the resting behaviors, 30% of the walking behaviors, and 100% of each of the remaining behaviors for training the random forest algorithm. The third analysis used a completely balanced distribution in which I used identical sample sizes of 500 observations for each behavior in the training dataset and the remaining observations to test and excluded behaviors with less than 500 observations. Based on these 3 analyses, I used the sampling distribution (i.e., uneven, subsampled, or balanced distribution) with the greatest predictive ability for further analyses.

To evaluate the ability to predict behaviors of ice bears, I used 3 different datasets to train the random forest models and evaluated the ability of each of these models. First, I used a random subset of the data from ice bears as the training dataset and the remaining data from ice bears to test predictions (testing dataset). Second, I used the data from captive polar bears as the training dataset. Third, I used the data from captive grizzly bears as the training dataset.

To evaluate the ability to predict behaviors of land bears, I conducted 4 additional analyses. First, I used a random subset of the data from land bears as the training dataset and the remaining data from land bears to test predictions (testing dataset). Second, I used the training data from ice bears as the training dataset. Third, I used the training data from captive polar bears as the training dataset. Fourth, I used the training data from captive grizzly bears as the training dataset.

To examine the effect of sampling frequency on the ability to discriminate behaviors, I subsampled the 16 Hz accelerometer data to lower data acquisition rates of 8 Hz and 4 Hz using SAS and repeated the predictive analyses above for both ice and land bears.

Predicted behaviors were categorized as true positive (TP) if they correctly matched the actual behavior, true negative (TN) if they correctly identified as a different behavior, false positive (FP) if they incorrectly identified the behavior, and false negative (FN) if they incorrectly identified as a different behavior. I evaluated the predictive abilities of these models based on Matthews' correlation coefficient (MCC; e.g., Basu et al. 2013, Martins et al. 2016), the percent precision, recall, and *F*-measure. I used MCC in place of accuracy due to the unbalanced nature of the dataset. MCC ($\frac{TP*TN-FP*FN}{\sqrt{(TP+FP)*(TP+FN)*(TN+FP)*(TN+FN)}}$), provides a measure of the agreement between the predicted and actual classifications where +1 represents a perfect prediction and -1 represents total disagreement (Matthews 1975). Precision is the proportion of positive classifications that were correctly classified ($\frac{TP}{TP+FP}$), recall is the probability that a behavior will be correctly classified ($\frac{TP}{TP+FN}$), and *F*-measure is the harmonic mean of precision and recall ($\frac{2\times precision\times recall}{precsion+recall}$). I used two sample *t*-tests to evaluate whether MCC, precision, and recall differed significantly using a 16 Hz sampling frequency compared to either an 8 Hz or 4 Hz sampling frequency based on the ice and land datasets.

RESULTS

Behaviors on the sea ice

Video collars on ice bears recorded 14 – 55 hours of video ($\bar{x}$ = 38 hours, SD = 17 hours, *n* = 5). For predicting the behavior of ice bears, I collected a total of 140 hours of video-linked accelerometer data from ice bears, 37 hours from captive polar bears, and 72 hours from captive grizzly bears. I identified 10 different behaviors from ice bears with resting, walking, and eating being the most prevalent (Table 1.4). Ice bears ate recently killed adult, subadult, or pup ringed seals (*Pusa hispida*), seal carcasses, bowhead whale carcasses (*Balaena mysticetus*), or unidentifiable carcasses. Captive polar bears consumed fish and captive grizzly bears ate dry omnivore chow. Captive grizzly bears also grazed on grass, which was excluded from analyses predicting behaviors of ice bears, but was included as eating for predicting behaviors of land bears.

The models using an uneven distribution of behaviors in which I used 70% of each behavior from ice bears and all of the available data from captive polar or grizzly bears exhibited 5% greater predictive ability overall compared to the subsampled distribution and 7% greater predictive ability overall compared to the balanced distribution based on *F*-measure (Table 1.5). In particular, the datasets with an uneven distribution exhibited greater ability to discriminate less frequent behaviors such as swimming, eating, and running (Table 1.5). Therefore, I used the datasets with uneven distributions for subsequent analyses (Table 1.4).

The model with training data from ice bears had an OOB error rate of 2.0% and exhibited the greatest predictive abilities for all 10 behaviors (Figure 1.2) compared to all other models tested. The models with training data from captive polar bears and grizzly bears had OOB error rates of 3.7% and 0.5% respectively, indicating both models performed well in discriminating captive behaviors. Both the ice bear and captive polar bear models exhibited strong predictive ability for identifying resting and walking behaviors in wild bears (>90% MCC, precision, recall, and *F*-measure; Table 1.6, Table 1.7). Predictive abilities for other behaviors varied with swimming and head shaking exhibiting strong predictive ability using the ice bear model (>75% MCC, precision, recall, and *F*-measure), but lower predictive ability for eating, running, pouncing, grooming, digging, and rolling (Figure 1.2, Tables 1.6,1.8). The model from ice bears had particularly greater ability than the captive polar bear model for swimming, pouncing, and digging (Figure 1.2, Table 1.7). The captive grizzly bear model provided weaker ability to distinguish behaviors of ice bears for walking, eating, and grooming (<65% MCC and *F*-measure), but reliably distinguished resting (Figure 1.2, Table 1.9).

Using the model from ice bears, eating had a high rate of false positive classifications resulting from digging behavior being incorrectly classified as eating (Table 1.8) as well as a high rate of false negative classifications with eating behavior incorrectly classified as either resting or walking (Table 1.8). A post-hoc test using only feeding behavior while eating a recently killed ringed seal within the training and testing datasets failed to improve the ability to discriminate eating (MCC = 0.61, precision = 0.67, recall = 0.56, *F*-measure = 0.61). Additionally, running was often misclassified as walking, whereas rolling was often misclassified as resting (Table 1.8).

The most important predictors using the model from ice bears were static acceleration in the heave (staticY) and surge directions (staticX), wet/dry conductivity (wetdry), and frequency at the dominant power spectrum in the surge direction (fdpsX; Figure 1.3). Differences in the intensity of behaviors were discernible in the ODBA measures with head shaking having the greatest ODBA and resting having the lowest (Table 1.10). Eating and swimming showed similar mean ODBA values, but had differing mean static acceleration values (Table 1.10). Eating and grooming had low values of static acceleration in the heave direction (staticY), which was indicative of a head down posture. Walking and running exhibited periodic undulating patterns in static acceleration in the heave direction (staticY; Figures 1.4, 1.5), which was indicative of the bear's head moving up and down as it stepped. Wet/dry conductivity while swimming was lower for wild polar bears ($\bar{x}$ = 81.9, sd = 81.5) than captive polar bears ($\bar{x}$ = 205.3, sd = 57.8) and lower than all other behaviors (all $\bar{x} > 234$). A post-hoc test excluding the conductivity variable reduced the ability of the algorithm to correctly identify swimming behaviors using the training dataset for ice bears (MCC = 0.47, precision = 0.77, recall = 0.29, *F*-measure = 0.42) with a high rate of swimming behaviors misclassified as resting.

Behaviors on land

Video collars on land bears recorded 19 – 36 hours of video ($\bar{x}$ = 27 hours, SD = 12 hours, *n* = 2) and in total 36 hours of video-linked accelerometer data were collected for the behaviors of interest. I identified 5 different behaviors from land bears with resting being the most prevalent followed by eating (Table 1.3). Eating on land consisted of berries, primarily crowberries (*Empetrum nigrum*).

The model with training data from land bears had an OOB error rate of 0.5% and had the greatest success in discriminating on land behaviors (Figure 1.6, Table 1.11). All behaviors except for grooming and head shaking, had MCC, precision, recall, and *F*-measure values >90% using the model from land bears (Figure 1.6, Table 1.11). In particular, the model from land bears was able to distinguish eating (MCC = 0.95, precision = 0.95, recall = 0.96, *F*-measure = 0.95), which was not possible with the other datasets. The model with training data from ice bears had success in discriminating resting behaviors on land (MCC = 0.60, precision = 0.96, recall = 1.0, *F*-measure = 0.98) and walking on land (MCC = 0.82, precision = 0.89, recall = 0.76, *F*-measure = 0.82), but eating was often misclassified as resting or walking (FP). The captive polar bear model performed similarly to the model from ice bears for discriminating behaviors on land (Figure 1.6). The captive grizzly bear model performed poorer for discriminating walking on land, but otherwise performed similarly to the models from ice bears and captive polar bears (Figure 1.6).

Sampling frequency

The OOB error rate using the data from ice bears increased from 2.0% to 2.2% using an 8 Hz sampling frequency and 2.6% using a 4 Hz sampling frequency. OOB error rate using data from land bears increased from 0.5% to 0.6% at 8 Hz and 0.8% at 4 Hz. Predictive ability using an 8 Hz sampling frequency was nearly identical to 16 Hz among all behaviors using the dataset from ice bears ($t_{58} = 0.70$, $p = 0.24$) and land bears ($t_{28} = 0.61$, $p = 0.27$) based on MCC, precision, and recall. Predictive ability using a 4 Hz sampling frequency was lower than predictive ability using 16 Hz for ice bears ($t_{55} = 1.8$, $p = 0.04$), but not for land bears ($t_{27} = 0.59$, $p = 0.28$). In particular, the ability to discriminate the high intensity behaviors of pouncing and head shaking declined using a 4 Hz sampling rate (Figure 1.7).

DISCUSSION

These results show that tri-axial accelerometers in combination with measures of conductivity can reliably distinguish the three most common behaviors of wild polar bears (resting, walking, and swimming; (Stirling 1974, Latour 1981, Hansson and Thomassen 1983, Lunn and Stirling 1985)). This will provide a method to remotely document the activity budgets of these far-ranging animals, which can be further linked with location data from satellite collars to examine the effects of habitat on behavior and energy expenditure. These results indicate that differences among habitats and species can impact the ability to discriminate behaviors in wild individuals using accelerometers. I found no loss in predictive ability using an 8 Hz sampling frequency, which would allow for twice the battery longevity of a 16 Hz rate and reduce the computational power needed for analyses. Although accelerometer studies on smaller species appear to require greater sampling frequencies (e.g., >30 Hz; (Broell et al. 2013, Brown et al. 2013)), the results in this study are similar to Rekvik (2015) from captive grizzly bears and Wang et al. (2015)

from captive mountain lions (*Puma concolor*), which both found little loss in predictive ability at sampling frequencies ≥8 Hz.

Habitat effects

The results in this study indicate accelerometer signatures on the sea ice are similar to signatures on land for most behaviors, but eating berries by land bears had a distinct signature that the ice bear model and captive bear models misclassified as grooming, resting, or walking. This highlights the value in linking observational and accelerometer data from wild subjects over multiple time periods and habitats and the importance of accounting for as many behaviors as possible in training datasets. Knowledge of eating frequency and duration would provide insight in determining foraging success, an important determinant of individual reproductive success and survival (Stirling et al. 1999, Regehr et al. 2007, 2010). Although I had success discriminating eating events by land bears I had lower precision and recall in discriminating eating events by ice bears. This was likely related in part to the movement pattern of bears eating berries, in which they typically stood with their head down and grazed. Conversely, bears eating on the sea ice exhibited a variety of positions including standing, sitting, and lying down, and both tore pieces of food from seals or gnawed on carcasses. Since most kill events involve bears pouncing on their seal prey (Stirling 1988, Derocher 2012), it may be feasible to identify successful kills based on the combination of a pouncing signature followed by eating signatures (e.g., Williams et al. 2014), but this requires further evaluation. Additionally, feeding on a seal would typically last prolonged periods, hence, if the model primarily predicted eating over a prolonged period this could be used as an indication of a feeding event, but this also requires further evaluation.

Use of captive animals and surrogate species

The ability to discriminate behaviors was greatly improved by including data from free-ranging polar bears rather than using data from captive bears alone. However, resting and walking could be reliably discriminated using data from either captive or wild polar bears. This illustrates the value of collecting data from captive individuals when data collection is difficult or impossible from wild counterparts. However, data from captive grizzly bears exhibited poorer performance for predicting active behaviors in wild polar bears. This may be related to differences in walking kinematics between polar and grizzly bears as well as potential differences in limb lengths between the species (Renous et al. 1988). Additionally, polar bears have longer necks relative to their body size than other ursid species (DeMaster and Stirling 1981), which could also affect accelerometer signatures from a neck-worn collar. Although Campbell et al. (2013) proposed the use of surrogate species to predict the behaviors of other species, the findings in this study suggest polar bear accelerometer signatures are likely species- and habitat-specific, at least for distinguishing specific behaviors. The grizzly bear model did reliably distinguish resting behavior in wild polar bears, which suggests that surrogate species could be used to distinguish coarse activity patterns such as active versus inactive (e.g., Gervasi et al. 2006, Ware et al. 2015).

The analyses in this study indicate conductivity measures are needed to reliably discriminate swimming. Greater conductivity measures in captive polar bears that were swimming in fresh water likely caused the poorer performance for discriminating swimming in wild polar bears that were swimming in salt water. For pouncing, captive polar bears pounced on large plastic barrels, which resulted in similar measures of ODBA as wild counterparts, but had different signatures of static acceleration (i.e., body posture). Digging by wild bears, which was often through snow and ice into subnivean lairs to locate seals, exhibited greater ODBA measures and slightly different static acceleration than captive bears digging in snow and ice. These results suggest some behaviors of captive bears may not fully reflect behaviors of their wild counterparts and thus further illustrate the value of collecting simultaneous observational data (e.g., video) from free-ranging individuals to calibrate accelerometer-based behavioral data.

Accelerometer attachment

Regardless of which training dataset was used, I found lower precision and recall for predicting five of the behaviors tested for bears on the sea ice. Eating, grooming, and rolling had high rates of misclassifications as resting whereas running and digging had high rates of misclassifications as walking. These results suggest the random forest algorithm could be prone to slightly overestimate the amount of true resting and walking behaviors in quantifying activity budgets. The lower precision and recall I found for discriminating some behaviors was likely due in part to the attachment of the accelerometer on a collar. Although a number of studies have successfully discriminated behaviors using accelerometers on collars (Watanabe et al. 2005, Martiskainen et al. 2009, Soltis et al. 2012, McClune et al. 2014, Rekvik 2015, Wang et al. 2015, Lush et al. 2016), many of these studies limited their analyses to 4 or 5 behaviors or documented high misclassification rates for distinguishing some behaviors. Wang et al. (2015) similarly reported low accuracy of accelerometers on collars for predicting eating and grooming by captive mountain lions and Lush et al. (2016) reported low accuracy for predicting some behaviors in wild brown hares (*Lepus europaeus*) including grooming. Attachment of the accelerometer to a collar as opposed to attachment directly on the animal, likely introduces noise in the data due to independent collar motion (i.e., the collar must be fitted to ensure animals do not remove it, but loose enough to accommodate potential changes in body mass) and may reduce the ability of the accelerometer to detect some low intensity movements (Shepard et al. 2008). The effect of independent collar motion is evident in the large values of ODBA I found when bears shook their heads. This behavior may be useful for identifying the end of a swim as bears are known to shake and roll in the snow following a swim. Additionally, the ability to discriminate head shaking, allows for excluding it from potential energetic analyses using accelerometers. Use of a higher sampling frequency than was used in this study (i.e., >16 Hz) could potentially improve the ability to discriminate some fine-scale body movements (Nathan et al. 2012) such as eating, though Wang et al. (2015) sampled at 64 Hz and had low accuracy in discriminating eating behaviors by captive mountain lions.

Video calibration

Having video-linked observational data from camera-mounted collars on wild polar bears was the most practical method to calibrate accelerometers on free-ranging individuals. However, because the animal's body was not visible in the video, some behaviors may have been incorrectly classified. For example, distinguishing walking versus running was often challenging as was determining when bears were actively swimming versus resting in the water. Both of these could have contributed to the misclassifications between running and walking and swimming and resting. Additionally, the models had greater success discriminating behaviors as sample sizes increased. Although unbalanced datasets are known to affect the predictive ability of random forest algorithms (Chen et al. 2004), I found the inclusion of larger sample sizes in the training dataset was more important than imbalance. This highlights the value of calibrating accelerometers from multiple individuals over prolonged periods.

Conclusions

The results in this study underscore the importance of thoroughly validating accelerometers for use in remote detection of behavior, ideally on a species- and habitat-specific level. The use of tri-axial accelerometers, as shown here, will enable detailed assessments of polar bear behaviors to better understand polar bear habitat use and the implications for energy demands. For example, measures of acceleration could be combined with measures of oxygen consumption from captive bears while resting, walking, and swimming to both quantify activity budgets and estimate the energetic costs of these behaviors (e.g., Wilson et al. 2006, 2012, Halsey et al. 2009*a*, 2011*a*, Gómez Laich et al. 2011, Williams et al. 2014). Future advances are needed that would enable remote transmission of raw accelerometer data to further enhance the applicability of these devices to animals occurring in remote environments and obviate the need for sensor recovery. As declines in sea ice are expected to increase the activity rates of polar bears across much of their range (Derocher et al. 2004, Molnár et al. 2010, Sahanatien and Derocher 2012), the use of accelerometers provide a method to monitor the impacts of habitat change on activity and energy budgets to better understand the implications for body condition, reproductive success, and survival of this Arctic apex predator.

Table 1.1. Polar bears and grizzly bears wearing collars with tri-axial accelerometers that were video recorded (captive bears) or that wore video-equipped collars (wild bears).

Species	**Sex**	**Age Class**	**Body Mass (kg)**	**Location**
Polar Bear	Female	Adult	288	Alaska Zoo
Polar Bear	Female	Adult	212	Oregon Zoo
Polar Bear	Female	Adult	237	San Diego Zoo
Grizzly Bear	Female	Adult	126	Washington State University
Grizzly Bear	Female	Adult	126	Washington State University
Polar Bear	Female	Adult	173	southern Beaufort Sea
Polar Bear	Female	Adult	176	southern Beaufort Sea
Polar Bear	Female	Adult	199	southern Beaufort Sea
Polar Bear	Female	Adult	172	southern Beaufort Sea
Polar Bear	Female	Subadult	141	southern Beaufort Sea
Polar Bear	Male	Subadult	186	Akimiski Island
Polar Bear	Female	Subadult	140	Akimiski Island

Table 1.2. Video recording schedules used by GPS-equipped video camera collars deployed on polar bears on the sea ice of the southern Beaufort Sea and on land on Akimiski Island, Nunavut.

Year – Location	Time of Day[a]	Video recording duty cycle
2014 – Sea Ice	8 am – 1 pm	1 min : 2 min
2014 – Sea Ice	1 pm – 9 pm	30 sec : 2 min
2015 – Sea Ice	8 am – 1 pm	1 min : 2 min
2015 – Sea Ice	1 pm – 10 pm	30 sec : 2 min
2015 – Sea Ice[b]	8 am – 6 pm	1 min : 2min
2015 – Sea Ice[b]	6 pm – 10 pm	30 sec : 2 min
2015 – Land	7 am – 11 am	Continuous
2015 – Land	11 am – 8 pm	1 min : 2 min

[a] Times for sea ice deployments are Alaska Daylight Time. Times for on land deployments are Eastern Daylight Time.

[b] Two collars in 2015 were set to record using the following duty cycle.

Table 1.3. Parameters extracted from tri-axial accelerometer and conductivity data and used in random forest models to predict wild polar bear behaviors. Respective acceleration measures from the surge (X), heave (Y), sway (Z), and magnitude (Q) axes.

Parameter	**Label**	**Definition**
Static acceleration (*g*)	staticX, staticY, staticZ, staticQ	Mean static acceleration along the surge, heave, sway, and magnitude axes.
Maximum dynamic body acceleration (*g*)	mdbaX, mdbaY, mdbaZ, mdbaQ	Maximum dynamic body acceleration along the surge, heave, sway, and magnitude axes
Standard deviation dynamic body acceleration (*g*)	stdbaX, stdbaY, stdbaZ, stdbaQ	Standard deviation dynamic body acceleration along the surge, heave, sway, and magnitude axes.
Overall dynamic body acceleration (*g*)	odbaX, odbaY, odbaZ, ODBA	Mean dynamic acceleration body acceleration along the surge, heave, and sway axes. ODBA = odbaX+odbaY+odbaZ
Dominant power spectrum ($g^2 Hz^{-1}$)	dpsX, dpsY, dpsZ, dpsQ	Maximum power spectral density of dynamic acceleration along the surge, heave, sway, and magnitude axes.
Frequency at the dominant power spectrum (Hz)	fdpsX, fdpsY, fdpsZ, fdpsQ	Frequency at the maximum power spectral density of dynamic acceleration along the surge, heave, sway, and magnitude axes.
Mean wetdry	wetdry	Mean conductivity determination of whether the tag is wet or dry (range 0–255).

Table 1.4. Number of 2 s long behaviors used in random forest training datasets for predicting behaviors of wild polar bears. Ice bears: polar bears on the sea ice of the southern Beaufort Sea. Land bears: polar bears on Akimiski Island, Nunavut.

Behavior	**Captive polar bears**	**Captive grizzly bears**	**Wild ice bears**	**Wild land bears**
Rest	53656	104838	163301	43132
Walk	8962	33059	36083	958
Swim	423	0	703	0
Eat	2108	973	2100	1529
Run	0	0	943	0
Pounce	458	0	49	0
Groom	3729	432	1138	289
Dig	405	0	1194	0
Head shake	86	14	435	19
Roll	87	0	1473	0

Table 1.5. Performance of a random forest model testing the effect of sampling distributions on the predictive ability of accelerometer data in discriminating the behaviors of bears on the sea ice as verified by video data. MCC: Matthews' correlation coefficient.

Behavior	**MCC**	**Precision**	**Recall**	***F*-measure**
Uneven distribution				
Rest	0.973	0.992	0.997	0.994
Walk	0.971	0.964	0.989	0.976
Swim	0.887	0.957	0.823	0.885
Eat	0.674	0.677	0.677	0.677
Run	0.709	0.835	0.604	0.701
Pounce	0.700	0.833	0.588	0.690
Groom	0.417	0.658	0.266	0.379
Dig	0.532	0.712	0.400	0.513
Head Shake	0.818	0.839	0.798	0.818
Roll	0.754	0.821	0.696	0.753
Sub-sampled distribution				
Rest	0.954	0.999	0.983	0.991
Walk	0.970	0.988	0.962	0.975
Swim	0.765	0.621	0.943	0.749
Eat	0.516	0.333	0.807	0.472
Run	0.474	0.294	0.769	0.425
Pounce	0.807	0.923	0.706	0.800
Groom	0.301	0.137	0.672	0.227
Dig	0.487	0.483	0.493	0.488
Head Shake	0.734	0.598	0.902	0.719
Roll	0.533	0.348	0.820	0.489
Balanced distribution				
Rest	0.855	1.000	0.931	0.964
Walk	0.918	0.990	0.876	0.929
Swim	0.579	0.350	0.960	0.513
Eat	0.539	0.495	0.595	0.541
Run	0.376	0.168	0.854	0.281
Groom	0.206	0.059	0.781	0.110
Dig	0.426	0.294	0.626	0.400
Head Shake	0.446	0.214	0.932	0.348
Roll	0.584	0.419	0.821	0.555

Table 1.6. Performance of a random forest model using accelerometer data from polar bears on the sea ice to predict behaviors from bears on the sea ice as verified by video data. MCC: Matthews' correlation coefficient.

Behavior	**MCC**	**Precision**	**Recall**	***F*-measure**
Rest	0.973	0.992	0.997	0.994
Walk	0.971	0.964	0.989	0.976
Swim	0.887	0.957	0.823	0.885
Eat	0.674	0.677	0.677	0.677
Run	0.709	0.835	0.604	0.701
Pounce	0.700	0.833	0.588	0.690
Groom	0.417	0.658	0.266	0.379
Dig	0.532	0.712	0.400	0.513
Head Shake	0.818	0.839	0.798	0.818
Roll	0.754	0.821	0.696	0.753

Table 1.7. Performance of a random forest model using accelerometer data from captive polar bears to predict behaviors from bears on the sea ice as verified by video data. MCC: Matthews' correlation coefficient.

Behavior	**MCC**[a]	**Precision**	**Recall**	***F*-measure**
Rest	0.914	0.996	0.966	0.981
Walk	0.958	0.942	0.989	0.965
Swim	0.534	0.517	0.555	0.535
Eat	0.454	0.385	0.550	0.453
Pounce	0.342	0.133	0.882	0.231
Groom	0.158	0.078	0.361	0.128
Dig	0.140	0.320	0.063	0.105
Head Shake	0.713	0.783	0.650	0.710
Roll	0.435	0.928	0.205	0.336

Table 1.8. Cross-validation comparing predicted behaviors (rows) from accelerometer analyses of polar bears on the sea ice to actual behaviors (columns) confirmed by video recordings. Correct classifications are denoted in bold. See Table 1.6 for performance statistics in predicting behaviors.

	Rest	**Walk**	**Swim**	**Eat**	**Run**	**Pounce**	**Groom**	**Dig**	**Head Shake**	**Roll**
Rest	**69760**	31	33	99	1	0	281	28	0	111
Walk	115	**15295**	10	111	153	4	15	102	26	41
Swim	6	2	**246**	1	0	0	1	0	0	1
Eat	35	51	2	**608**	1	0	45	145	0	11
Run	0	44	0	1	**243**	0	0	1	1	1
Pounce	0	0	0	0	0	**10**	0	2	0	0
Groom	17	2	0	33	0	0	**129**	13	0	2
Dig	2	16	0	44	0	2	9	**203**	0	9
Head Shake	2	6	0	0	3	0	0	2	**146**	15
Roll	45	13	8	1	1	1	5	2	10	**437**

Table 1.9. Performance of a random forest model using accelerometer data from captive grizzly bears to predict behaviors from bears on the sea ice as verified by video data.

Behavior	**MCC**[a]	**Precision**	**Recall**	***F*-measure**
Rest	0.639	0.894	0.988	0.939
Walk	0.605	0.860	0.498	0.631
Eat	0.104	0.138	0.089	0.108
Groom	0.018	0.087	0.004	0.008
Head Shake	0.794	0.850	0.743	0.793

[a] Matthews' correlation coefficient

Table 1.10. Mean (standard deviation) static acceleration (*g*) in the surge (X), heave (Y), and sway (Z) directions, and overall dynamic acceleration (ODBA (*g*)) derived from accelerometers deployed on 3 captive polar bears, 2 captive grizzly bears, 5 polar bears on the sea ice, and 2 polar bears on land.

	Captive Polar Bears				**Captive Grizzly Bears**				**Wild Polar Bears–Sea Ice**				**Wild Polar Bears–Land**			
Behavior	**staticX**	**staticY**	**staticZ**	**ODBA**	**staticX**	**staticY**	**staticZ**	**ODBA**	**staticX**	**staticY**	**staticZ**	**ODBA**	**staticX**	**staticY**	**staticZ**	**ODBA**
Rest	-0.06 (0.25)	-0.74 (0.30)	-0.06 (0.55)	0.04 (0.06)	0.13 (0.20)	-0.36 (0.61)	0.26 (0.60)	0.01 (0.03)	-0.07 (0.29)	-0.51 (0.38)	-0.25 (0.69)	0.02 (0.07)	-0.22 (0.29)	-0.58 (0.34)	-0.09 (0.65)	0.01 (0.03)
Walk	-0.10 (0.19)	-0.95 (0.06)	0.10 (0.20)	0.26 (0.08)	0.24 (0.14)	-0.90 (0.18)	0.21 (0.08)	0.32 (0.09)	-0.03 (0.17)	-0.99 (0.06)	-0.14 (0.22)	0.45 (0.14)	-0.09 (0.14)	-0.99 (0.04)	-0.13 (0.12)	0.29 (0.07)
Swim	-0.11 (0.43)	-0.51 (0.36)	-0.01 (0.61)	0.32 (0.21)					-0.10 (0.50)	-0.56 (0.36)	-0.37 (0.42)	0.40 (0.28)				
Eat	-0.26 (0.45)	-0.80 (0.15)	0.06 (0.24)	0.26 (0.09)	0.59 (0.18)	-0.76 (0.09)	0.16 (0.16)	0.30 (0.14)	-0.40 (0.41)	-0.76 (0.15)	-0.07 (0.25)	0.36 (0.14)	-0.49 (0.12)	-0.87 (0.08)	-0.11 (0.07)	0.17 (0.07)
Run									0.02 (0.15)	-0.91 (0.13)	-0.10 (0.22)	1.42 (0.63)				
Pounce	-0.73 (0.34)	-0.46 (0.13)	0.16 (0.21)	1.52 (0.31)					-0.45 (0.26)	-0.55 (0.19)	-0.11 (0.20)	1.51 (0.44)				
Groom	-0.50 (0.34)	-0.67 (0.27)	0.10 (0.31)	0.19 (0.23)	0.42 (0.31)	-0.74 (0.29)	0.27 (0.16)	0.09 (0.08)	-0.26 (0.38)	-0.71 (0.30)	0.00 (0.45)	0.21 (0.12)	-0.45 (0.20)	-0.77 (0.14)	-0.33 (0.24)	0.08 (0.03)
Dig	-0.64 (0.17)	-0.71 (0.13)	-0.07 (0.20)	0.31 (0.08)					-0.48 (0.39)	-0.70 (0.20)	-0.09 (0.22)	0.45 (0.22)				
Head Shake	0.02 (0.29)	-0.70 (0.26)	0.58 (0.37)	2.81 (0.67)	-0.09 (0.19)	-0.73 (0.23)	0.48 (0.20)	3.16 (0.66)	-0.26 (0.37)	-0.61 (0.34)	0.36 (0.46)	2.24 (0.79)	-0.09 (0.30)	-0.91 (0.14)	0.01 (0.28)	1.85 (0.87)
Roll	-0.18 (0.21)	0.35 (0.37)	0.35 (0.60)	1.19 (0.62)					-0.09 (0.37)	-0.20 (0.47)	0.09 (0.66)	0.98 (0.58)				

Table 1.11. Performance of a random forest model using accelerometer data from polar bears on land to predict behaviors from bears on land as verified by video data.

Behavior	**MCC**[a]	**Precision**	**Recall**	***F*-measure**
Rest	0.979	0.998	0.999	0.999
Walk	0.957	0.950	0.966	0.958
Eat	0.950	0.947	0.956	0.951
Groom	0.742	0.894	0.618	0.731
Head Shake	0.845	1.000	0.714	0.833

[a] Matthews' correlation coefficient

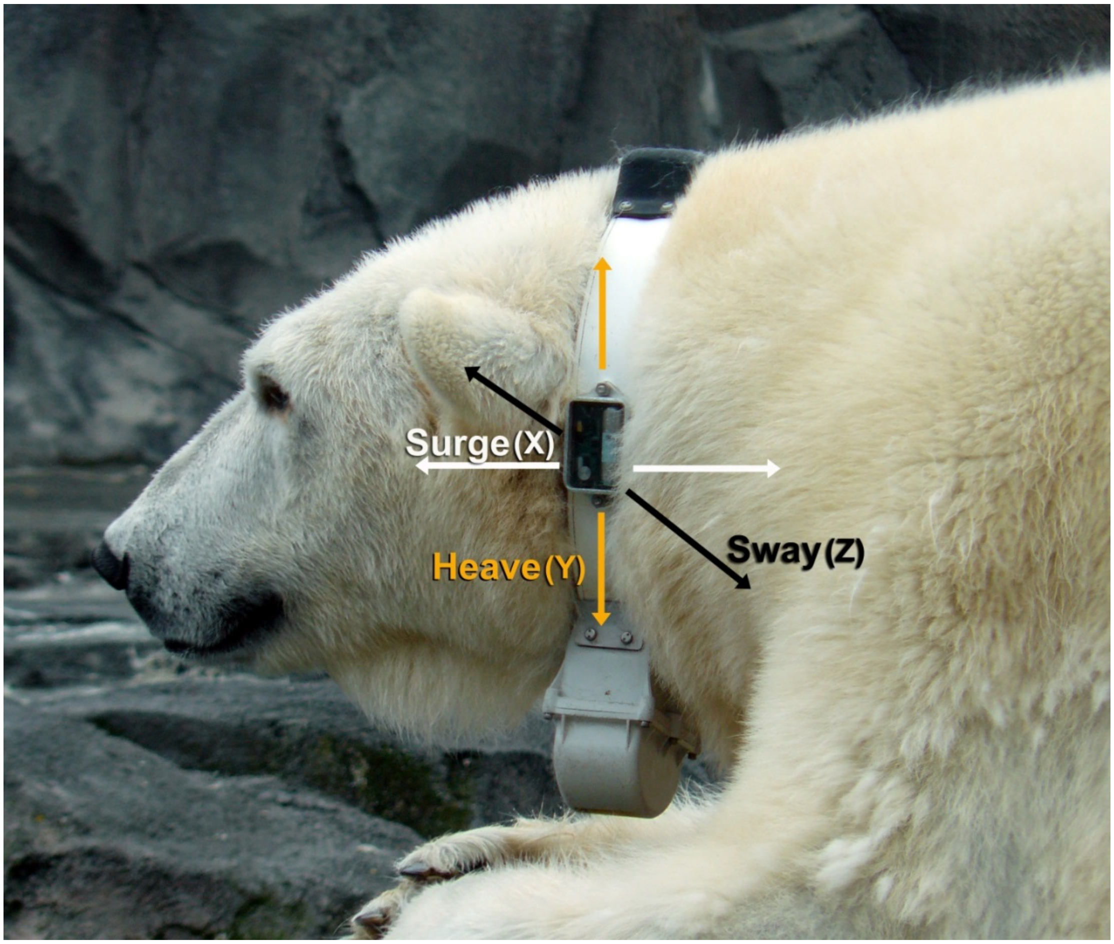

Figure 1.1. Orientation of an archival logger containing a tri-axial accelerometer attached to a collar for use on polar and grizzly bears.

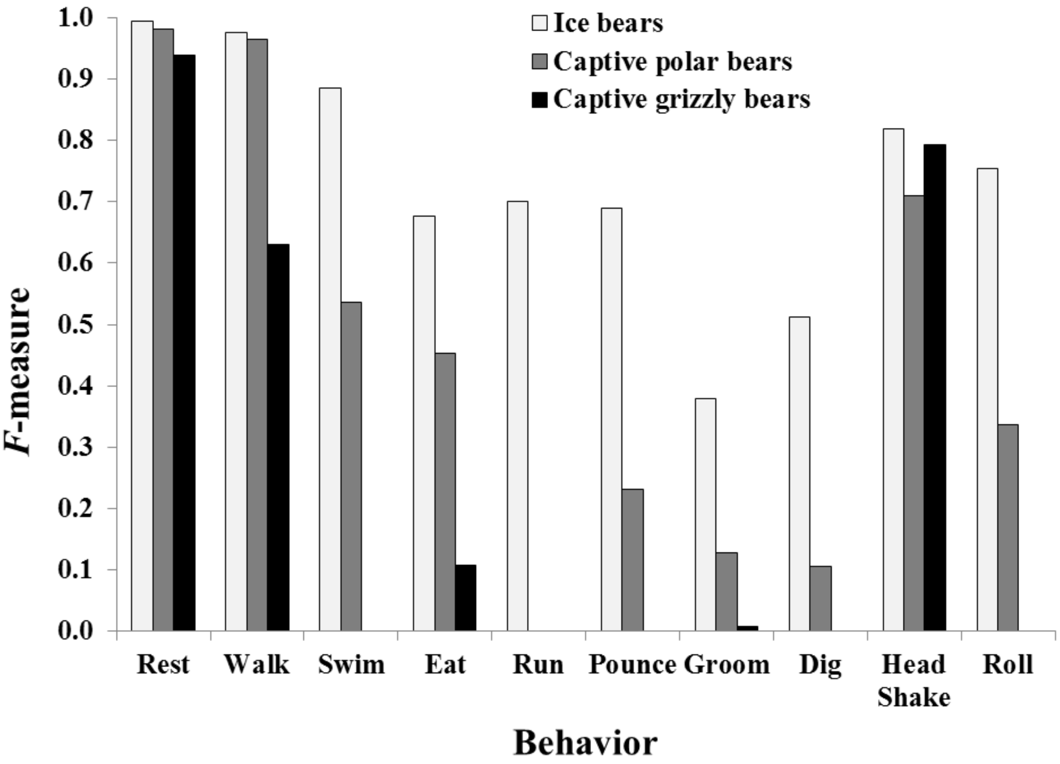

Figure 1.2. Ability (*F-measure*) of the random forest model to predict 10 behaviors of polar bears on the sea ice from 3 different training datasets of accelerometer data. Ice bears: polar bears on the sea ice of the southern Beaufort Sea.

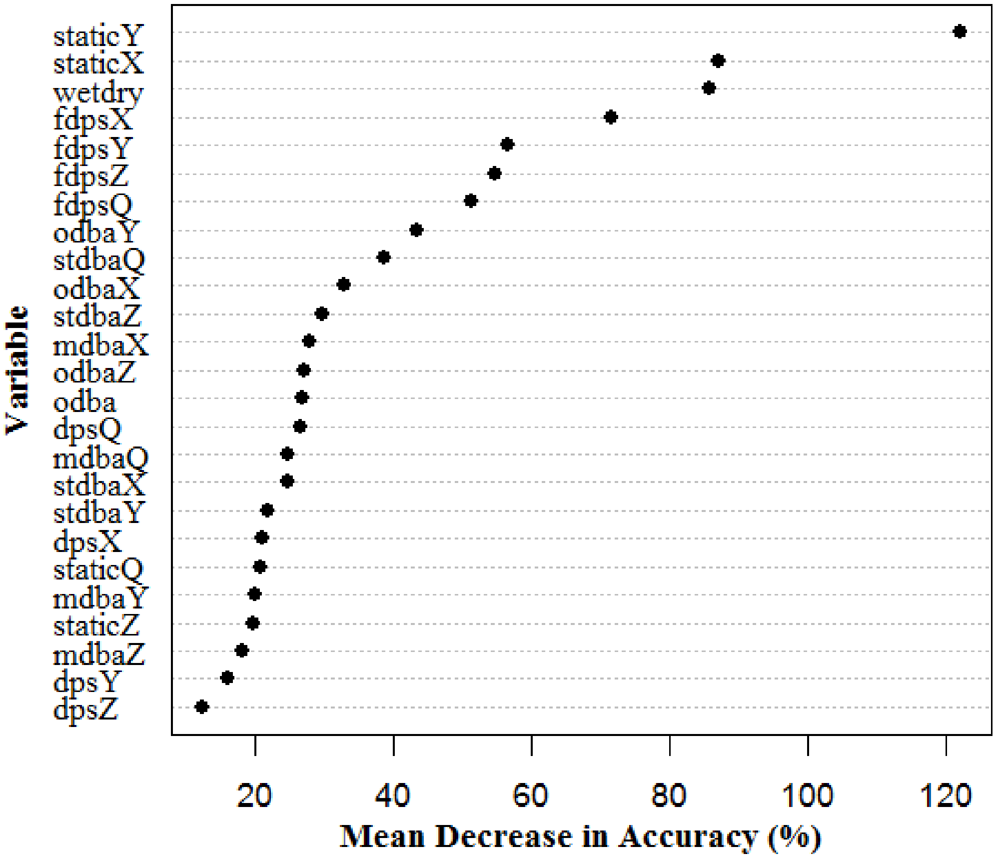

Figure 1.3. Variable importance plot from the random forest model of accelerometer data from polar bears on the sea ice. The importance plot provides a relative ranking of parameters in which higher values indicate parameters that contributed more toward classification accuracy. Mean decrease in accuracy is normalized by dividing by the standard errors of the parameters (i.e., *z*-score). See Table 1.3 for description of parameters.

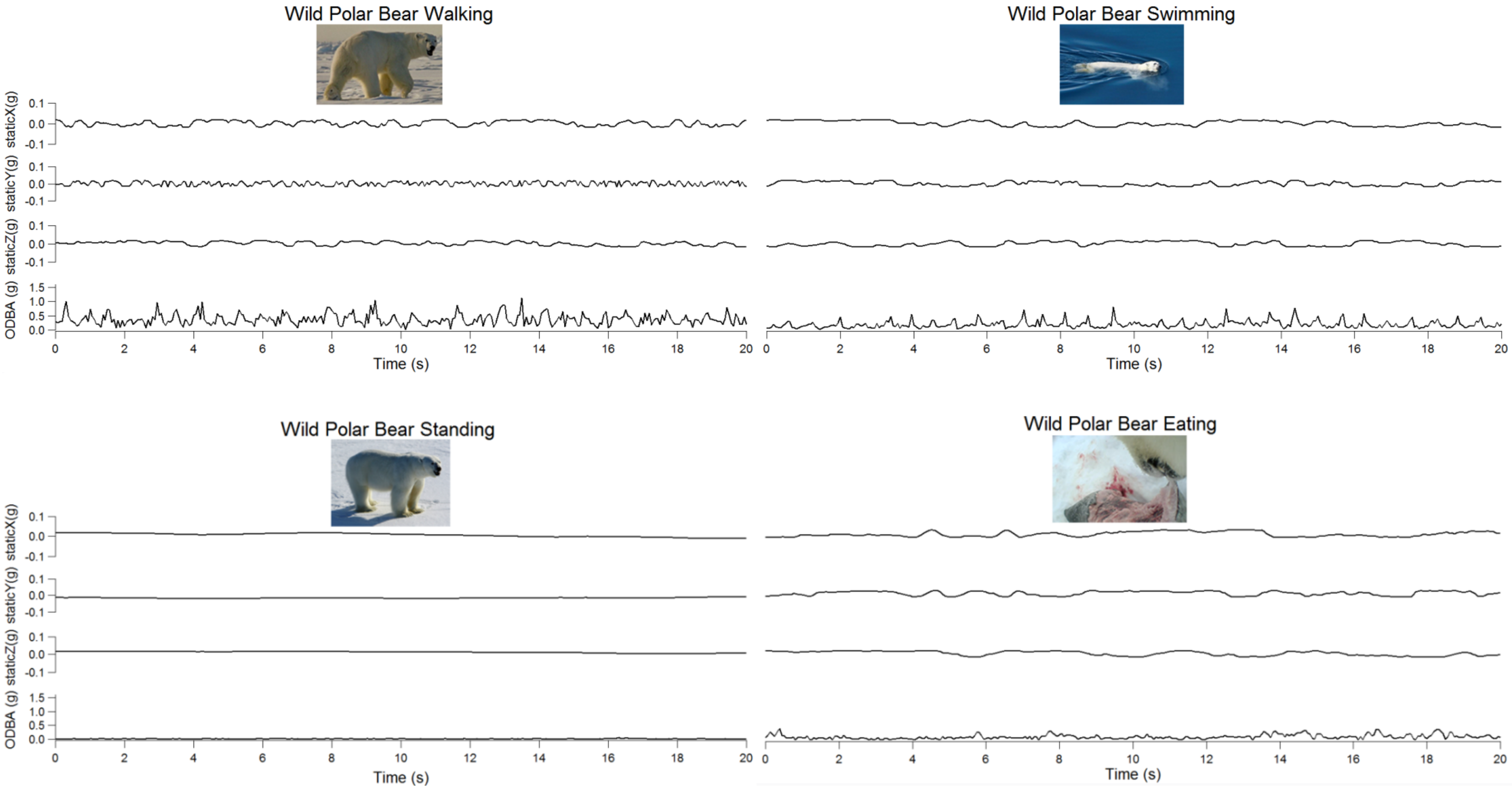

Figure 1.4. Accelerometer signatures of static acceleration in the surge (X), heave (Y), and sway (Z) directions and overall dynamic acceleration (ODBA) while walking, swimming, standing, and eating a seal from an adult female polar bear on the sea ice of the southern Beaufort Sea.

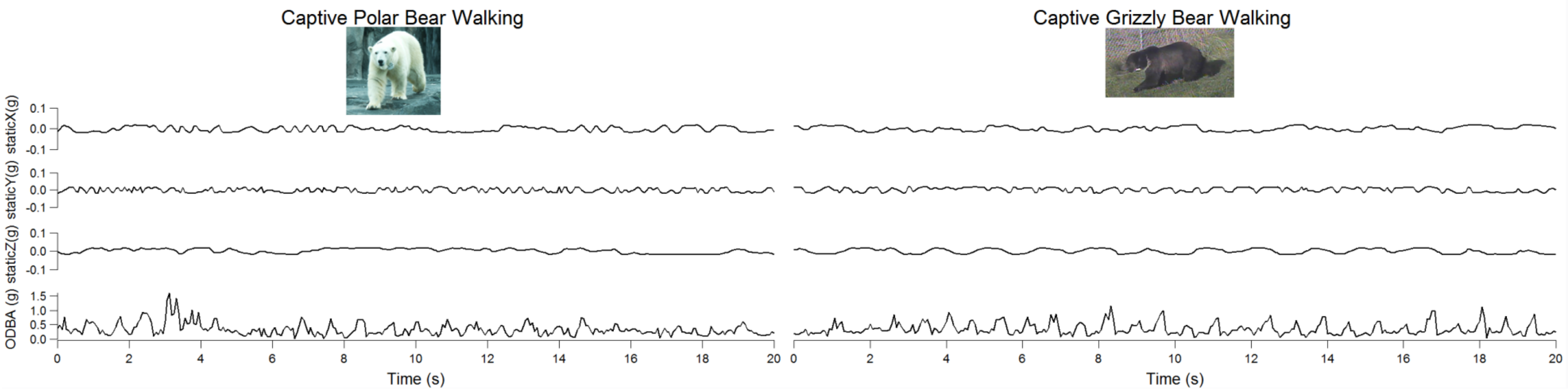

Figure 1.5. Accelerometer signatures of static acceleration in the surge (X), heave (Y), and sway (Z) directions and overall dynamic acceleration (ODBA) while walking from a captive adult female polar bear (left) compared to a captive adult female grizzly bear (right).

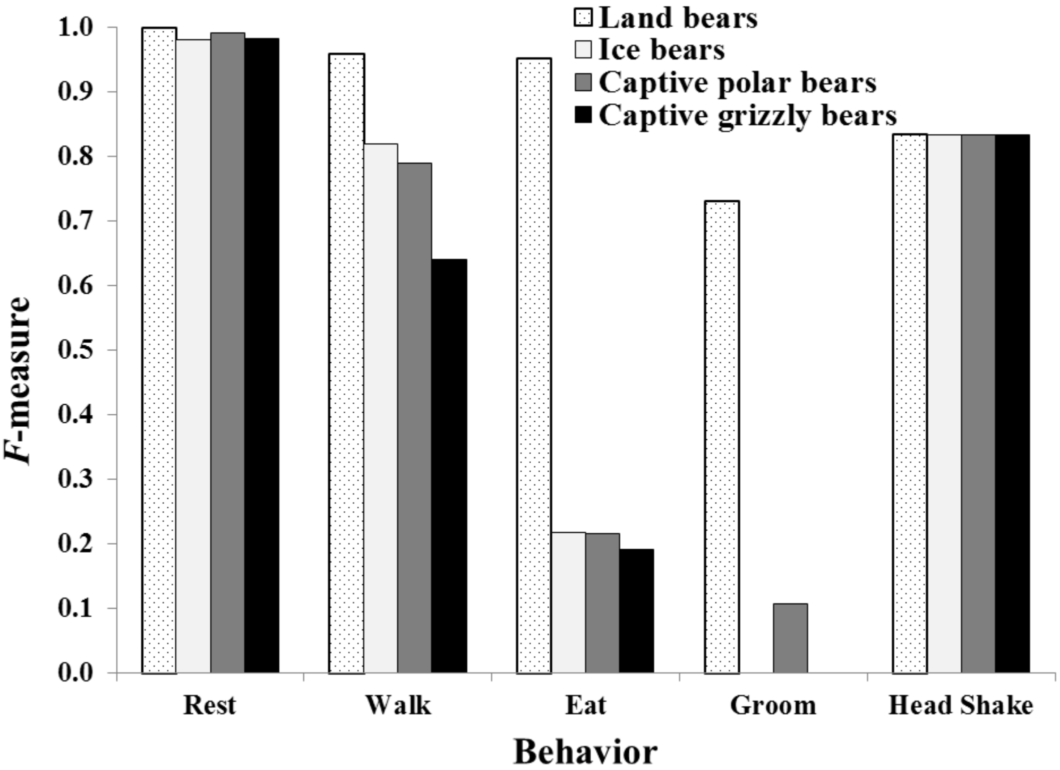

Figure 1.6. Ability (*F-measure*) of a random forest model to predict behaviors of polar bears on land from 4 different training datasets. Ice bears: polar bears on the sea ice of the southern Beaufort Sea. Land bears: polar bears on Akimiski Island, Nunavut.

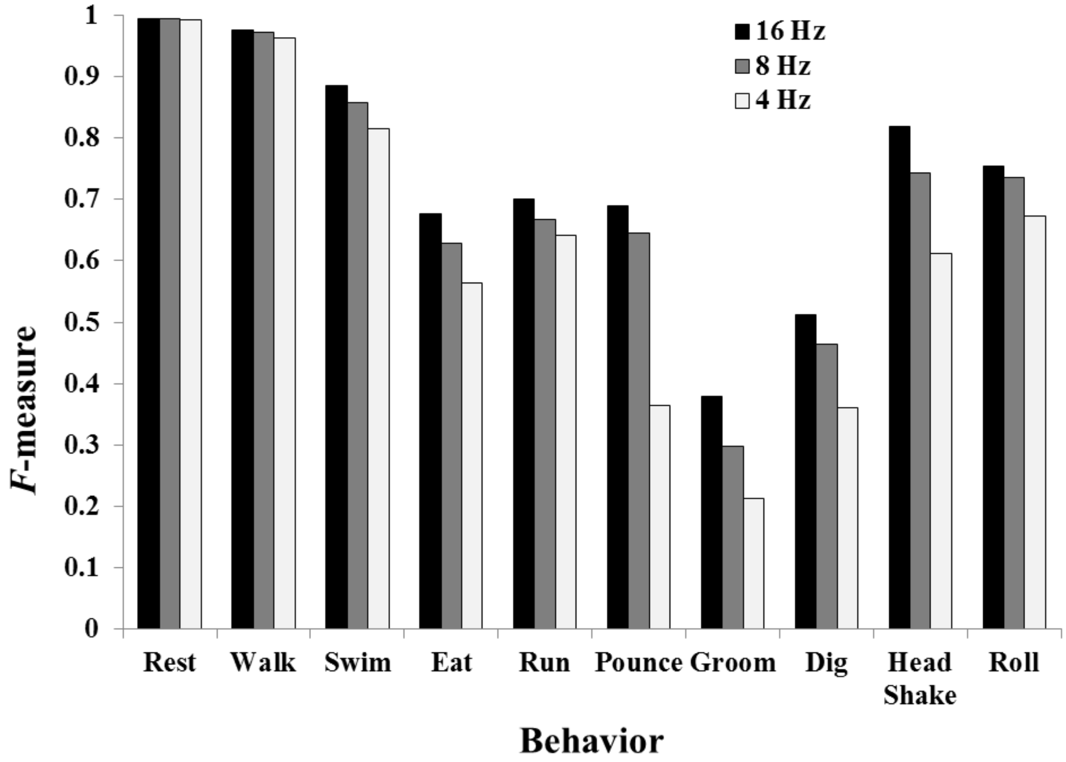

Figure 1.7. Ability (*F-measure*) of a random forest model to predict behaviors of polar bears on the sea ice using 3 different accelerometer sampling frequencies.

Chapter 2[‡]

Energetic costs of locomotion in bears: Is plantigrade locomotion energetically economical?

ABSTRACT

Ursids are the largest mammals to retain a plantigrade posture. This primitive posture has been proposed to result in reduced locomotor speed and economy relative to digitigrade and unguligrade species, particularly at high speeds. Previous energetics research on polar bears (*Ursus maritimus*) found locomotor costs were more than double predictions for similarly-sized quadrupedal mammals, which could be a result of their plantigrade posture or due to adaptations to their Arctic marine existence. To evaluate whether polar bears are representative of terrestrial ursids or distinctly uneconomical walkers, this study measured the mass-specific metabolism, overall dynamic body acceleration, and gait kinematics of polar bears and grizzly bears (*U. arctos*) trained to rest and walk on a treadmill. At routine walking speeds, I found polar bears and grizzly bears exhibited similar costs of locomotion and gait kinematics, but differing measures of overall dynamic body acceleration. Minimum cost of transport while walking in the two species (2.21 J kg^{-1} m^{-1}) was similar to predictions for similarly-sized quadrupedal mammals, but these costs doubled (4.42 J

[‡] A version of this chapter has been published as: Pagano, A.M., A.M. Carnahan, C.T. Robbins, M.A. Owen, T. Batson, N. Wagner, A. Cutting, N. Nicassio-Hiskey, A. Hash, and T.M. Williams. 2018. Energetic costs of locomotion in bears: Is plantigrade locomotion energetically economical? Journal of Experimental Biology 221:doi:10.1242/jeb.175372.

kg^{-1} m^{-1}) at speeds ≥ 5.4 km h^{-1}. Similar to humans, another large plantigrade mammal, bears appear to exhibit a greater economy while moving at slow speeds.

INTRODUCTION

A plantigrade posture in which the heel makes contact with the ground during a step is considered to be an ancestral form of locomotion (Lovegrove and Haines 2004). This posture has been shown to enhance locomotor economy while walking in humans, despite a reduced economy while running relative to digitigrade or unguligrade postures, which enable greater stride length and elastic storage (Carrier 2016). Members of the family Ursidae represent the largest mammals to have retained a plantigrade posture (Brown and Yalden 1973), which likely increases their dexterity for digging and climbing and enhances support for their large body mass (McLellan and Reiner 1994), but may impose a reduced energetic economy during locomotion (Lovegrove and Haines 2004, Shine et al. 2015).

Ursids represent a small family of large-bodied terrestrial mammals with a diverse range of diets from specialist carnivores, specialist herbivores, to generalist omnivores. Energetics research on ursids has largely focused on their abilities to reduce metabolism during hibernation (e.g., Watts et al. 1987, Watts and Cuyler 1988, Watts and Jonkel 1988, Tøien et al. 2011). Resting metabolic rates (RMRs) have also been examined in many ursids (Hurst 1981, Watts et al. 1987, McNab 1992, Tøien et al. 2011, Fei et al. 2016). Giant pandas (*Ailuropoda melanoleuca*) (Fei et al. 2016) and sloth bears (*Melursus ursinus*) (McNab 1992) exhibit RMRs 18% and 41% less than predictions for similarly-sized mammals (Kleiber 1975), while polar bears

(Hurst et al. 1991, Watts et al. 1991, Chapter 4) and black bears (*U. americanus*) (Tøien et al. 2011) exhibit RMRs 62% and 23% greater than predictions. This increased maintenance cost in polar bears, and to a lesser extent in black bears, is likely a result of their carnivorous diet, whereas giant pandas are a specialist herbivore and sloth bears an insectivore, both of which impose a lower energetic cost than carnivory (McNab 1986). Despite this understanding of baseline energetic costs in ursids, the energetic costs of locomotion have received less attention and has only been examined in polar bears, whose energetic cost of walking is more than twice that predicted for similarly-sized quadrupedal mammals (Øritsland et al. 1976, Hurst et al. 1982*a*, Watts et al. 1991). Yet, it remains unknown whether this high cost of transport is found across the Ursidae, potentially as a result of plantigrade locomotion, or whether polar bears are distinctly uneconomical walkers due to their carnivorous, marine, and semi-aquatic lifestyle (Williams 1999, Williams et al. 2002).

Despite the paraphyletic relationship between polar bears and grizzly bears (Talbot and Shields 1996), polar bears exhibit a number of physiological and behavioral adaptations from grizzly bears likely as a consequence of their marine existence. In addition to being the most carnivorous of the bear species (Stirling and Derocher 1990), polar bears have larger paws (potentially as an adaptation for swimming; (DeMaster and Stirling 1981), reduced forelimb dexterity (Iwaniuk et al. 2000), and exhibit distinct running kinematics using a transverse gallop compared to the rotary gallop of grizzly bears (Renous et al. 1988). Additionally, a study using tri-axial accelerometers tested the ability of data from grizzly bears to serve as proxies for discriminating basic behaviors in polar bears and found that data from grizzly bears failed to reliably discriminate polar bear behaviors (Chapter 1). This suggests differences in morphology and body movements between the two species while performing similar behaviors (Chapter 1).

To evaluate whether polar bears have uniquely high energetic costs of locomotion among ursids, I examine the energetic costs of resting and locomotion in polar bears and grizzly bears. I measure the oxygen consumption, overall dynamic body acceleration (ODBA), stride length, and stride frequency of captive polar bears and grizzly bears while at rest in a metabolic chamber and walking on a motorized treadmill. I test the hypotheses that polar bears differ from grizzly bears in their relationships between speed and oxygen consumption, ODBA, stride length, or stride frequency. I compare the costs of locomotion of polar bears and grizzly bears to similar measures from other plantigrade mammals, digitigrade carnivores, and to estimates based on allometric relationships. I further evaluate the relationship between oxygen consumption and ODBA in polar bears and grizzly bears as a proxy of energy expenditure. In other species, ODBA is strongly correlated with energy expenditure due to the relationship between acceleration and muscle contraction (Wilson et al. 2006, Gleiss et al. 2011), enabling the use of accelerometers to measure energy expenditure in free-ranging animals (e.g., Wilson et al. 2006, 2012, Halsey et al. 2009*a*, 2011*b*, Gómez Laich et al. 2011, Williams et al. 2014). For example, ODBA has been used to measure instantaneous energetics (e.g., Williams et al. 2014) and to evaluate the energy landscapes of wild animals (e.g., Wilson et al. 2012, Shepard et al. 2013). This is based on the assumption that movement is the primary factor influencing variability in energy expenditure (Costa and Williams 1999, Wilson et al. 2006, Gleiss et al. 2011). If such relationships are similar in ursids, it could provide a method to remotely measure their energy expenditure. Additionally, I assess the potential influence of differences in body composition on the oxygen consumption measurements taken from grizzly bears to evaluate whether differences in body fat or lean body mass strongly influence energy expenditure. Lastly, I evaluate the locomotor speeds of polar bears walking and running on the sea ice to assess whether preferred locomotor speeds in the wild conform to my energetic predictions.

MATERIALS AND METHODS

Experimental design

Oxygen consumption ($\dot{V}O_2$) was measured via open-flow respirometry, as well as stride frequency, stride length, and ODBA in polar bears and grizzly bears. Measurements were made within a sealed metabolic chamber (2.7 m × 0.9 m × 1.2 m) constructed of polycarbonate walls that were reinforced with a steel frame (Technical Services, Washington State University, Pullman, WA, USA) and mounted on the surface of a variable-speed treadmill (T1 Trotter horse treadmill, Horse Gym USA, LLC, Wellington, FL, USA). The body composition of grizzly bears was measured using deuterium oxide. The movement rates of free-ranging female polar bears were measured while walking and running on the sea ice of the Beaufort Sea.

Animals

One polar bear at the San Diego Zoo and 7 grizzly bears at Washington State University were used for metabolic, acceleration, and gait kinematic measurements (Table 2.1). Additionally, a polar bear at the Oregon Zoo was used for acceleration and gait kinematic measurements (Table 2.1). The polar bear at the San Diego Zoo was trained over 5 months and conditioned to rest while lying in sternal recumbency and to walk on the moving treadmill while receiving food (i.e., meat and fish) every 20 sec. The polar bear at the Oregon Zoo was trained over 8 months to walk on the moving treadmill while receiving food every 20 sec. The grizzly bears were similarly trained over 2 months and conditioned to rest while lying in sternal recumbency and walk on the moving treadmill while receiving food every 10–20 sec. Research was approved by the Animal Care and Use Committees of the University of California, Santa Cruz, the U.S. Geological Survey, Alaska Science Center, the San Diego Zoo Global, Oregon Zoo, and Washington State University (Protocols 04780 and 04952). Polar bear research was further authorized under U.S. Fish and Wildlife Service Marine Mammal Permit MA77245B.

To measure locomotor speeds in free-ranging bears, 1 subadult and 5 adult female polar bears without dependent young were captured on the sea ice of the Beaufort Sea in April 2015 and 2016. Polar bears were located from a helicopter and immobilized with a rapid-injection dart (Palmer Cap-Chur Equipment, Douglasville, GA) containing zolazepam-tiletamine (Telazol®) (Stirling et al. 1989). Procedures were approved by the Animal Care and Use Committees of the University of California, Santa Cruz and the U.S. Geological Survey, Alaska Science Center.

Research was authorized under U.S. Fish and Wildlife Service Marine Mammal Permit MA690038.

Metabolic measurements

$\dot{V}O_2$ measurements were collected over 6–13 min intervals with a minimum of 5 minutes of steady-state levels of behavior to ensure equilibration. For both species, at least 1 resting measurement was taken following an overnight fast to ensure a post-absorptive state. For the grizzly bears, a subsequent resting measurement was taken 3 hours after feeding to evaluate the potential effects of specific dynamic action on $\dot{V}O_2$ measurements. Food intake per session ranged from 728–963 g (polar bear) and 2000–2300 g (grizzly bears).

A vacuum pump (FlowKit Mass Flow Generator - 2000, Sable Systems International, Inc., Las Vegas, NV, USA) was used to draw air in along the lower edge of the treadmill at 700 L min^{-1} during measurements. Flow rates were monitored continuously and maintained oxygen levels ≥20% to avoid hypoxic conditions. Sub-samples of air from the exhaust port of the chamber were drawn through a series of 6 columns, filled with desiccant (Drierite, W. A. Hammond Drierite, Xenia, OH, USA), and scrubbed of carbon dioxide (Sodasorb, W.R. Grace & Co, Chicago, IL, USA) before entering the oxygen analyzer (Sable Systems International, Inc.). The percent of oxygen in the expired air was monitored continuously and recorded values once per second using Expedata Analysis software (Sable Systems International, Inc.). Air temperatures within the chamber ranged from 22.2–24.6°C ($\bar{x}$ = 23.9°C) for polar bears and 18.6–34.3°C ($\bar{x}$ = 28.9°C) for grizzly bears. I converted values to $\dot{V}O_2$

using equation 4B from Withers (Withers 1977) assuming a respiratory quotient of 0.78. All values were corrected to standard temperature and pressure, dry. The entire system was calibrated prior to measurements with dry ambient air (20.95% O_2) and periodically with dry N_2 gas (Fedak et al. 1981). Body mass was measured using a platform scale. I estimated net minimum cost of transport (COT_{MIN}) as the slope and postural cost of activity as the y-intercept of the relationship between $\dot{V}O_2$ (ml O_2 kg^{-1} s^{-1}) and speed (m s^{-1}) (Taylor et al. 1982). I estimated total cost of transport (COT_{TOT}) by dividing $\dot{V}O_2$ by speed.

Gait kinematics

I measured stride frequency (strides sec^{-1}) and stride length (m) at each speed using video from a high-speed camera (Panasonic, Lumix FZ300, 120 frames s^{-1}) and a high-definition video camera (Sony, HDR-CX260V, 1080 HD, 60p) positioned perpendicular to the treadmill and analyzed with video editing and motion analysis software (Corel Video Studio Pro X5, Corel Corp., Ottawa, Ontario, Canada; ProAnalyst, Xcitex, Woburn, MA, USA). Stride frequency was measured as the average interval for 25 cycles of the front right foot (Heglund and Taylor 1988).

Overall dynamic body acceleration

I mounted archival loggers (TDR10-X-340D, Wildlife Computers, Inc., Redmond, WA, USA) to the side of collars such that they were on the bears' left side of the neck (see Figure 1.1 in Chapter 1). Archival loggers measured tri-axial acceleration (m s^{-2}) at 16 Hz (range ±20 m s^{-2}) while bears were resting and walking within the metabolic chamber. I also included acceleration and $\dot{V}O_2$ measurements collected from the same polar bear (264 kg) at the San Diego Zoo while she rested during a previous study (Chapter 4). I estimated the $\dot{V}O_2$ of the polar bear at the Oregon Zoo based on the relationship between speed and $\dot{V}O_2$ derived below. I converted accelerometer measures from m s^{-2} to g (1 g = 9.81 m s^{-2}). I used a 2 s running mean of the raw acceleration data to calculate static acceleration (gravitational acceleration) and subtracted the static acceleration from the raw acceleration data to calculate dynamic acceleration (Wilson et al. 2006, Shepard et al. 2008). I calculated ODBA as the absolute sum of dynamic acceleration across the 3 axes (Wilson et al. 2006).

Body composition

I measured the body composition of the 7 grizzly bears via deuterium oxide (D_2O). I collected an initial blood sample to serve as a baseline measure of D_2O. I then injected each bear intravenously with a precisely weighed (± 0.01 g, Ohaus Scout Pro, Parsippany, NJ, USA) dose of 0.05 g/kg of 99.9% enriched D_2O (Cambridge Isotope Laboratories, Inc., Tewksbury, MA, USA) with NaCl added to make it 0.9% isotonic and sterilized using a 0.2 μ Millipore filter. On injection, the syringe was back washed with blood to ensure all D_2O had been injected into the bear. For non-anesthetized bears, I collected a final blood sample 60 minutes after the injection of D_2O to allow isotope equilibration (Rigano et al. 2017). For anesthetized bears, I collected a final blood sample 120 minutes after the injection of D_2O to allow isotope equilibration (Farley and Robbins, 1994). I collected blood in evacuated tubes without anticoagulants and centrifuged tubes to separate serum from red blood cells. I stored serum frozen in cryogenic vials at -20°C until analysis.

Serum samples were analyzed for D_2O concentration (Metabolic Solutions, Inc., Nashua, NH, USA). I calculated total body water as the ratio of the amount of D_2O injected to the concentration of D_2O in the body at equilibration per the plateau method (Speakman 1997, equation 17.11). I used measures of total body water to determine measures of total body fat based on Farley and Robbins (1994), where: % total body fat = 96.85 – 1.33×(% total body water). Lean body mass was calculated by subtracting total body fat from body mass.

Preferred locomotor speeds

I measured the movement rates (km hr^{-1}) of 6 female polar bears over 3–13 days while walking or running on the sea ice. Movement rates were derived from global positioning system (GPS) collars (Exeye, LLC., Bristow, VA) with a GPS fix rate every 5 or 10 minutes. Location data were transmitted via the Iridium satellite system. I used a continuous time correlated random walk (CRAWL) model (Johnson et al. 2008, Johnson 2016) in program R (R Core Team 2014) to predict locations on a 10 minute interval based on GPS locations. The CRAWL model accounts for variable location quality and sampling intervals and I assigned GPS location data an accuracy of 30 m (Frair et al. 2010). I calculated the minimum distance travelled between two successive predicted locations as the great-circle distance (i.e., distance accounting for the earth’s curvature), and calculated movement rate by dividing distance by the duration between predicted locations (i.e., 10 minutes) in SAS (version 9.3, SAS Institute Inc., Cary, NC). I identified walking and running movements based on archival loggers (TDR10-X-340D, Wildlife Computers, Inc.) attached to the GPS collars, which measured tri-axial acceleration (m s^{-2}) continuously at 16 Hz (range ±20 m s^{-2}). Walking and running were discriminated within the accelerometer data using a random forest model (Breiman 2001) in program R (RandomForest package, (R Core Team 2014) as described in Chapter 1. I linked these accelerometer-derived behaviors with their corresponding predicted location data by calculating the percent time spent walking or running between predicted locations (i.e., 10 minutes) in SAS. If ≥ 95% of the time between predicted locations was classified as walking or running, I considered the movement rate during this interval to be indicative of walking or running.

Analyses

I combined the polar bear $\dot{V}O_2$ measurements while walking collected in this study with $\dot{V}O_2$ measures similarly recorded using open-flow respirometry from 7 sub-adult polar bears (2 females and 5 males) walking and running walking on a treadmill that ranged in body mass from 110–235 kg (Øritsland et al. 1976, Hurst et al. 1982*a*, *b*, Watts et al. 1991). I used least-squares linear regression to evaluate the relationship between $\dot{V}O_2$ and speed. Although Hurst et al. (1982*a*) proposed a curvilinear relationship between $\dot{V}O_2$ and speed in polar bears as a result of measurements at speeds ≥ 5.4 km hr^{-1}, I evaluated $\dot{V}O_2$ measurements at speeds ≥ 5.4 km hr^{-1} separately as data from free-ranging polar bears indicate they rarely walk this fast (Whiteman et al. 2015) and the predicted gait transition speed for 100–250 kg animals is 5.7–5.3 km hr^{-1} (Heglund and Taylor 1988). I used analysis of covariance (ANCOVA) to evaluate whether the relationships between $\dot{V}O_2$ and speed differed between speeds < 5.4 and ≥ 5.4 km hr^{-1}. For grizzly bears, I similarly used least-squares linear regression to evaluate the relationship between $\dot{V}O_2$ and speed. I used ANCOVA to evaluate whether the intercepts and slopes differed between polar bears and grizzly bears in their relationships between $\dot{V}O_2$ and speed. I further used least-squares linear regression to evaluate the relationship between $\dot{V}O_2$ and ODBA and speed and ODBA and used ANCOVA to evaluate whether the relationship between $\dot{V}O_2$ and ODBA differed between species. I used ANCOVA to evaluate whether the relationship between stride frequency and speed as well as stride length and speed differed between species. I used a repeated measures ANOVA to evaluate the effect of age, body mass, lean body mass, fat mass, and specific dynamic action on grizzly bear $\dot{V}O_2$. We calculated the mean and distribution of walking and running speeds measured in free-ranging female polar bears on the sea ice. All analyses were conducted in program R (R Core Team 2014) and differences of $P \leq 0.05$ were considered significant.

RESULTS

Metabolic rates

RMRs of the adult female polar bear averaged 0.27 ml O_2 g^{-1} h^{-1} (SE = 0.01, n = 5) with a low of 0.25 ml O_2 g^{-1} h^{-1}. In combination with measures previously collected from sub-adult male and female polar bears (Hurst 1981, Watts et al. 1991), the post-absorptive RMR of polar bears averages 0.23 ml O_2 g^{-1} h^{-1} (SE = 0.02, n = 6).

Grizzly bears remained active during resting measurements (e.g., head and limb movements) and, thus, their RMRs are akin to zero velocity measurements (i.e., y-intercept) relating to the postural effect of activity (Taylor et al. 1970, Schmidt-Nielsen 1972). Zero-velocity metabolic rates of the grizzly bears while post-absorptive averaged 0.55 ml O_2 g^{-1} h^{-1} (SE = 0.11, $n = 5$) with a low of 0.30 ml O_2 g^{-1} h^{-1}. Zero velocity metabolic rates of the grizzly bears 3 hours postprandial averaged 0.50 ml O_2 g^{-1} h^{-1} (SE = 0.04, $n = 5$) with a low of 0.36 ml O_2 g^{-1} h^{-1}.

I found a significant difference in the slope ($F_{1,107} = 6.87$, $P = 0.01$) and intercept ($F_{1,108} = 58.21$, $P < 0.001$) in the relationship between $\dot{V}O_2$ and speed for bears walking < 5.4 km h^{-1} (Figure 2.1A) and bears walking ≥ 5.4 km h^{-1} (Figure 2.2A). Polar bear metabolic rates while walking < 5.4 km h^{-1} exhibited a linear relationship between $\dot{V}O_2$ (ml O_2 g^{-1} h^{-1}) and speed (km h^{-1}): $\dot{V}O_2 = 0.44 + 0.12\times\text{speed}$ ($r^2 = 0.42$, $P < 0.001$, $n = 35$) and averaged 1.5× rates predicted for terrestrial carnivores based on body mass and speed (Taylor et al. 1982). At speeds ≥ 5.4 km h^{-1}, polar bear $\dot{V}O_2$ exhibited a linear relationship with speed: $\dot{V}O_2 = 0.41 + 0.22\times\text{speed}$ ($r^2 = 0.32$, $P < 0.001$, $n = 37$, Figure 2.2A). At speeds ≤ 4.6 km h^{-1}, grizzly bear $\dot{V}O_2$ similarly exhibited a linear relationship with speed: $\dot{V}O_2 = 0.50 + 0.13\times\text{speed}$ ($r^2 = 0.82$, $P < 0.001$, $n = 39$) and averaged 1.7× rates predicted for terrestrial carnivores based on body mass and speed (Taylor et al. 1982). I found no difference in the slope ($F_{1,70} = 0.06$, $P = 0.80$) or intercept ($F_{1,71} = 3.56$, $P = 0.06$) in the relationship between $\dot{V}O_2$ and speed between the two species at speeds < 5.4 km h^{-1}. Combining data from the 2 species, at speeds < 5.4 km h^{-1} I found a linear relationship between $\dot{V}O_2$ and speed: $\dot{V}O_2 = 0.50 + 0.11\times\text{speed}$ ($r^2 = 0.64$, $P < 0.001$, $n = 74$, Figure 2.1A). Postural cost of activity (i.e., y-intercept) was 0.50 ml O_2 g^{-1} h^{-1} or 2.2 times greater than predictions based on body mass (Taylor et al. 1982). Net COT_{MIN} was 0.11 ml O_2 kg^{-1} m^{-1} (2.21 J kg^{-1} m^{-1}), or 1.1 times greater than predictions based on body mass (Figure 2.3) (Taylor et al. 1982). COT_{TOT} was lowest at 1.2 m s^{-1} (4.3 km h^{-1}) (Figure 2.4). At speeds ≥ 5.4 km h^{-1}, net COT_{MIN} was 0.22 ml O_2 kg^{-1} m^{-1} (4.42 J kg^{-1} m^{-1}) (Figure 2.3).

Gait kinematics

Bears exhibited plantigrade gaits with the toes and metatarsals flat on the ground (Figure 2.5). I found no difference in the slope ($F_{1,28} = 0.93$, $P = 0.34$) or intercept ($F_{1,29} = 2.43$, $P = 0.13$) in the relationship between stride frequency and speed or stride length and speed ($F_{1,28} = 2.26$, $P = 0.14$; $F_{1,29} = 2.08$, $P = 0.16$; respectively) between the two species. Stride frequency (strides s^{-1}) increased linearly with speed: Stride frequency = $0.21 + 0.16\times\text{speed}$ ($r^2 = 0.88$, $P < 0.001$, $n = 32$, Figure 2.1B). Stride length (m) increased linearly with speed: Stride length = $0.71 + 0.15\times\text{speed}$ ($r^2 = 0.76$, $P < 0.001$, $n = 32$, Figure 2.1C).

Overall dynamic body acceleration

The relationship between $\dot{V}O_2$ (ml O_2 g^{-1} h^{-1}) and ODBA (g) differed in the slope ($F_{1,29} = 5.49$, $P = 0.03$) and intercept ($F_{1,30} = 4.92$, $P = 0.03$) between the species. This difference appeared to be predominantly driven by differences in dynamic body acceleration in the sway (z) dimension (Figure 2.6). Polar bear $\dot{V}O_2$ increased linearly as a function of ODBA: $\dot{V}O_2 = -0.90 + 12.33\times\text{ODBA}$ ($r^2 = 0.84$, P

< 0.001, $n = 18$, Figure 2.7A). Polar bear speed was also strongly predicted by ODBA: Speed = -2.92 + 16.25×ODBA ($r^2 = 0.92$, $P < 0.001$, $n = 18$). Grizzly bear $\dot{V}O_2$ increased linearly as a function of ODBA: $\dot{V}O_2 = -0.05 + 2.03 \times \text{ODBA}$ ($r^2 = 0.76$, $P < 0.001$, $n = 15$, Figure 2.7B). Grizzly bear speed was also strongly predicted by ODBA: Speed = -4.62 + 16.12×ODBA ($r^2 = 0.81$, $P < 0.001$, $n = 15$).

Body composition

Grizzly bears exhibited little variation in body composition (Fig. S1). On average, grizzly bears consisted of 19.6% total body fat (s.e.m. = 1.5, $n = 7$) and 58.1% total body water (s.e.m. = 1.1, $n = 7$). Body mass ($F_{1,12} = 41.3$, $p < 0.001$), age ($F_{1,12} = 8.4$, $p = 0.01$), and specific dynamic action ($F_{1,12} = 12.4$, $p = 0.004$) had significant effects on zero velocity metabolic rates of grizzly bears, but not lean body mass ($F_{1,12} = 0.03$, $p = 0.86$) or fat mass ($F_{1,12} = 0.003$, $p = 0.95$).

Preferred locomotor speeds

Walking and running speeds of female polar bears on the sea ice over 10 minute intervals averaged 3.4 km h^{-1} (SE = 0.04, $n = 533$, Figure 2.2B) and ranged from 0.4 to 10.0 km h^{-1}. Only 3% of these movements were ≥ 5.4 km h^{-1} (Figure 2.2B).

DISCUSSION

Contrary to previous energetic studies on polar bears, the results from this study indicate that polar bears and grizzly bears are energetically similar to other quadrupedal mammals while walking. In humans, a plantigrade posture while walking has been shown to reduce the cost of transport relative to a digitigrade posture, but incurs a 61% increase in cost of transport while running (Cunningham et al. 2010). The results from this study similarly indicate at routine walking speeds both polar bears and grizzly bears exhibit costs of transport that are similar to predictions from other quadrupedal mammals based on their body mass (Taylor et al. 1982), but at speeds ≥ 5.4 km h^{-1} costs of transport doubled, greatly exceeding predictions.

Hurst et al. (1982*a*) proposed a curvilinear relationship between speed and energy expenditure in polar bears as a result of these disproportionately high energetic costs at speeds ≥ 5.4 km h^{-1}. However, data from free-ranging polar bears indicate they rarely move this fast (Figure 2.2B, (Whiteman et al. 2015), which suggests these speeds are likely non-preferred and may require an uneconomical gait. I found total cost of transport was lowest at 4.3 km h^{-1}, which is almost 1 km h^{-1} greater than mean walking speeds measured in polar bears on the sea ice over 10 minute periods. Additionally, field movements would be expected to impose greater energetic costs relative to movements on a treadmill (Bidder et al. 2017). Shine et al. (2015) documented a lack of a trotting gait in grizzly bears and reported transition speeds of ≥ 7.2 km h^{-1} for running walks and ≥ 10.8 km h^{-1} for canters. Walking involves storing and recovering energy with each stride via an exchange between gravitational-potential and kinetic energies through an inverted pendulum (Cavagna et al. 1977). However, the benefits of these pendulum mechanics decline at both low and high speeds (Cavagna et al. 1977). At high speeds, animals can trot, run, or hop, which allows energy to be conserved through elastic energy recovery (Cavagna et al. 1977). Yet, given their plantigrade posture, bears would be expected to have reduced energy-savings from elastic energy recovery relative to unguligrade or digitgrade mammals (Reilly et al. 2007, Cunningham et al. 2010). In humans, plantigrade locomotion enhances pendular mechanics and reduces ground collisional losses in kinetic energy while walking, at the expense of reduced elastic storage at higher speeds (Cunningham et al. 2010). At present, no data exist on the mechanics of polar bears at speeds between 5.4 and 7.2 km h^{-1} to better evaluate the causes of these disproportionate energetic costs, and $\dot{V}O_2$ of grizzly bears has not been examined at speeds > 4.6 km h^{-1}. Although polar bears seldom walk at these speeds in the wild (Figure 2.2B, Whiteman et al. 2015), future research evaluating the gait kinematics and cost of transport of bears at speeds ≥ 5.4 km h^{-1} would better elucidate the aerobic performance of ursids compared to other quadrupedal mammals.

At routine walking speeds, polar bears and grizzly bears exhibited similar energetic costs and gait kinematics. Despite their evolutionary divergence from grizzly bears, which has enabled polar bears to exist within the Arctic marine environment and facilitated abilities to swim long distances (Pagano et al. 2012, Pilfold et al. 2017), these adaptations appear to have had little effect on their costs of transport while walking compared to their closest living relative. This result is contrary to most semi-aquatic mammals that have higher costs of transport than strict terrestrial or aquatic mammals (Williams 1999, Williams et al. 2002), and suggests that polar bears are primarily adapted for walking and may incur high energetic costs while swimming (Durner et al. 2011, Griffen 2018).

Despite walking costs that were similar to those of other quadrupedal mammals, both polar bears and grizzly bears have postural costs that are more than double predictions based on other quadrupedal mammals (Taylor et al. 1982). This result is consistent with high resting metabolic rates (Hurst et al. 1991, Watts et al. 1991, Chapter 4) and high field metabolic rates in polar bears (Chapter 4). Taylor et al. (1970) found postural costs ranged from 1.3 to 2.1 times RMR in a variety of terrestrial mammals and Cavagna et al. (1977) proposed that this elevated cost may reflect the cost of lifting the center of mass against gravity. However, the postural costs I found are greater than those reported in other large terrestrial mammals. For example, in elephants (*Elephas maximus*), postural costs were 1.4 times greater than predictions (Langman et al. 2012), while in pumas (*Puma concolor*) postural costs were 1.6 times greater than predictions (Williams et al. 2014). Hence, this increased postural cost in polar bears and grizzly bears may in part be a result of their plantigrade posture as more erect limb postures (e.g., digitigrade and unguligrade) are known to have lower muscle mass and greater effective mechanical advantage (Biewener 1989, Reilly et al. 2007). I recommend further research explore the potential causes of these high postural costs in polar bears and grizzly bears. These high costs of activity have important energetic implications for free-ranging polar bears, which appear to be increasing their movement and activity rates in response to climate change (Durner et al. 2017).

Similar to behavior discrimination using tri-axial accelerometers (Chapter 1), I found the relationship between ODBA and $\dot{V}O_2$ differed between species. This difference appeared to be primarily driven by differences in the sway (z) dimension between species (Figure 2.6C), which suggests greater side-to-side movement by the grizzly bears while walking. Yet, such movements did not appear to influence the gait kinematics or locomotor costs between species. Since the accelerometers in this study were attached to collars on the neck, these movements may reflect differences in head and neck motions between species rather than limb or center of mass movements. Halsey et al. (2009*b*) found body mass explained most of the variation in the relationship between $\dot{V}O_2$ and ODBA among species. The adult female grizzly bears wearing accelerometers in this study differed by an average of 89 kg from the adult female polar bears wearing accelerometers, which may have also influenced their side-to-side movements. The results of this study support Halsey et al.'s (2009*b*) finding that the relationship between ODBA and $\dot{V}O_2$ is species-specific. I recommend further evaluation of the effect of body mass on the relationship between ODBA and $\dot{V}O_2$ in ursids. In particular, ursids are known for extreme seasonal fluctuations in body mass as a result of changes in food availability and winter dormancy (Nelson et al. 1983) and such changes may affect the relationship between ODBA and $\dot{V}O_2$ even on an intraspecific level. Furthermore, the relationships I derived between ODBA and $\dot{V}O_2$ resulted in negative intercepts for both species, which suggests that these relationships need to be further developed in order to use ODBA as a proxy for energy expenditure in these species.

Polar bears and grizzly bears put on the majority of their body fat from the late spring to early fall and the data in this study were collected prior to the onset of considerable fat accumulation. I found little variability in the body composition of the grizzly bears measured in this study and no effect of lean body mass or fat mass on zero velocity $\dot{V}O_2$ measures. I further found little difference in grizzly bear $\dot{V}O_2$ measures based on whether bears were post-absorptive or 3 hours postprandial, which suggests that specific dynamic action had little effect on metabolic measurements. Although measurements of the body composition of the polar bears in this study were not feasible, the body composition of grizzly bears were similar to the body composition of wild polar bears in the spring (Pagano et al. 2017) and wild grizzly bears in the spring (Hilderbrand et al. 2000) and thus reflect costs when bears are in lower states of fat storage. Results from northern elephant seal pups (*Mirounga angustirostris*) indicate little effect of storage fat on energy expenditure and indicate lean body mass to be a stronger predictor of changes in $\dot{V}O_2$ than body mass (Rea and Costa 1992). Fat mass similarly had little effect on basal metabolism in adult harp seals (*Pagophilus groenlandicus*) (Aarseth et al. 1999) or RMR in humans (Segal et al. 1989). In dogs, lean body mass had a stronger effect on RMRs than fat mass, but both effects were significant (Speakman et al. 2003). These results suggest that as bears accumulate body fat over their annual cycle they may not experience a commensurate increase in energy expenditure (Molnár et al. 2009). I recommend further research specific to ursids better elucidate this relationship.

Polar bears and grizzly bears are known to travel extensive distances and have large home ranges relative to other mammals (Ferguson et al. 1999, McLoughlin et al. 1999, McLoughlin and Ferguson 2000), yet they are primarily ambush and opportunistic predators that typically catch prey through sit-and-wait and stalk behaviors rather than chasing down prey (Stirling 1974, Stirling and Derocher 1990, Garneau et al. 2007, Chapter 4). The results from this study provide the physiological basis for these seemingly contradictory behaviors. Both species exhibit economical costs of walking, which is facilitated by their plantigrade posture. However, like humans, this comes at the expense of a less economical cost while moving at higher speeds. Observations of polar bears chasing down flightless geese (Iles et al. 2013) have inspired analyses, which found this hunting strategy to be energetically profitable (Gormezano et al. 2016). Nevertheless, the results from this study highlight the elevated energetic demands for polar bears to chase down their prey compared to traditional sit-and-wait tactics. This reinforces the importance of Arctic sea ice to enable polar bears to efficiently capture prey.

Table 2.1. Summary of animals used in this study.

Species & Individual	**Sex**	**Age**	**Body Mass (kg)**	**Location**
Polar Bear 1	Female	31	242	Oregon Zoo
Polar Bear 2	Female	16	235	San Diego Zoo
Grizzly Bear 1	Male	15	253	Washington State University
Grizzly Bear 2	Male	15	239	Washington State University
Grizzly Bear 3	Female	14	164	Washington State University
Grizzly Bear 4	Female	12	143	Washington State University
Grizzly Bear 5	Female	12	142	Washington State University
Grizzly Bear 6	Male	2	126	Washington State University
Grizzly Bear 7	Female	2	95	Washington State University

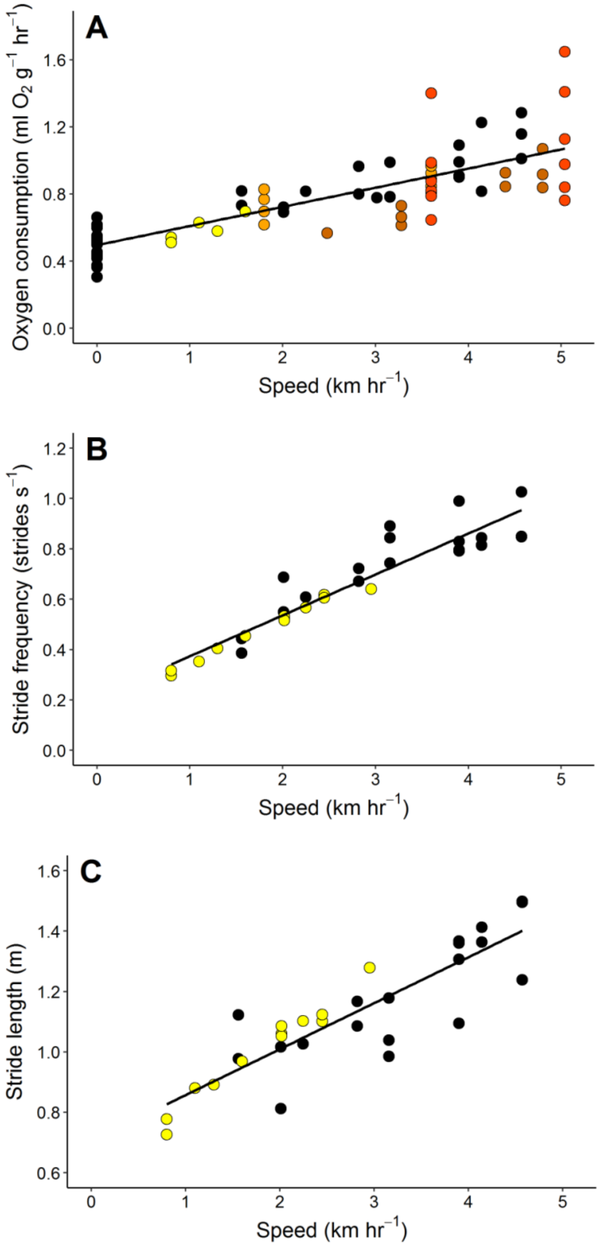

Figure 2.1. Relationship between oxygen consumption, gait kinematics, and locomotor speed in polar bears and grizzly bears. A. Least-squares regression (solid line) of mass-specific oxygen consumption in relation to locomotor speed for polar bears and grizzly bears on a treadmill. Points represent individual steady-state measurements for polar bears (yellow circles, present study; orange circles, (Hurst et al. 1982*a*); dark-orange circles, (Øritsland et al. 1976); orange-red circles, (Watts et al. 1991)) and grizzly bears (black circles). **B.** Least-squares regression (solid line) between stride frequency and speed in polar bears (yellow circles) and grizzly bears (black circles. **C.** Least-squares regression (solid line) between stride length and speed in polar bears (yellow circles) and grizzly bears (black circles).

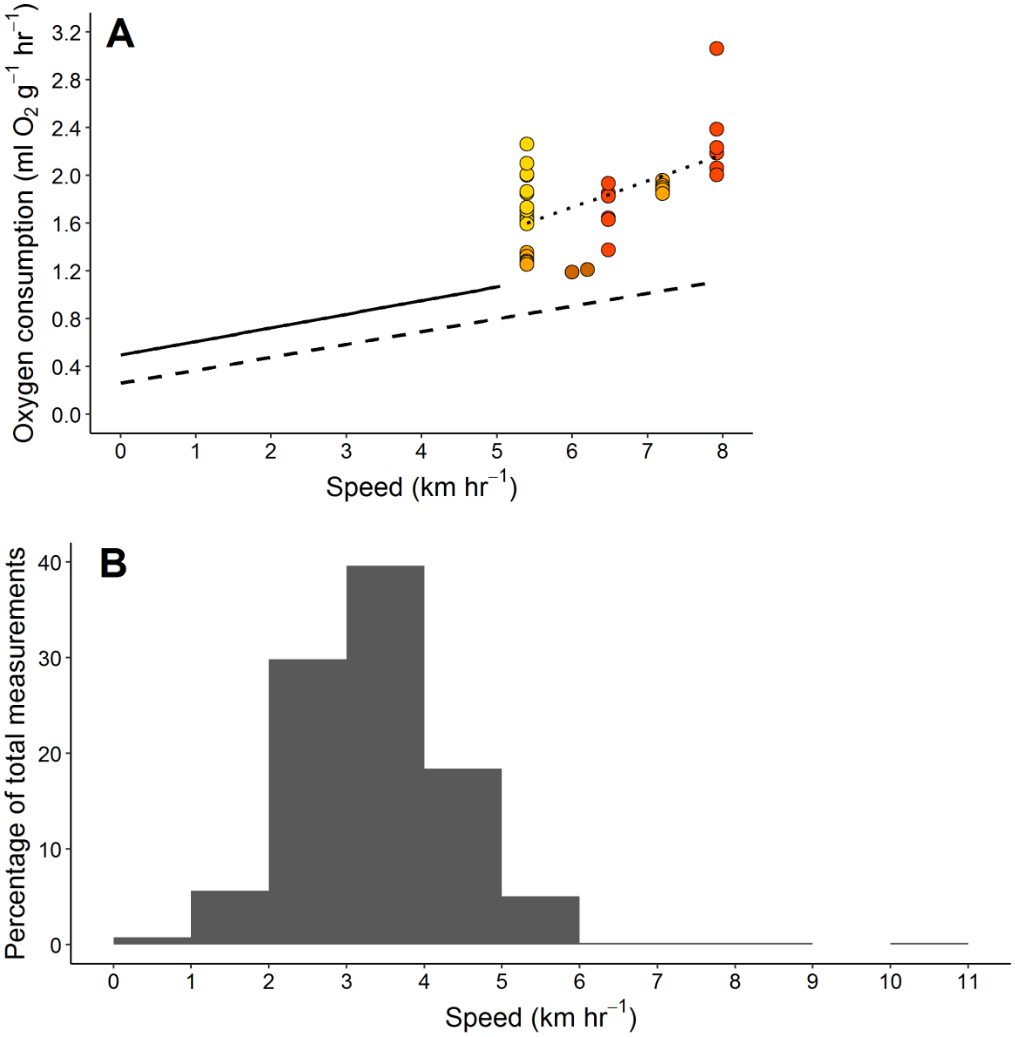

Figure 2.2. Relationship between oxygen consumption and locomotor speed for bears moving on a treadmill and locomotor speeds of free-ranging polar bears while walking and running on the sea ice. **A.** Mass-specific oxygen consumption in relation to locomotor speed. Points represent individual steady-state measurements for polar bears (orange circles, (Hurst et al. 1982*a*); yellow circles, (Hurst et al. 1982*b*); dark-orange circles, (Øritsland et al. 1976); orange-red circles, (Watts et al. 1991)). The solid line is the least-squares regression from polar bears and grizzly bears at < 5.4 km h^{-1} (Figure 2.1A) and the dotted line is the least-squares regression from polar bears at ≥ 5.4 km h^{-1} (see text for regression statistics). The dashed line is the predicted relationship derived from other terrestrial carnivores (Taylor et al. 1982). **B.** Frequency distribution of walking and running speeds over 10 minute intervals from 6 female polar bears on the sea ice of the Beaufort Sea in April 2015 and 2016 ($n = 533$).

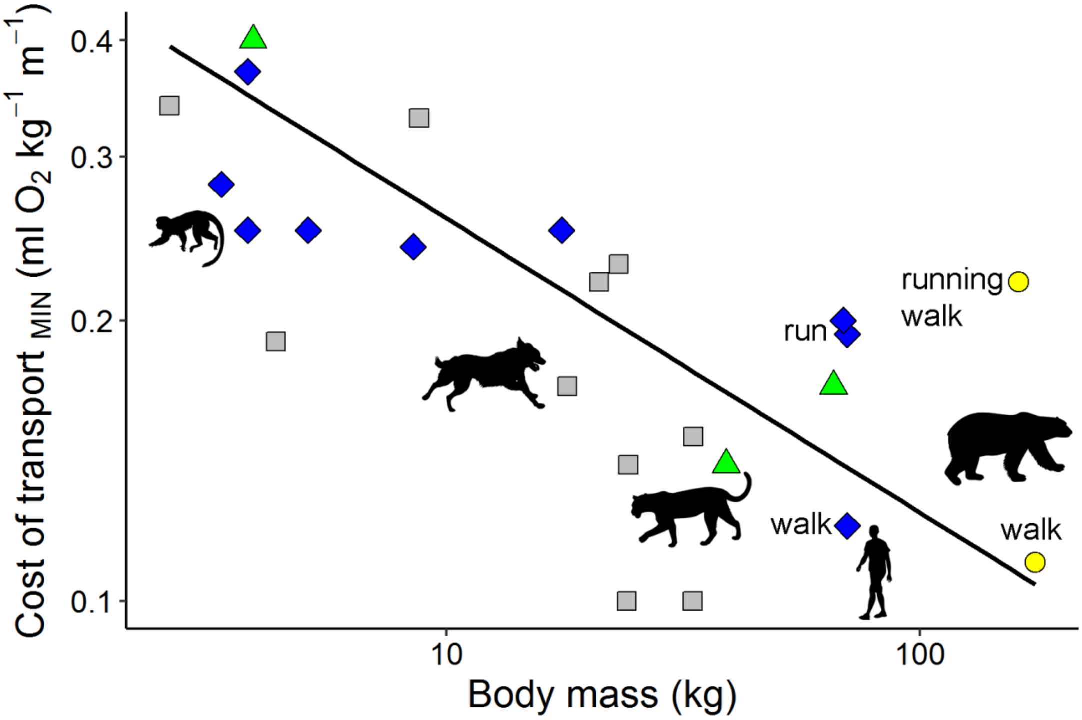

Figure 2.3. Net minimum cost of transport (COT_{MIN}) in digitigrade carnivores and plantigrade mammals. Digitigrade carnivores: canids (grey squares, (Taylor et al. 1982, Bryce and Williams 2017)) and felids (green triangles, (Taylor et al. 1982, Williams et al. 2014)). Plantigrade mammals: primates (blue diamonds, (Taylor et al. 1982, Cunningham et al. 2010)) and ursids (yellow circles, present study). The solid line is the predicted relationship for COT_{MIN} of quadrupedal mammals (Taylor et al. 1982).

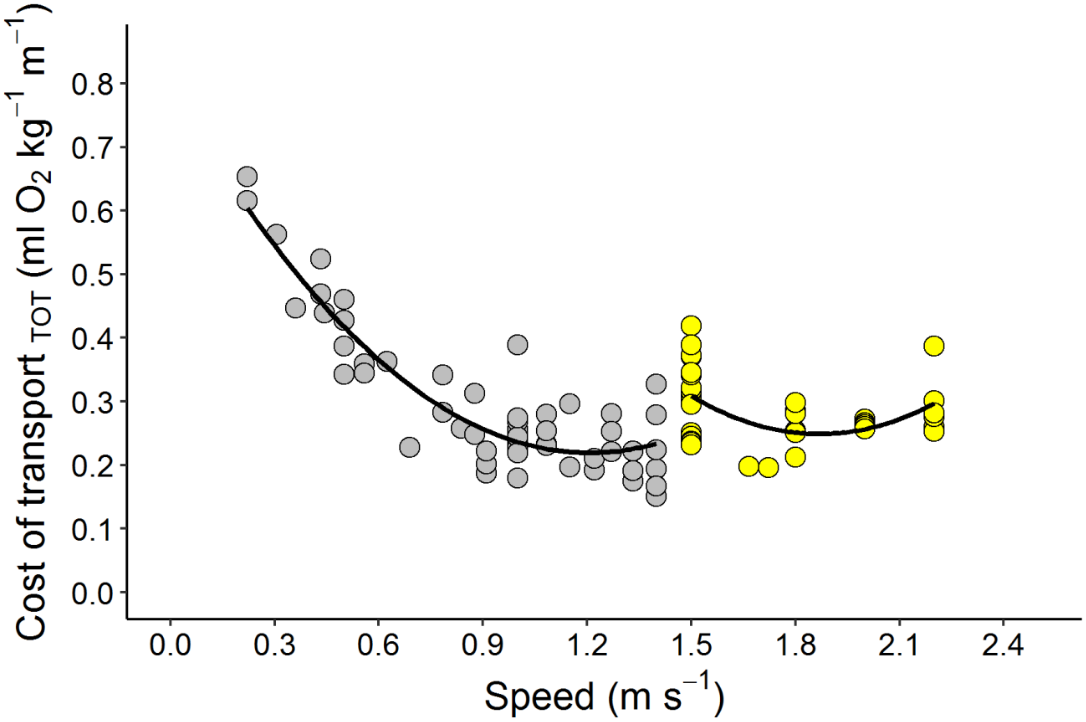

Figure 2.4. Mass-specific total cost of transport (COT_{TOT}) in relation to locomotor speed in polar bears and grizzly bears. Polar bears and grizzly bears while walking at < 1.5 m s^{-1} (grey circles) and polar bears at ≥ 1.5 m s^{-1} (yellow circles). The equation describing the second-order polynomial relationship between COT_{TOT} and walking speed at < 1.5 m s^{-1} is $COT_{TOT} = 0.40 \times speed^2 - 0.96 \times speed + 0.80$, ($r^2 = 0.83$). The equation describing the second-order polynomial relationship between COT_{TOT} and speed at ≥ 1.5 m s^{-1} is $COT_{TOT} = 0.44 \times speed^2 - 1.64 \times speed + 1.78$, ($r^2 = 0.22$).

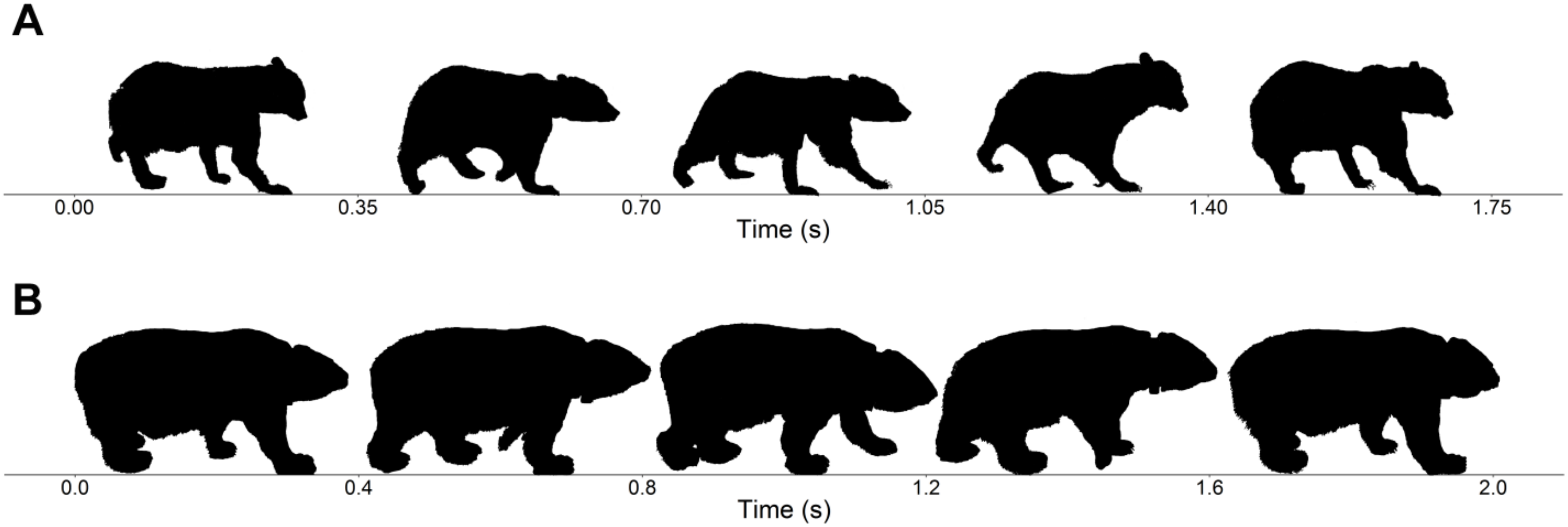

Figure 2.5. Plantigrade walking gait of the grizzly bear and polar bear. A. Single walking stride of an adult female grizzly bear moving on a treadmill at 2.8 km h^{-1} over 1.75 seconds. **B.** Single walking stride of an adult female polar bear moving on a treadmill at 2 km h^{-1} over 2 seconds.

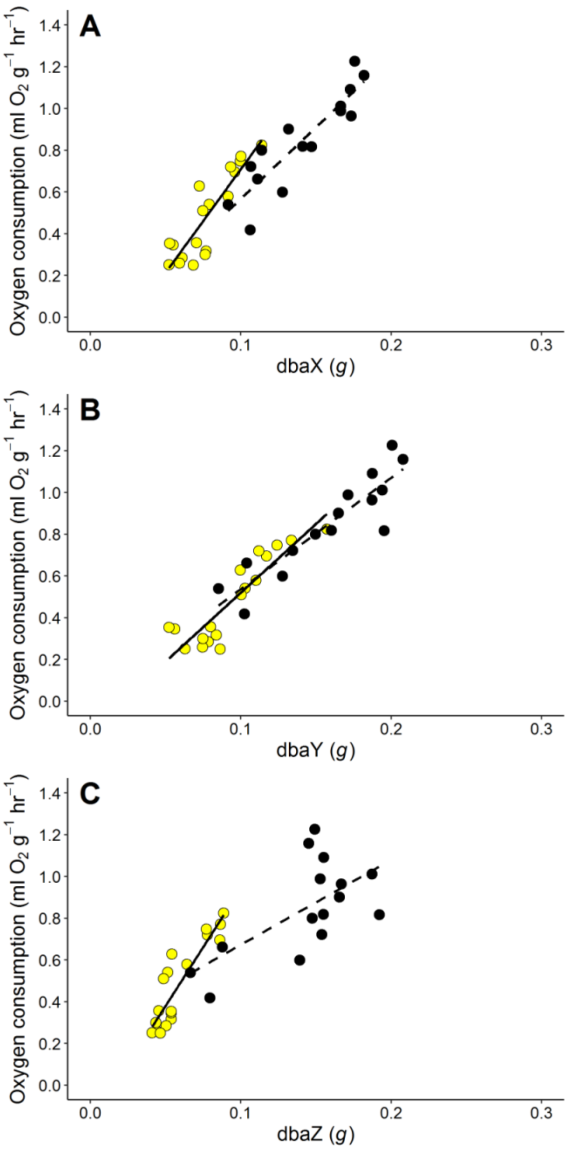

Figure 2.6. Relationship between oxygen consumption and dynamic body acceleration (dba) in polar bears and grizzly bears. Least-squares regression of mass-specific oxygen consumption and mean absolute dba in the surge (X; **A.**), heave (Y; **B.**), and sway (Z; **C.**) dimension from 2 adult female polar bears (yellow circles, solid line) and 3 adult female grizzly bears (black circles, dashed line) resting and walking on a treadmill. Points are mean steady-state measurements.

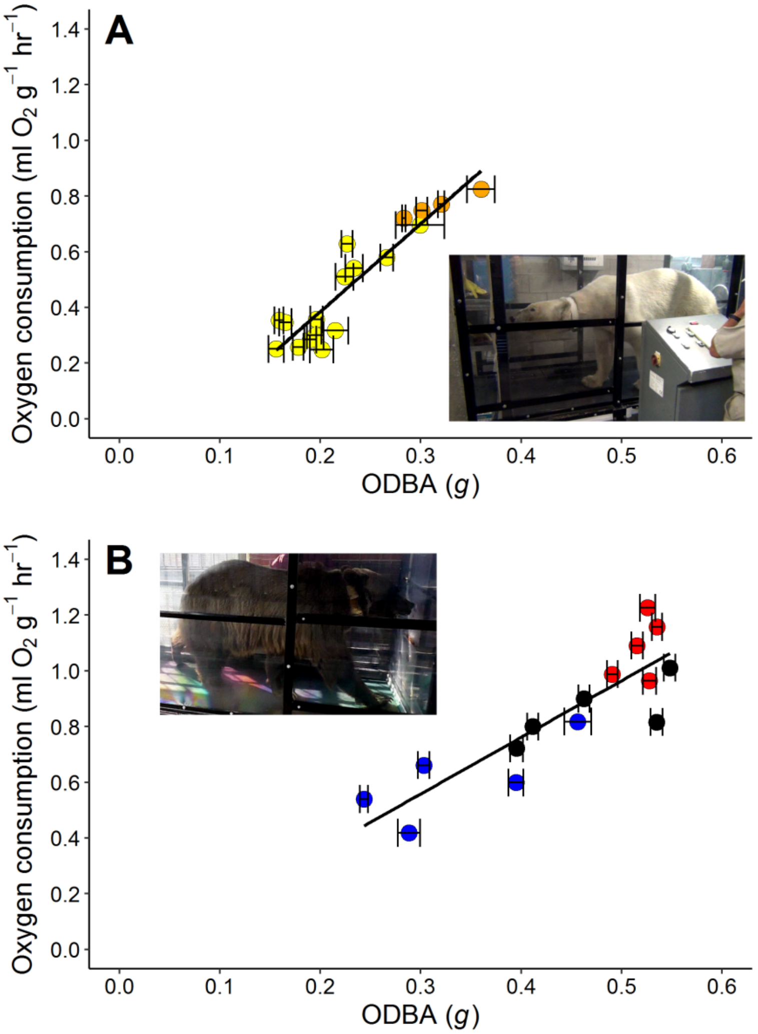

Figure 2.7. Relationship between oxygen consumption and overall dynamic body acceleration (ODBA) in polar bears and grizzly bears. A. Least-squares regression of mass-specific oxygen consumption and mean ODBA from 2 adult female polar bears (Polar Bears 1-2 (yellow and orange circles, respectively)) resting and walking on a treadmill. Points are mean (± SE) steady-state measurements (see text for regression statistics). **B.** Least-squares regression of mass-specific oxygen consumption and mean ODBA from 3 adult female grizzly bears (Grizzly Bears 3-5 (red, blue, and black circles, respectively)) resting and walking on a treadmill. Points are mean (± SE) steady-state measurements (see text for regression statistics).

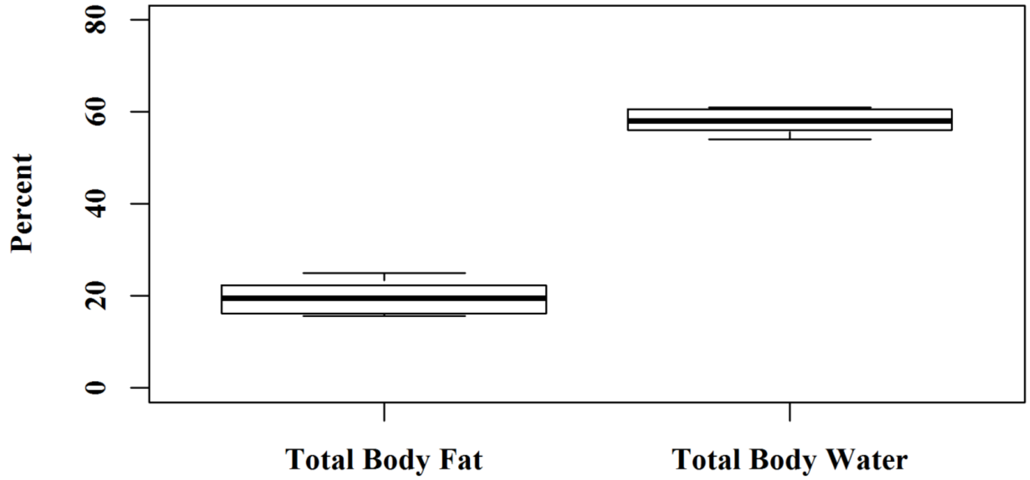

Fig. 2.8. Body composition of 7 grizzly bears based on deuterium oxide injection. Percent total body fat and total body water (median, 1st and 3rd quartiles, maximum, and minimum).

Chapter 3

Energetic costs of aquatic locomotion in a subadult polar bear

ABSTRACT

Polar bears (*Ursus maritimus*) are the only marine mammal to rely on walking as its primary form of locomotion. Yet, polar bears are known as strong swimmers and have been documented swimming extensive distances. To assess the energetic costs of aquatic locomotion in polar bears, I measured the oxygen consumption and stroke frequency of a subadult polar bear while resting in the water and swimming and diving in a water flume. The polar bear used pectoral paddling to swim at the surface and dive. Mean stroke costs while swimming and diving averaged 13.6 J kg^{-1} $stroke^{-1}$, which is 1.3 to 7.9 times greater than stroke costs measured in other semi-aquatic and marine mammals. Similar to other semi-aquatic mammals, subadult polar bears appear to exhibit uneconomical costs of aquatic locomotion. Future energetic measures are needed from adult polar bears while surface swimming to further quantify the costs of swimming in this species and to assess the energetic implications of increases in swimming rates in free-ranging polar bears.

INTRODUCTION

Most marine mammals rely on swimming as their primary form of locomotion. These animals have evolved specialized morphologies, physiologies, and behaviors that have enabled them to efficiently move through an aquatic environment (Williams 1999). Such adaptations include body streamlining, specialized plantar surfaces for propulsion, and abilities to remain submerged for extended durations (Williams 1989). Contrary to most marine mammals, polar bears (*Ursus maritimus*) rely on walking as their primary form of locomotion. As a consequence, they exhibit little evidence of body streamlining or abilities to remain submerged for extended durations. The longest dive recorded for a polar bear is 3 min and 10 s (Stirling and van Meurs 2015), a relatively brief period compared to other marine mammals (Ponganis 2015). Nevertheless, polar bears do exhibit large forepaws relative to other bear species, potentially as an adaptation for swimming (DeMaster and Stirling 1981, Griffen 2018), and exhibit some distinct physiological and behavioral adaptations from other bear species likely as a consequence of their marine existence (Chapter 4).

Polar bears are considered strong swimmers (Øritsland 1969, 1970, Stirling 1974, 1988, DeMaster and Stirling 1981) and satellite telemetry data has revealed polar bears swimming extensive distances up to 687 km (Durner et al. 2011, Pagano et al. 2012, Pilfold et al. 2017). Polar bears have also been documented swimming and diving for seals, kelp, fish, and other prey (Stirling 1974, Russell 1975, Furnell and Oolooyuk 1980, Dyck and Romberg 2007, Stirling and van Meurs 2015, Laforest et al. 2018). Yet, a recent study found the costs of swimming to be 5 times greater than walking based on modeled costs derived from internal body temperature data from 2 wild swimming polar bears (Griffen 2018). Such costs have important implications for polar bear body condition, reproductive success, and survival as long-distance swims in some regions of the Arctic appear to be increasing in frequency as a result of declines in Arctic sea ice (Pagano et al. 2012, Pilfold et al.

2017). However, the 2 bears studied by (Griffen 2018) were both lactating, which may have inflated their energetic costs, and many of the parameters used to convert internal body temperature to energy expenditure were based on measures derived from other mammal species. Furthermore, the energetic costs of swimming in polar bears have yet to be measured using indirect calorimetry methods to better assess the implications of polar bear swimming on overall energy expenditure.

To improve estimates of the costs of aquatic locomotion in polar bears, I measured the oxygen consumption and stroke frequency of a subadult polar bear while resting in the water and swimming and diving within a water flume. I compare these costs of aquatic locomotion to modeled swimming costs in polar bears, resting and walking costs in polar bears, and the costs of swimming in other species of semi-aquatic and marine mammals.

MATERIALS AND METHODS

Oxygen consumption ($\dot{V}O_2$) was measured via open-flow respirometry in a 166.5 kg yearling female polar bear at the Oregon Zoo while simultaneously measuring her stroke frequency. Measurements were made within a sealed metabolic chamber (2.9 m × 1.4 m × 0.6 m) constructed of polycarbonate, reinforced with a steel frame (Carter2Systems, Inc., Hillsboro, OR, USA) that was mounted to the concrete walls of a 1.6 m deep pool. Water was circulated at approximately 0.6 km hr^{-1} within the chamber using an electric motor (Fastlane, Endless Pools, Inc., Aston, PA, USA).

The bear was trained over 11 months and conditioned to rest in still water while standing on its hind legs or bracing itself against the sides of the wall (Figure 3.1) and to swim and dive against a current in the flume (Figure 3.1) while receiving food (i.e., fish) every 10 – 20 sec. During each measurement session the bear swam into the chamber and a resting measurement was recorded for a minimum of 10 min before each swimming session. Following resting measurements, the water pump was turned on and the bear was enticed to swim and dive by dropping fish into the water column. Each swimming and diving measurement was recorded for a minimum of 10 min. Food intake per resting or swimming session ranged from 625–950 g fish. Measurement sessions occurred at varying times during the day. The first session per day occurred in the morning following an overnight fast to ensure a post-absorptive state.

A vacuum pump (FlowKit Mass Flow Generator - 2000, Sable Systems International, Inc., Las Vegas, NV, USA) was used to draw air at 500 L min^{-1} during measurements. Flow rates were monitored continuously and maintained oxygen levels ≥20% to avoid hypoxic conditions. Sub-samples of air from the exhaust port of the chamber were drawn through a series of 6 columns, filled with desiccant (Drierite, W. A. Hammond Drierite, Xenia, OH, USA), and scrubbed of carbon dioxide (Sodasorb, W.R. Grace & Co, Chicago, IL, USA) before entering the oxygen analyzer (Sable Systems International, Inc.). The percent of oxygen in the expired air was monitored continuously and recorded values once per second using Expedata Analysis software (Sable Systems International, Inc.). Air temperatures within the chamber ranged from 21.8–28.0°C ($\bar{x}$ = 24.4°C) and water temperatures ranged from 23.0–24.4°C ($\bar{x}$ = 23.7°C). I converted values to $\dot{V}O_2$ using equation 4B from Withers (1977) assuming a respiratory quotient of 0.78. All values were corrected to standard temperature and pressure, dry. I calibrated the entire system prior to measurements with dry ambient air (20.95% O_2) and daily with dry N_2 gas (Fedak et al. 1981).

I measured stroke frequency of the forepaws (strokes sec^{-1}) using video from a high-definition video camera (Sony, Tokyo, Japan; HDR-CX260V, 1080 HD, 60p) positioned either above or in front of the flume and a second high-definition video camera (GoPro, San Mateo, CA, USA; Hero 3+, 1080 HD, 60p) camera positioned in front of the flume at the water line. I analyzed the video footage with video editing and motion analysis software (Corel Video Studio Pro X5, Corel Corp., Ottawa, Ontario, Canada; ProAnalyst, Xcitex, Woburn, MA, USA).

I compared $\dot{V}O_2$ during resting sessions while the bear was post-absorptive to $\dot{V}O_2$ measures while the bear was post-prandial to evaluate the potential effects of specific dynamic action on $\dot{V}O_2$ measurements. Given the variable behavior of the bear during locomotor measurements (i.e., both swimming and diving within the flume) I could not measure her locomotor speed. Hence, I converted oxygen consumption rates while the bear swam and dove to stroke costs (J kg^{-1} $stroke^{-1}$) to enable comparison with other studies.

RESULTS

$\dot{V}O_2$ measurements while resting in the water averaged 0.39 ml O_2 g^{-1} h^{-1} (SE = 0.02, *n* = 7) and was identical among sessions in which the bear was post-absorptive ($\bar{x}$ = 0.39 ml O_2 g^{-1} h^{-1}, SE = 0.06, *n* = 3) or post-prandial ($\bar{x}$ = 0.39 ml O_2 g^{-1} h^{-1}, SE = 0.02, *n* = 4). This resting metabolic rate (RMR) in water is 1.7 times greater than the mean post-absorptive RMR reported for polar bears (0.23 ml O_2 g^{-1} h^{-1}; Chapter 2) and 1.1 times less than the postural cost of activity reported for polar bears (0.44 ml O_2 g^{-1} h^{-1}; Chapter 2). $\dot{V}O_2$ measurements while swimming and diving averaged 0.59 ml O_2 g^{-1} h^{-1} (SE = 0.02, *n* = 6), which would be equivalent to the energy expended by a polar bear walking at 1.3 km hr^{-1} (Chapter 2).

Swimming was performed primarily by pectoral paddling with alternate strokes of the forelimbs (Figure 3.2). Some propulsive motions of the hind limbs were also observed (Figure 3.2). The bear was positively buoyant and swam with her head and portions of her back above the water surface (Figure 3.2). Stroke frequency while swimming and diving averaged 0.25 Hz (SE = 0.02, *n* = 6). Stroke costs averaged 13.6 J kg^{-1} $stroke^{-1}$ (SE = 0.8, *n* = 6). This is 1.5 times greater than polar bear stride costs while walking on a treadmill (9.0 J kg^{-1} $stride^{-1}$; Chapter 2) and greater than previously documented costs in semi-aquatic or marine mammals, except humans (*Homo sapiens*) (Figure 3.3).

DISCUSSION

Despite their reliance on the marine environment, subadult polar bears appear to have relatively high energetic costs of aquatic locomotion. Similar to other semi-aquatic mammals, polar bears exhibit little streamlining, have small propulsive appendages relative to aquatic mammals, and primarily swim at the water surface (Fish 2000). At the surface, drag can be up to 5 times greater than submerged swimming (Hertel 1966), resulting in considerably greater costs of transport while surface swimming (Williams 1989). Like most semi-aquatic mammals, polar bears are paddle swimmers, which has been shown to be a particularly uneconomical form of locomotion due to energy lost through inertia, non-thrust movements during power strokes, and increased drag during recovery strokes (Fish 1992). Yet, unlike most paddlers, polar bears primarily swim by pectoral paddling (Fish and Baudinette 2008). Fish and Baudinette (2008) found pectoral paddling in ferrets (*Mustela putorius*) to be more economical than quadrupedal paddling used by mink (*Neovison vison*) (Williams 1983) and suggested that bipedal swimming was more economical than quadrupedal swimming. Nevertheless, I found subadult polar bear stroke costs to be greater than costs documented in other species of semi-aquatic mammals, except humans who are considered exceptionally uneconomical surface swimmers (Prange and Schmidt-Nielsen 1970, Schmidt-Nielsen 1972, Williams et al. 1992). Humans using whole-body front-crawl swimming exhibited 1.9 times greater stroke costs than the polar bear in this study (26.3 J kg^{-1} $stroke^{-1}$; Morris et al. 2017), while Australian water rats (*Hydromys chrysogaster*) exhibited the next highest stroke costs (10.2 J kg^{-1} $stroke^{-1}$; Fish and Baudinette 1999), which were 1.3 times less than the polar bear in this study. Marine mammals at preferred swimming speeds exhibited stroke costs on average 4.4 times less than the stroke costs measured in this study (Williams et al. 2017). Based on stroke costs, the cost per stroke was 50% greater relative to the cost per stride measured in polar bears walking on a treadmill (Chapter 2), which is similar to the difference between stride and stroke costs found in Australian water rats who swim by pelvic paddling (Fish and Baudinette 1999). Hence, the findings from this study appear to corroborate the high energetic costs of swimming in wild adult polar bears that were modeled by Griffen (2018).

However, the results of this study should be interpreted as a preliminary assessment. Although Watts et al. (1991) found resting metabolic rates of 2 subadult polar bears to be similar to Kleiber (1975) predictions, the immature age of this bear suggests that her resting metabolic rate should be greater than rates in adults (Brody 1945, Lavigne et al. 1986). Furthermore, the behavior of the bear in which she both swam and dove during measurements prevented us from measuring her swim speed to calculate relationships between metabolic rate and speed. Additionally, it is expected that polar bears in the wild are primarily surface swimming during long distances swims (Pagano et al. 2012), whereas the bear in this study both swam on the surface and dove. Polar bears deposit large quantities of subcutaneous fat (Pond and Ramsay 1992, Pond et al. 1992), increasing their buoyancy (Harrington 1965, Aars and Plumb 2010, Derocher 2012), which would be further aided by their pelage (Fish et al. 2002, Derocher 2012). Hence, diving costs in polar bears could potentially be greater than surface swimming costs as a result of overcoming the force of buoyancy (Butler 2000). Furthermore, polar bears would also be expected to have greater thermoregulatory costs in Arctic waters relative to the temperate water temperatures in this study (Scholander et al. 1950, Øritsland 1969, Griffen 2018). Although Whiteman et al. (2015) speculated that polar bears may be capable of regional heterothermy to minimize heat loss while swimming, this remains untested. I recommend future research examine the costs of surface swimming in adult polar bears at variable speeds and in variable water temperatures to better quantify the costs of swimming in wild polar bears.

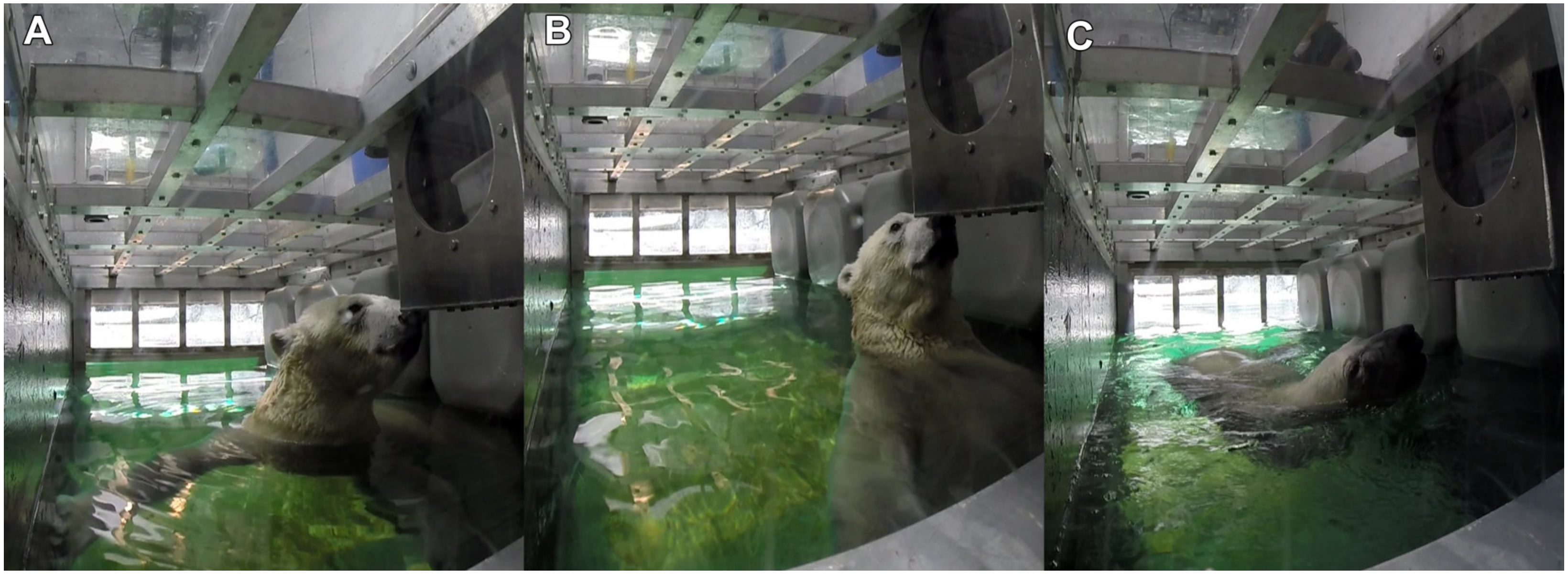

Figure 3.1. Resting and swimming behaviors of a subadult polar bear. **A.** Subadult female polar bear resting in the water in the metabolic chamber while bracing itself against the walls at the water surface; **B.** subadult female polar bear resting in the water in the metabolic chamber while standing on its hindlegs; and **C.** subadult female polar bear swimming against a current in the flume.

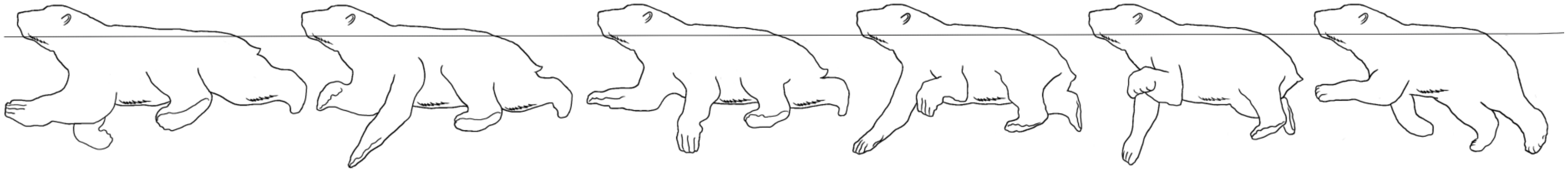

Figure 3.2. Swimming pattern of a subadult polar bear. The first image shows the left forelimb at the beginning of the power phase of the stroke cycle. In the recovery phase (fourth and fifth images), the limb is brought close to the body and moved forward to return to the power phase (last image).

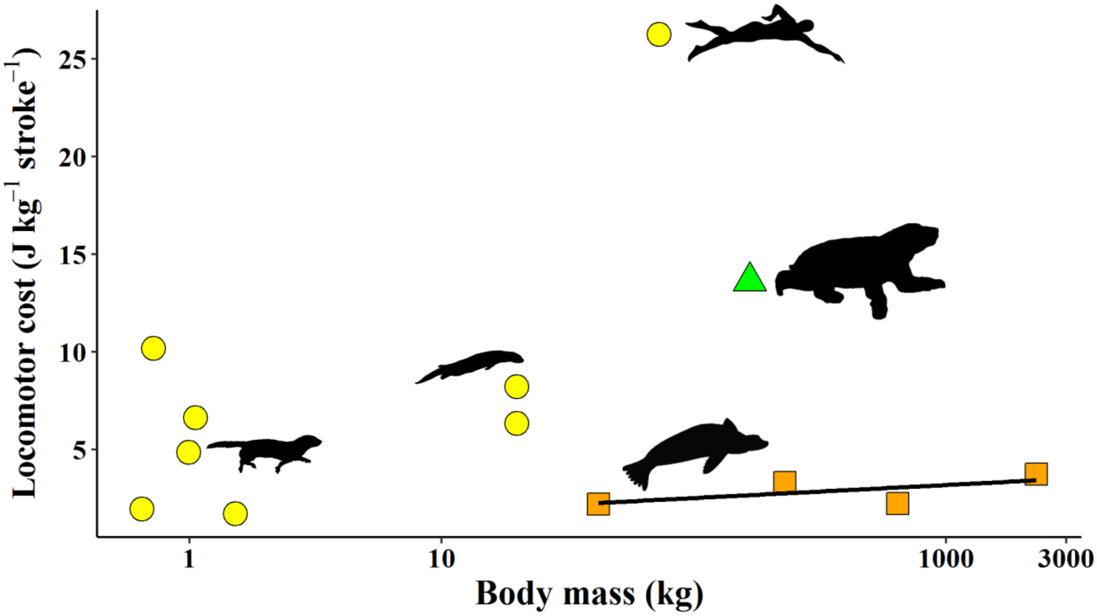

Figure 3.3. Mean stroke costs in a polar bear, semi-aquatic, and marine mammals. Polar bear (green triangle). Semi-aquatic mammals (yellow circles): muskrats (*Ondatra zibethicus*) (Fish 1982, 1984), mink (Williams 1983), ferrets (Fish and Baudinette 2008), platypus (*Ornithorhynchus anatinus*) (Fish et al. 1997), Australian water rats (Fish and Baudinette 1999), sea otters (*Enhydra lutris*) surface swimming and submerged swimming (Williams 1989), and elite front-crawl swimming in humans (Morris et al. 2017). Marine mammals (orange squares): bottlenose dolphins (*Tursiops truncatus*) (Williams et al. 2017), harbor porpoises (*Phocoena phocoena*) (Williams et al. 2017), beluga whales (*Delphinapterus leucas*) (Williams et al. 2017), and killer whales (*Orcinus orca*) (Williams et al. 2017). The solid line is the least squares linear regression for marine mammals (Williams et al. 2017).

Chapter 4[‡]

High-energy, high-fat lifestyle challenges an Arctic apex predator, the polar bear

ABSTRACT

Regional declines in polar bear (*Ursus maritimus*) populations have been attributed to changing sea ice conditions, but with limited information on the causative mechanisms. By simultaneously measuring field metabolic rates, daily activity patterns, body condition, and foraging success of polar bears moving on the spring sea ice, I found that high metabolic rates (1.6 times greater than previously assumed) coupled with low intake of fat-rich marine mammal prey resulted in an energy deficit for more than half of the bears examined. Activity and movement on the sea ice strongly influenced metabolic demands. Consequently, increases in mobility resulting from ongoing and forecasted declines in and fragmentation of sea ice are likely to increase energy demands and may be an important factor explaining observed declines in body condition and survival.

INTRODUCTION

As the most carnivorous and only marine-living ursid, polar bears are unique among bears in their reliance on marine mammal prey. Evolution of this Arctic apex predator included behavioral and physiological adaptations that distinguish polar bears from terrestrial bears (Berta 2012), which has made them dependent on the sea

---

[‡] A version of this chapter has been published as: Pagano, A.M., G.M.Durner, K.D. Rode, T.C. Atwood, S.N. Atkinson, E. Peacock, D.P. Costa, M.A. Owen, and T.M. Williams. 2018. High-energy, high-fat lifestyle challenges an Arctic apex predator, the polar bear. Science 359:568-572.

ice and may increase their vulnerability to climate change (Laidre et al. 2008). As a consequence of living in this labile marine habitat, polar bears occupy expansive home ranges that are considerably larger than those occupied by other ursids (Stirling and Derocher 1990) or predicted for similarly-sized terrestrial carnivores (Ferguson et al. 1999). They also exhibit remarkable abilities to swim for extended distances (Pagano et al. 2012). However, such long-distance movements, whether walking or swimming, necessitate substantial energetic resources to satisfy locomotor demands (Hurst et al. 1982*b*, Griffen 2018). Historically, sufficient resources were afforded through the availability of fatty, energy-dense seal prey, which could be hunted efficiently from the sea ice (Stirling 1974). Presently, the sea ice minimum extent across the Arctic is decreasing at a rate of 14% per decade, spring break-up is occurring earlier, and fall freeze-up, later (Stroeve et al. 2014). This decline in sea ice is likely reducing access to, and abundance of, seal prey (Stirling and Derocher 1993).

Because metabolism determines the rate at which organisms require energy from their environment (Brown et al. 2004), measures of polar bear metabolic rates provide an important metric for linking declines in Arctic sea ice to polar bear survival. Changes in energy balance resulting from increased energy expenditure or reductions in foraging opportunities could lead to declines in body condition, survival, and reproductive success. Previous studies have reported that walking costs for polar bears are greater than predicted for other similarly-sized mammals (Hurst et al. 1982*a*, *b*). Yet, models predicting polar bear annual field metabolic rates (FMRs) assumed that FMRs would be relatively low due to the bear’s sit-and-wait style of hunting and theorized ability to reduce metabolism while fasting (Stirling and Øritsland 1995, Kingsley 1998), similar to denning bears (Nelson et al. 1983, Stirling and Øritsland 1995). However, measures of mass loss and body temperature suggest that metabolic rates of fasting polar bears during the summer are in fact greater than those of denning bears (Atkinson et al. 1996, Robbins et al. 2012, Whiteman et al. 2015). Despite this improved understanding of fasting metabolism, no study has provided quantitative estimates of the FMRs of active polar bears on the sea ice where they spend most, and in many areas of their range all, of the year.

I measured the FMRs of female polar bears (*n* = 9) during April, 2014 – 2016 in the Beaufort Sea (Figure 4.1) over 8 – 11 days each year using doubly-labeled water (DLW). On the same animals, I deployed global positioning system (GPS) equipped video camera collars and archival loggers with tri-axial accelerometers and conductivity sensors to determine activity and behavior to assess the causes of variation in FMRs (Figure 4.1). I determined individual energetic balance using video-derived observations of foraging and measures of blood biochemistry, body mass, and body composition. Additionally, I measured the resting metabolic rate (RMR) of a captive adult female polar bear using open-flow respirometry to assess baseline energetic costs of the species relative to free-ranging polar bears and other mammals.

MATERIALS AND METHODS

Study design

The objectives of this study were to measure the field metabolic rates, activity rates, and foraging success rates of female polar bears. I simultaneously used DLW, GPS-equipped video camera collars, archival loggers with tri-axial accelerometers and conductivity sensors, and measures of blood biochemistry on female polar bears on the sea ice. Sample sizes and randomization were limited by the logistical constraints of locating and relocating free-ranging bears. I further measured the resting metabolic rate of a captive adult female polar bear to assess baseline energetic costs in the species relative to other bear species and other mammals.

Captures

I captured subadult and adult female polar bears without dependent young on the sea ice of the Beaufort Sea north of Prudhoe Bay, Alaska in April 2014, 2015, and 2016 (Figure 4.1). Polar bears were located from a helicopter and immobilized with a rapid-injection dart (Palmer Cap-Chur Equipment, Douglasville, GA) containing zolazepam-tiletamine (Telazol®) (Stirling et al. 1989). Following immobilization, I weighed bears using an electronic load cell suspended from an aluminum tripod. Bears that had not been previously captured were aged based on counts of cementum annuli from an extracted vestigial premolar (Calvert and Ramsay 1998). Procedures were approved by the Animal Care and Use Committees of the University of California, Santa Cruz and the U.S. Geological Survey, Alaska Science Center. Research was authorized under U.S. Fish and Wildlife Service Marine Mammal Permit MA690038.

Doubly-labeled water

Following immobilization, I inserted an external jugular catheter to facilitate blood sampling and administration of isotopes. An initial blood sample was collected to serve as a baseline measure of ^{18}O (oxygen-18) and ^{2}H (deuterium). The bear was then injected intravenously with a precisely weighed dose containing 0.12 – 0.25 g kg^{-1} of 97% enriched ^{18}O (Isoflex USA, San Francisco, CA) and 0.06 – 0.10 g kg^{-1} of 99.9% enriched ^{2}H (Isotec, Inc., Miamisburg, OH or Cambridge Isotope Laboratories, Inc., Tewksbury, MA) with NaCl added to make it 0.9% isotonic and sterilized using a 0.2 μ Millipore filter. On injection, the syringe was back washed with blood three times to ensure all the DLW had been injected into the bear. The bear was kept immobilized for 2 hours after the injection of DLW to allow isotope equilibration (Arnould 1990, Farley and Robbins 1994). I collected serial blood samples 60, 90, and 120 minutes after dosing to evaluate equilibration curves (Speakman 1997). I recaptured bears 8 – 11 days later to obtain a blood sample to measure final enrichment. At recapture, I weighed bears to measure changes in body mass. In 2015 and 2016, I dosed recaptured bears with 0.09 – 0.14 g kg^{-1} of 99.9% enriched deuterated water (D_2O, Cambridge Isotope Laboratories, Inc.) and collected serial blood samples 60 and 90 minutes after dosing to measure changes in body composition between captures (Farley and Robbins 1994, Atkinson and Ramsay 1995, Atkinson et al. 1996, Hilderbrand et al. 1998). Blood was collected in 10 ml glass evacuated tubes without anticoagulants (Serum Vacutainer, Becton Dickinson, Franklin Lakes, NJ) and centrifuged to separate serum from red blood cells. Serum was stored frozen in 2 ml cryogenic vials (Corning, Inc., Corning, NY) at -20°C until analysis.

Serum samples were analyzed for the concentrations of ^{18}O and ^{2}H (Metabolic Solutions, Inc., Nashua, NH). I calculated CO_2 production using the plateau method and Speakman’s two-pool equation (Speakman 1997), which has been shown to be best suited for large mammals [(Speakman 1997, Speakman et al. 2001, Sparling et al. 2008), but see (Dalton et al. 2014)]. I used results from ^{2}H dilution to evaluate total body water (TBW) of bears at initial capture and recapture (2015 and 2016) and used TBW to determine fat and lean body mass (LBM) based on the equations of Farley and Robbins (1994) . In 2015 and 2016, I used mean percent TBW that incorporated changes in TBW at recapture. In 2014, I assumed percent TBW remained constant between capture and recapture. I used the mean group dilution space ratio in calculating CO_2 production (Speakman 1997). I converted CO_2 production to metabolic rate using a respiratory quotient of 0.76 (26.32 kJ per liter CO_2). This value was derived from respiratory exchange ratio data collected from solitary adult female polar bears on the sea ice of the Beaufort Sea by a previous study during spring in 2009 and 2010 ($\bar{x} = 0.76$, SE = 0.015, $n = 12$) (Whiteman 2014). Nutritional demands were determined from the caloric value and digestibility of ringed seals in polar bears (Stirling and McEwan 1975, Best 1985) as ringed seals are the primary prey of female polar bears in the Beaufort Sea in the spring (Thiemann et al. 2008, Rogers et al. 2015, McKinney et al. 2017). Ringed seal pups were mean total (fat + protein) caloric values from pups < 1 month old, carcasses were mean caloric values of protein from subadult and adult ringed seals, and subadults and adult ringed seals were mean caloric values of fat.

Urea/creatinine ratios

Serum samples from capture and recapture were analyzed using an Abaxis Vetscan VS2 chemistry analyzer (Abaxis, Inc., Union City, CA). Each sample was analyzed twice and average values were calculated. Blood urea nitrogen (BUN) values were divided by 0.466 to obtain urea concentrations (Nelson et al. 1984) and then divided by creatinine concentrations to obtain urea/creatinine ratios (U/C). I considered increases in U/C ratios between captures and recaptures as an indication of feeding during the sampling period. I considered U/C ratios ≤10 to be an indicator of fasting for >1 week (Derocher et al. 1990).

Video collars and archival loggers

I deployed GPS-equipped video camera collars (Exeye, LLC., Bristow, VA) and archival loggers (TDR10-X-340D, Wildlife Computers Inc., Redmond, WA) on individuals dosed with DLW to associate behavior with metabolic rate. Three of the archival loggers deployed in 2014 failed within 12 hours of deployment. The other six archival loggers functioned for the duration of the deployments. The GPS receiver on one of the collars (bear #5) failed 4 days after deployment. Video cameras were programmed to record at varying frequencies during daylight periods (Table 4.1) with sunrise during this period occurring around 6 am Alaska Daylight Time (AKDT) and sunset occurring around 10 pm (AKDT). Video cameras were programmed to turn off if the temperature of the collar was ≤ -17 °C to protect video equipment. Two collars in 2014 and 2015 were additionally equipped with side-mounted cameras as an alternative if the main cameras failed or the lens became obstructed by snow or ice. Video collars including accelerometers and release mechanisms weighed 1.6 – 2.1 kg (0.8% – 1.5% of body mass of bears in this study). GPS fix rate was every 30 minutes in 2014, every 10 minutes in 2015, and every 5 minutes in 2016. Location data were transmitted via the Iridium satellite system. To evaluate differences in movement rates and distances traveled among bears, I used a continuous time correlated random walk (CRAWL) model (Johnson et al. 2008, Johnson 2016) in program R (R Core Team 2014) to predict locations on a 30 minute interval based on GPS locations. The CRAWL model accounts for variable location quality and sampling intervals and I assigned GPS location data an accuracy of 30 m (Frair et al. 2010). I calculated minimum distance travelled between two successive predicted locations as the great-circle distance (i.e., distance accounting for the earth's curvature), and calculated movement rate by dividing distance by the duration between predicted locations (i.e., 30 minutes) in SAS (version 9.3, SAS Institute Inc., Cary, NC).

Archival loggers recorded tri-axial acceleration (m s^{-2}) at 16 Hz (range ±20 m s^{-2}), time-of-day, and wet/dry conductions at 1 Hz (via an on-board conductivity sensor) continuously from the time of deployment until recovery. I calculated activity patterns using recovered accelerometer and conductivity data as well as daytime activity patterns using the video collar data. Resting behaviors included sleeping, standing, sitting, and still-hunting (Chapter 1). I calculated activity to be the proportion of time a bear was not engaged in resting behaviors. Behaviors were derived from the accelerometer and conductivity data using a random forest algorithm (Breiman 2001) in R (‘RandomForest’ package) (Chapter 1). I used the R package ‘maptools’ (Bivand and Lewin-Koh 2017) to link GPS coordinates with the timing of sunrise and sunset to examine diurnal and nocturnal differences in activity and movement rates. I quantified foraging success based on visual observations of feeding within the video collar data. I linked accelerometer-derived behaviors with corresponding predicted location data by calculating the percent time spent in each behavior class between predicted locations (i.e., 30 minutes) in SAS. I treated the dominant behavior (e.g., ≥50%) between each location as indicative of the primary behavior at the ensuing location. I plotted behavior-linked locations using the R packages ‘ggplot2’ (Wickham 2009) and ‘ggmap’ (Kahle and Wickham 2013).

Analyses

I evaluated the allometric relationship between individual FMRs and mean body mass between capture and recapture in comparison to predicted FMRs for marine and terrestrial mammalian carnivores (Nagy et al. 1999), terrestrial mammals in general (Nagy 2005), and predicted basal metabolic rates (Kleiber 1975). I used least-squares linear regression to evaluate the relationships between FMRs and activity levels derived from video collars and accelerometer/conductivity data, CRAWL-derived mean movement rates, and CRAWL-derived total distance traveled. I further used least-squares linear regression to evaluate the relationship between changes in U/C ratios and changes in body mass between capture and recapture. I compared the activity rates measured in this study to activity rates from other large terrestrial carnivores using measures from African lions (*Panthera leo*) (Hayward and Hayward 2007, Mogensen et al. 2011), coyotes (*Canis latrans*) (Gese et al. 1996), wolves (Theuerkauf et al. 2003, Bryce 2017), mountain lions (*Puma concolor*) (Seidensticker et al. 1973), and spotted hyenas (*Crocuta crocuta*) (Hayward and Hayward 2007, Kolowski et al. 2007). All analyses were conducted in program R with $\alpha = 0.05$.

Resting metabolic rate

The oxygen consumption ($\dot{V}O_2$) of a 16 year-old female polar bear (body mass = 264 kg) resting in a chamber at the San Diego Zoo was measured via open-flow respirometry. The polar bear was trained over 2 months to enter a polycarbonate and steel framed metabolic chamber (2.7 m × 0.9 m × 1.2 m) and conditioned to lay in sternal recumbency while receiving food (i.e., meat and fish) every 20 sec. $\dot{V}O_2$ measurements were collected over 11 – 13 min intervals on 3 days with 2 sessions per day (*n* = 6). The first session per day occurred in the morning following an overnight fast to ensure a post-absorptive state. Food intake per session ranged from 728 – 963 g. Air temperatures within the chamber during measurements ranged from 15.9 – 16.4°C ($\bar{x} = 16.2$°C), which were within the thermoneutral zone for a resting polar bear (Best 1976). A vacuum pump (FlowKit Mass Flow Controller, Sable Systems International, Inc., Las Vegas, NV) was used to draw air from the chamber at 450 – 500 L min^{-1}. Flow rates were monitored continuously and maintained oxygen levels ≥20% to avoid hypoxic conditions. Sub-samples of air from the exhaust port of the chamber were drawn through a series of 6 columns, alternatingly filled with desiccant

(Drierite, W. A. Hammond Drierite, Xenia, OH) and scrubbed of carbon dioxide (Sodasorb, W.R. Grace & Co, Chicago, IL) before entering the oxygen analyzer (Sable Systems International, Inc.). The percentage of oxygen in the expired air was monitored continuously and recorded values once per second using Expedata Analysis software (Sable Systems International, Inc.). I converted values to $\dot{V}O_2$ using equations from Withers (1977) and assumed a respiratory quotient of 0.76 as was used for DLW conversions. All values were corrected to standard temperature and pressure, dry. The entire system was calibrated prior to measurements with dry ambient air (20.95% O_2) and on 2 of the 3 days with dry N_2 gas (Fedak et al. 1981). Body mass was measured on the last day of $\dot{V}O_2$ measurements using a platform scale.

I compared the lowest resting measurement while post-absorptive to previously collected mean resting measurements that used open-flow respirometry on subadult male and female polar bears (Hurst 1981, Watts et al. 1991), hibernating adult female polar bears (Watts et al. 1987), hibernating adult male grizzly bears (*U. arctos*) (Watts and Jonkel 1988), male and female black bears (*U. americanus*) (Tøien et al. 2011), hibernating male and female black bears (Watts and Cuyler 1988, Tøien et al. 2011), adult and subadult male and female panda bears (*Ailuropoda melanoleuca*) (Fei et al. 2016), and female sloth bears (*Melursus ursinus*) (McNab 1992).

Procedures for captive measurements were approved by the Animal Care and Use Committees of the University of California, Santa Cruz, the U.S. Geological

Survey, Alaska Science Center, and the San Diego Zoo Global. Captive research was further authorized under U.S. Fish and Wildlife Service Marine Mammal Permit MA77245B.

RESULTS and DISCUSSION

Like other members of the order Carnivora whose diet is exclusively meat (McNab 1988), polar bears exhibit greater RMRs compared to predictions for other terrestrial mammals (i.e., derived from omnivores, carnivores, and foliovores, (RMR = 70×mass$^{0.75}$), (Kleiber 1975) (Figure 4.2). RMRs measured from a single captive polar bear over 6 sessions averaged 0.34 ml O_2 g^{-1} h^{-1} (SE = 0.01) with a low, post-absorptive (i.e., fasting) value of 0.30 ml O_2 g^{-1} h^{-1}, which converts to 37.1 mJ day^{-1}. On a mass-specific basis, this post-absorptive RMR was within 0.5 – 11.4% of post-absorptive RMRs previously reported for sub-adult polar bears (Hurst 1981, Watts et al. 1991), 17% greater than measurements from polar bears while denning (Watts et al. 1987), and 2 – 21% greater than other ursids while resting or denning (Figure 4.2). Thus, carnivory and large body mass set a comparatively high maintenance cost for polar bears that must be satisfied to remain in energetic balance.

As a result, the FMR of polar bears is high relative to predictions for terrestrial mammals generally (Nagy 2005) and consistent with expected levels derived solely from other mammalian carnivores (Nagy et al. 1999). The measured FMRs in this study averaged 1.6 times previously assumed values for polar bears (SE = 0.1, range = 1.0 – 2.6) (Stirling and Øritsland 1995, Kingsley 1998). Daily FMRs measured over 8 – 11 days, averaged 0.45 ml CO_2 g^{-1} h^{-1} (SE = 0.04, $n = 9$), which converts to 51.6 mJ day^{-1} (SE = 6.2, n = 9) or 12,324.7 kcal day^{-1}. These values ranged from 0.6 – 1.1 times predicted FMRs ($\bar{x}$ = 0.8, SE = 0.1) for similarly-sized marine and terrestrial mammalian carnivores (Nagy et al. 1999) and 2.5 – 5.2 times predicted RMRs based on body mass ($\bar{x}$ = 2.8, SE = 0.3) (Kleiber 1975) (Figure 4.3A, Table 4.2). Daily FMR was 1.5 – 2.8 times the post-absorptive RMR ($\bar{x}$ = 2.0, SE = 0.2) measured in this study. On average, daily FMR was 2.6 times (Robbins et al. 2012) and 4 times (Molnár et al. 2009) predicted values for male polar bears fasting on land.

To remain in energy balance with these elevated metabolic demands, polar bears have evolved hunting tactics to prey on high energy-content prey, such as ringed seals (*Pusa hispida*), and preferentially feed on their energy-dense blubber (Stirling and Øritsland 1995). Using these measures of daily FMR, I estimated that a solitary female bear on the spring sea ice would on average need to eat either 1 adult ringed seal, 3 subadult ringed seals, or 19 newborn ringed seal pups every 10 – 12 days to remain in energetic balance (Figure 4.4A). These estimates corroborate observations that bears in the early summer typically kill an adult/subadult ringed seal every 5 days (Stirling 1974). However, this rate of consumption would be necessary simply to energetically break-even. Polar bears put on the majority of their body fat in the late spring and early summer (Stirling and Øritsland 1995) and can reach a relative fatness of 1 kg fat per kg LBM (Atkinson and Ramsay 1995). To obtain this body condition, bears would either need to reduce their energy demands or increase their rate of food consumption.

Using video collar data, I documented bears' hunting behavior and foraging success. Ninety percent of the time, bears used sit-and-wait tactics to hunt seals, while stalking comprised the remaining 10% of hunts. Bears that successfully killed and ate adult/subadult ringed seals either gained or maintained body mass, while bears that only scavenged or showed no evidence of eating, lost mass (Figures 4.4B,C,D). Land-based remains of subsistence-harvested bowhead whale carcasses (*Balaena mysticetus*) provided an alternative food resource for two bears (Figures 4.4B, D), although 91% of their telemetry data were on the sea ice and away from this resource. Scavenging the muscle from previously-killed seals was also common (Figure 4.4D) and consistent with previous observations of polar bear foraging on the sea ice (Stirling 1974, Stirling and Øritsland 1995).

Four bears lost ≥ 10% of their body mass over the 8 – 11 day period (Figure 4.4B, Table 4.2), with an average loss of 1% per day (1.95 kg day^{-1}). This is 4 times the % mass lost per day and 2.2 times the kg lost per day documented in fasting polar bears on land (Atkinson et al. 1996), which typically exhibit lower activity levels than the bears in this study (Whiteman et al. 2015). Nevertheless, this change in body mass is within the range of the % mass loss observed in other carnivores (Geffen et al. 1992, Williams et al. 1997). Of these four bears, one lost a greater amount of LBM than fat mass (Figure 4.4B, Table 4.2), which suggests she was in a prolonged fasting condition (Atkinson et al. 1996). This was confirmed with changes in serum urea/creatinine (U/C) ratios (an indicator of fasting for > 7 days) (Derocher et al. 1990) (Table 4.2). Additionally, changes in U/C ratios over the 8 – 11 day period were strongly positively correlated with changes in body mass ($r^2 = 0.62$, $p = 0.01$, $n = 9$).

Despite the use of efficient sit-and-wait hunting tactics, polar bears in the spring exhibited activity patterns typical of other large terrestrial carnivores. Activity rates (i.e., the proportion of time engaged in non-resting behaviors) derived from accelerometers, which recorded continuously throughout each day, ranged from 22% to 40% ($\bar{x} = 34\%$, SE = 2.8, $n = 6$, Figure 4.5C). Bears spent 28% of the time walking (SE = 2.3, $n = 6$) and only 0.3% of the time swimming (SE = 0.15, $n = 6$, Figure 4.5C). Activity rates derived from video collars (which recorded only during daylight hours) ranged from 13% to 60% of the day ($\bar{x} = 32\%$, SE = 5.1, $n = 9$, Figure 4.5D). These activity rates are similar to those observed for adult and subadult polar bears on the summer sea ice (34.6% of the time active) (Stirling 1974), but are greater than observations from a breeding adult female polar bear on the spring sea ice (26.7% active) (Stirling et al. 2016). Breeding females are known to exhibit reduced activity and devote less time to hunting compared to non-breeding individuals (Stirling et al. 2016). In the present study, 7 of the 9 bears interacted with at least one adult male. However, the activity levels I observed were greater than measures derived from activity sensors on adult female polar bears on the sea ice of the Beaufort Sea during April (25% active) (Whiteman et al. 2015) and solitary female polar bears on the sea ice in April (16.9% active) in the Canadian Arctic (Messier et al. 1992), indicating marked variability in the activity levels of this species depending on seasonal, geographical, and reproductive factors. The activity levels for polar bears were less than the activity levels documented in other bear species ($\bar{x}$ = 54% active) (Paisley and Garshelis 2006), but were similar to activity levels reported for other large terrestrial carnivores ($\bar{x}$ = 39% active).

Individuals exhibited diel differences in activity and movement rates, which may be indicative of a strategy to increase the time allocated to sit-and-wait hunting tactics during daylight hours when seals may be more likely to be in the water and using breathing holes (Stirling 1974), as ringed seals have been documented to haul out more frequently and reduce activity in water during dark hours in March and April (Kelly and Quakenbush 1990). I found activity (Figure 4.6) and movement rates were greater at night ($\bar{x}$ = 0.99 km/h, SE = 0.15, n = 10) than during the day ($\bar{x}$ = 0.79 km/h, SE = 0.12, n = 10), which was similarly reported by coastal indigenous observations (Nelson 1966).

Ultimately, the ability of polar bears to achieve energy balance is dictated by the acquisition of metabolizable energy versus expenditure from basal metabolism, specific dynamic action, thermoregulation, reproduction, growth, and locomotion (Costa and Williams 1999). I found that variation in daily FMR was primarily influenced by positive relationships with body mass (daily FMR = $0.0002\times\text{mass}^{2.41}$, $r^2 = 0.91$, $p < 0.001$, $n = 9$, Figure 4.3A), movement rate (daily FMR = 167.3×rate + 153.0, $r^2 = 0.82$, $p < 0.001$, $n = 9$, Figure 4.3B), and activity rate derived from video collars (daily FMR = 336.73×activity + 180.5, $r^2 = 0.60$, $p = 0.01$, $n = 9$, Figure 4.3C). I found a positive, but non-significant relationship between activity rate derived from accelerometers and daily FMR ($r^2 = 0.56$, $p = 0.09$, $n = 6$). I further found a positive relationship between overall FMR and total distance traveled (overall FMR = 0.006×distance + 1.5, $r^2 = 0.78$, $p = 0.003$, $n = 8$, Figure 4.3D). These relationships suggest that basal metabolism, locomotion, and activity were the primary drivers of energy expenditure for the polar bears in this study. This reinforces that there is a substantial cost of locomotion in polar bears relative to other quadrupedal mammals, as has been documented in captive treadmill studies (Hurst et al. 1982*b*). For example, bears with movement rates averaging ≥ 1.0 km h^{-1} ($n = 3$) had 1.5 times greater FMRs than bears that moved < 1.0 km h^{-1} ($n = 6$) (Figure 4.3B).

Admittedly, the activity levels and FMRs in this study may be biased low due to the effects of recovery post-capture. Based on movement rate and activity sensor data, recovery post-capture for polar bears may last 2 – 3 days (Rode et al. 2014*a*). Although one bear in this study successfully caught and ate an adult/subadult ringed seal less than 24 hours after being collared (Figure 4.5B), most bears exhibited lower activity rates during the first 24 hours after capture (Figures 4.7, 4.8). Hence, the FMRs and activity budgets presented in this study should be considered conservative levels for free-ranging polar bears.

I find that polar bears in the spring exhibit greater energetic demands than previous predictions (Stirling and Øritsland 1995, Kingsley 1998) both for maintenance functions and locomotion. Similar to other marine mammals, polar bears likely transitioned to the marine ecosystem to take advantage of abundant prey resources (Berta 2012) despite the increased energetic costs required for a marine and carnivorous existence (Williams et al. 2001). These demands necessitate access to high-energy content prey in the form of ringed and bearded seals (*Erignathus barbatus*).

More than half of the bears in this study lost body mass, meaning that over the period of observation their energy demand exceeded that gained by consuming prey. Although I cannot assess the effects of post-capture recovery on observed foraging rates, previous researchers reported that 42% of adult female polar bears in the Beaufort Sea during the spring from 2000-2016 had not eaten for ≥ 7 days prior to capture (Rode et al. 2018). This rate of fasting was 12% greater than measurements from 1983 –1999 (Rode et al. 2018), suggesting that spring ice conditions are affecting prey availability for polar bears even before the summer open water period. Additionally, access to optimal habitats (i.e., annual ice over the continental shelf) is expected to and in some areas has already declined as a result of climate change (Durner et al. 2009, Ware et al. 2017). Survival rates of cubs, body condition of adult females, body size of young, litter mass, and yearling numbers have also exhibited declines in some regions of the Arctic (Stirling et al. 1999, Bromaghin et al. 2015). Together with the data from this study on the cost of activity and energy acquisition (Figures 4.3, 4.4), these studies suggest that an increasing proportion of bears are unable to meet their energy demands. The results from this study indicate that further increases in activity and movement resulting from declining and increasingly fragmented sea ice are likely to increase the demand side of the energy balance ratio (Durner et al. 2017). Inherently high energy demands create a physiological constraint that makes it difficult for polar bears to compensate for both increases in activity and declines in the availability of energy-dense prey as habitats become more fragmented (Sahanatien and Derocher 2012). Hence, increases in movement and activity rates mediated by the loss of sea ice habitat are likely to have negative cascading effects on polar bear reproductive success and, ultimately, their populations.

Table 4.1. Video recording schedules. GPS-equipped video camera collars deployed on female polar bears on the spring sea ice of the Beaufort Sea.

Year	Time of day[a]	Video recording duty cycle
2014	8 am – 1 pm	1 min : 2 min
2014	1 pm – 9 pm	30 sec : 2 min
2015	8 am – 1 pm	1 min : 2 min
2015	1 pm – 10 pm	30 sec : 2 min
2015[b]	8 am – 6 pm	1 min : 2min
2015[b]	6 pm – 10 pm	30 sec : 2 min
2016	8 am – 10 pm	1 min : 2 min

[a] Times are Alaska Daylight Time.

[b] Two collars in 2015 were set to record using the following duty cycle.

Table 4.2. Polar bear field metabolic rates (FMRs) and changes in body mass, body composition, and blood biochemistry.

Bear	Age (years)	Duration (days)	Initial mass (kg)	Final mass (kg)	% mass change	Initial relative fatness (fat/LBM[a])	LBM[a] loss/ gain (kg)	Fat loss/ gain (kg)	FMR (kJ kg^{-1} day^{-1})	Initial U/C[b] ratio	Final U/C[b] ratio
1	8	7.7	144.7	162.4	12%	0.20	--	--	227.9	8.8	37.6
2	5	9.9	163.7	171.9	5%	0.22	--	--	226.6	22.7	69.4
3	6	9.1	196.0	172.8	-12%	0.27	--	--	363.6	71.5	26.1
4	5	9.0	172.4	155.6	-10%	0.30	--	--	247.7	11.9	10.7
5	4	9.2	198.7	179.6	-10%	0.28	-0.3	-18.7	290.1	35.4	9.5
6	5	10.0	171.9	170.6	-1%	0.20	-0.1	-1.2	274.0	21.5	36.5
7	3	10.6	140.6	126.6	-10%	0.30	-9.1	-5	214.1	9.9	8.9
8	6	8.0	202.3	215.9	7%	0.26	3.1	10.5	402.1	36.96	22.59
9	22	8.9	190.1	220.4	16%	0.17	7.5	22.9	337.4	4.67	60.8

[a] Lean body mass (LBM).

[b] Urea/creatinine ratio (U/C). Values ≤10 are considered to be an indicator of fasting for >1 week.

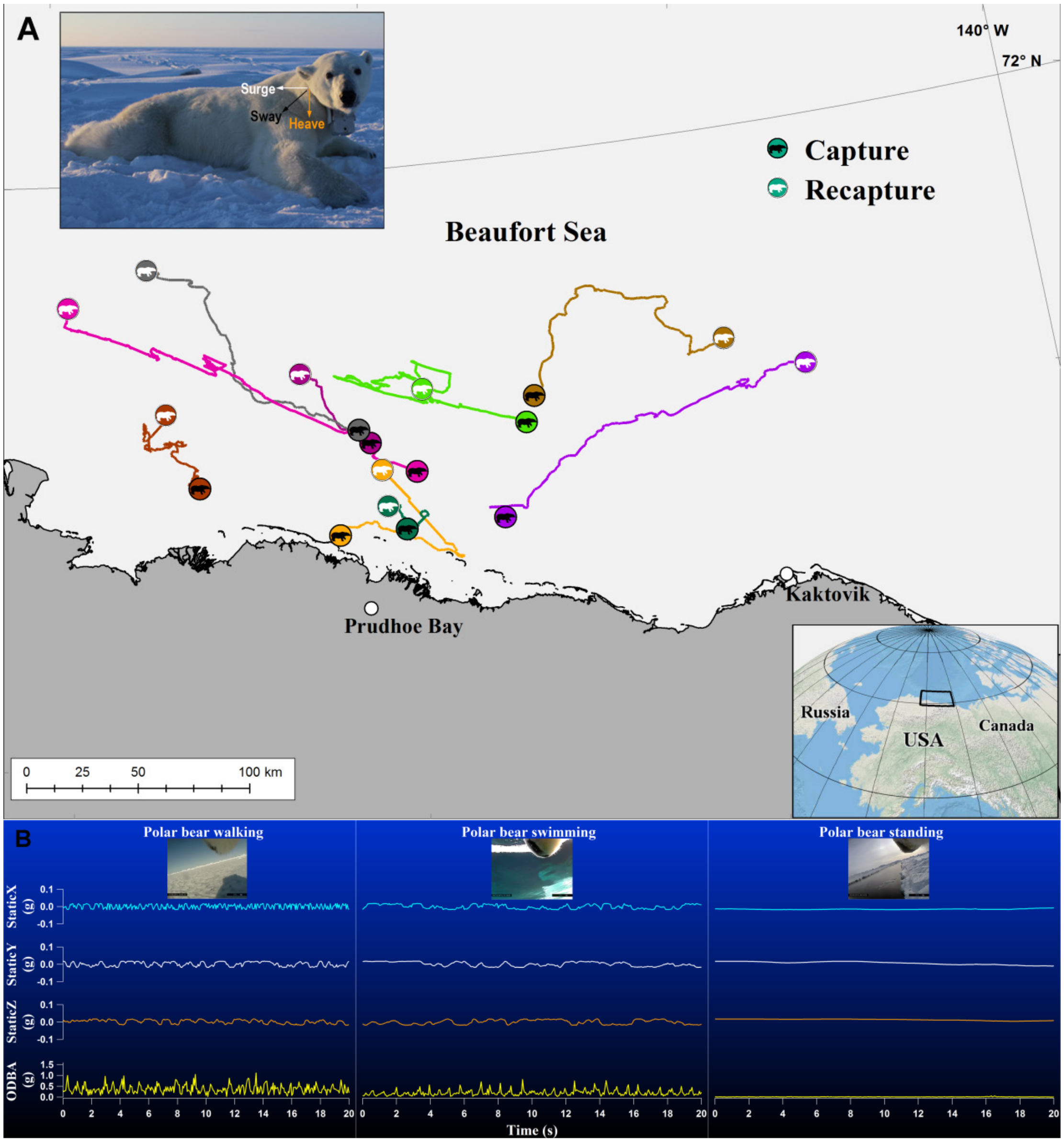

Figure 4.1. **Field movements and accelerometer signatures of polar bears in April 2014 to 2016**. **A.** Capture and recapture locations and GPS movement paths of nine female polar bears dosed with DLW and equipped with GPS-equipped video camera collars and archival loggers with tri-axial accelerometers and conductivity sensors. Gray area denotes land; white area shows sea ice cover. (Inset) Orientation of the accelerometer while attached to the video collar. **B.** Accelerometer signatures of static acceleration in the surge (x), heave (y), and sway (z) directions and overall dynamic body acceleration (ODBA) while walking, swimming, and standing. Images show the corresponding behaviors derived from the animal-borne video camera.

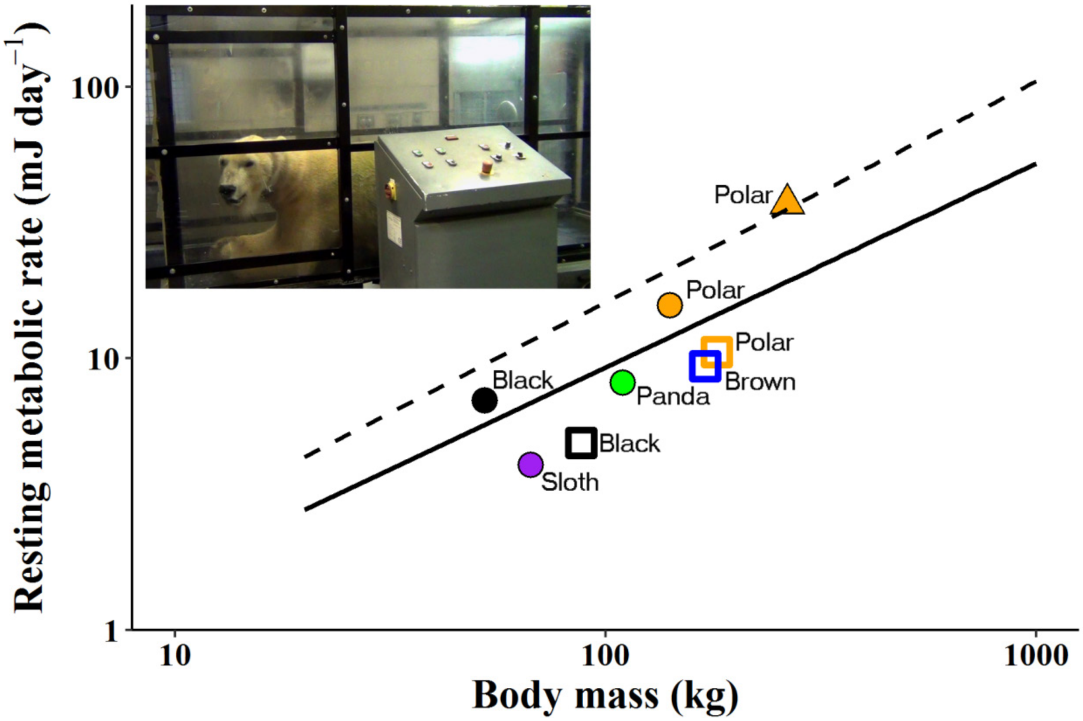

Figure 4.2. **Relationship between body mass and RMR in polar bears and other ursids.** RMR of an adult female polar bear (orange triangle, this study), compared with mean RMRs of subadult polar bears (orange circle), hibernating adult female polar bears (orange square), hibernating adult male grizzly bears (blue square), black bears (black circle), hibernating black bears (black square), adult and subadult panda bears (green circle), and female sloth bears (purple circle). Sources are available in the methods. The dashed line is the allometric regression for RMR in vertebrate-eating carnivores (McNab 1988). The solid line is the allometric regression for RMR in eutherian mammals (Kleiber 1975). (Inset) The adult female bear resting in the metabolic chamber from the present study.

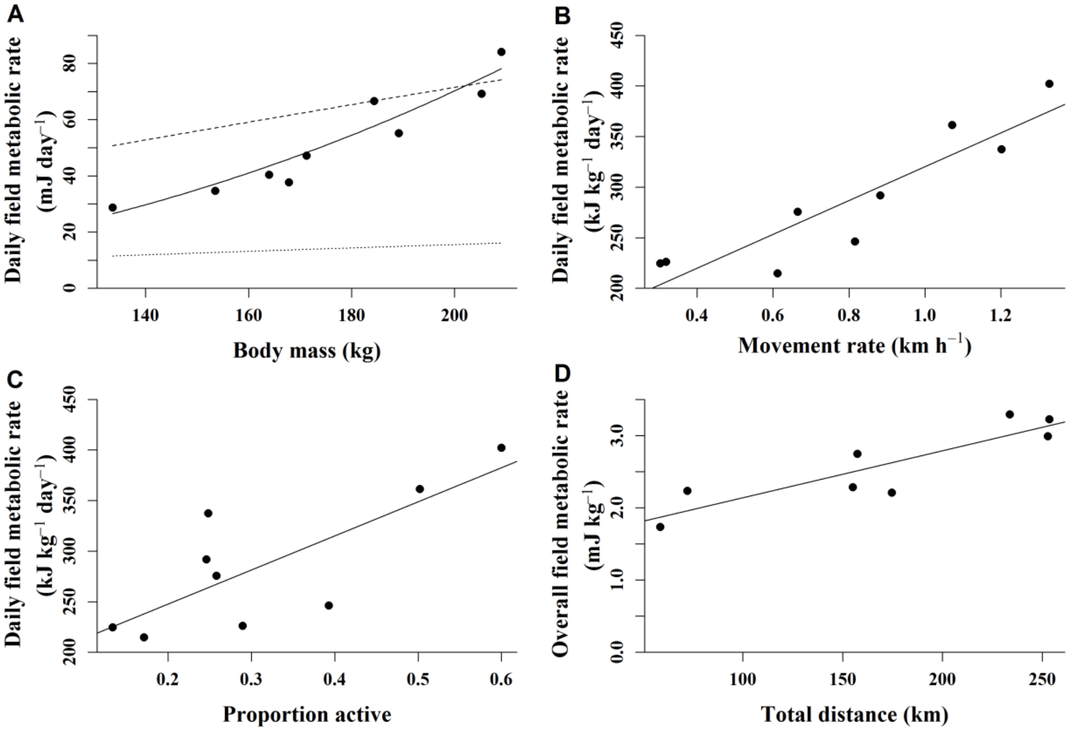

Figure 4.3. **FMR and overall FMR in relation to body mass, movement, and activity rate of polar bears. A.** Mean daily FMRs of female polar bears on the sea ice in relation to body mass. The allometric regression (solid line) is compared with predicted daily FMRs for marine and terrestrial mammalian carnivores (upper dashed line) (Nagy et al. 1999), and predicted daily RMRs (lower dotted line) (Kleiber 1975). **B.** Least squares regression (solid line) of mean daily mass-specific FMR in comparison with mean movement rate. **C.** Least squares regression (solid line) of mean daily mass-specific FMR in comparison with mean activity rate derived from video collars. **D.** Least squares regression (solid line) of overall mass-specific FMR in comparison with total distance moved over 8 to 11 days. Regression statistics are provided in the main text. Each point represents a single value for one bear in A. to D.

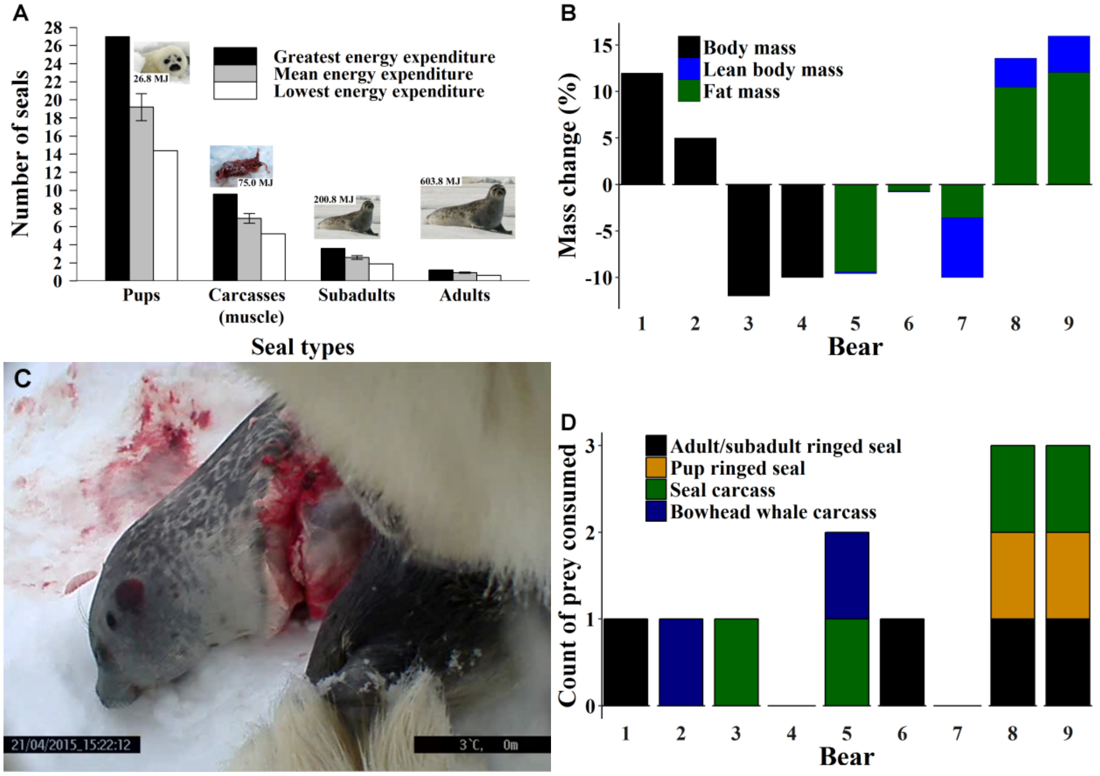

Figure 4.4. **Feeding demands, changes in body mass, and foraging success of polar bears. A.** Number of ringed seals required for a female polar bear to meet its energy demands over 10 to 12 days on the spring sea ice based on the greatest energy expenditure, mean (±SE) energy expenditure, and lowest energy expenditure. **B.** Changes in body mass, lean body mass, and fat mass of female polar bears on the sea ice over 8 to 11 days. Measures of changes in lean body mass and fat mass were only available for bears five to nine. Bar heights represent data for individual bears. **C.** Image of a polar bear eating a recently killed ringed seal. **D.** Prey type consumed by female polar bears. Bar heights represent data for individual bears.

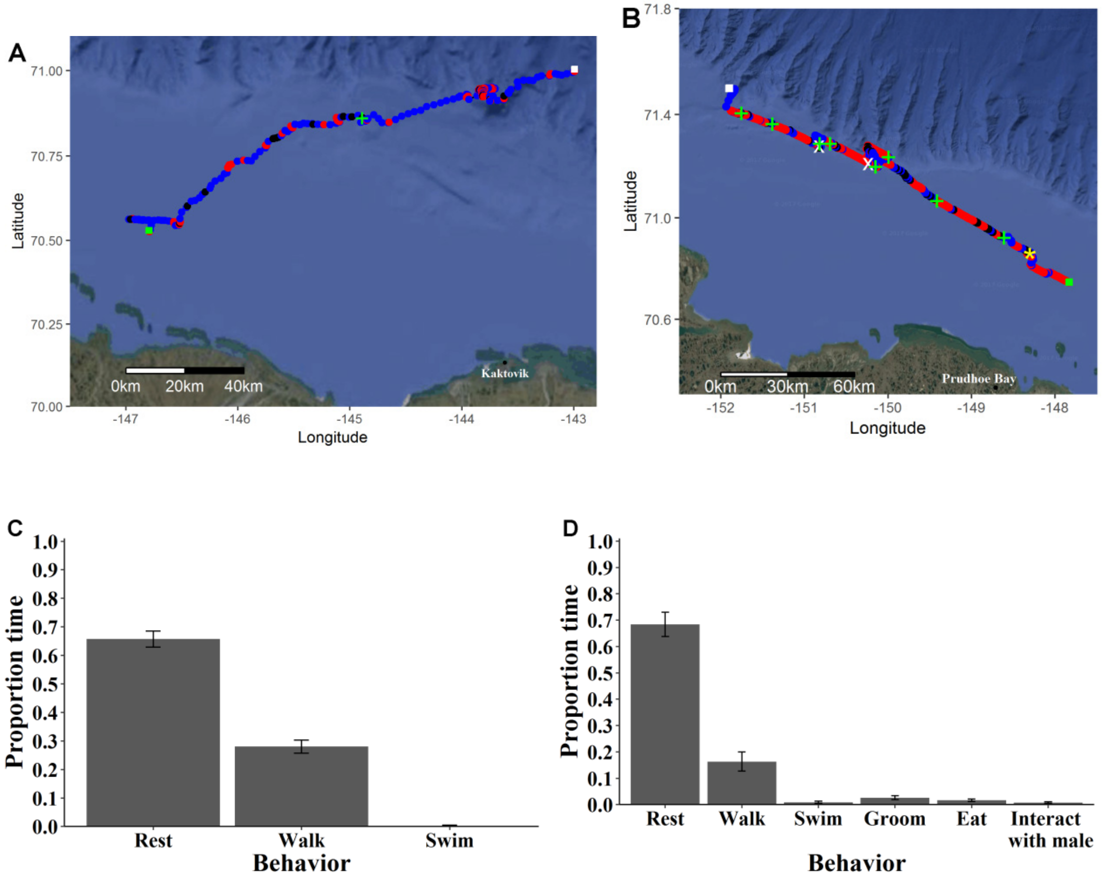

Figure 4.5. **Polar bear movement, foraging, and activity. A.** Movements of bear #3 over 9 days. **B.** Movements of bear #8 over 8 days. Figures show locations where bears were captured (green squares), recaptured (white squares), resting (red circles), walking (blue circles), exhibiting mixed behaviors (black circles), kill sites of seals (yellow asterisk), kills sites of seal pups (white crosses), or scavenging sites of seal carcasses (green pluses). **C.** Mean (± SE) activity using accelerometer data from 6 female polar bears over 8 – 11 days. **D.** Mean (± SE) daytime activity using video collar data from 9 female polar bears over 5 – 10 days.

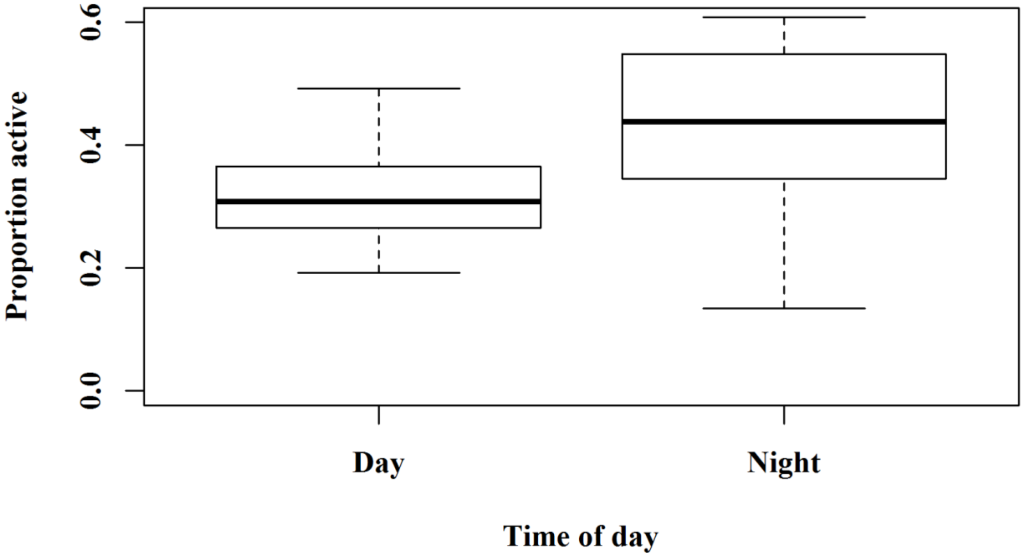

Figure 4.6. **Polar bear diel differences in activity.** Proportion of the day active (median, 1st and 3rd quartiles, maximum, and minimum) based on accelerometer data from 7 female polar bears on the spring sea ice of the southern Beaufort Sea over 8 – 13 days. Day was from sunrise to sunset and night was from sunset to sunrise.

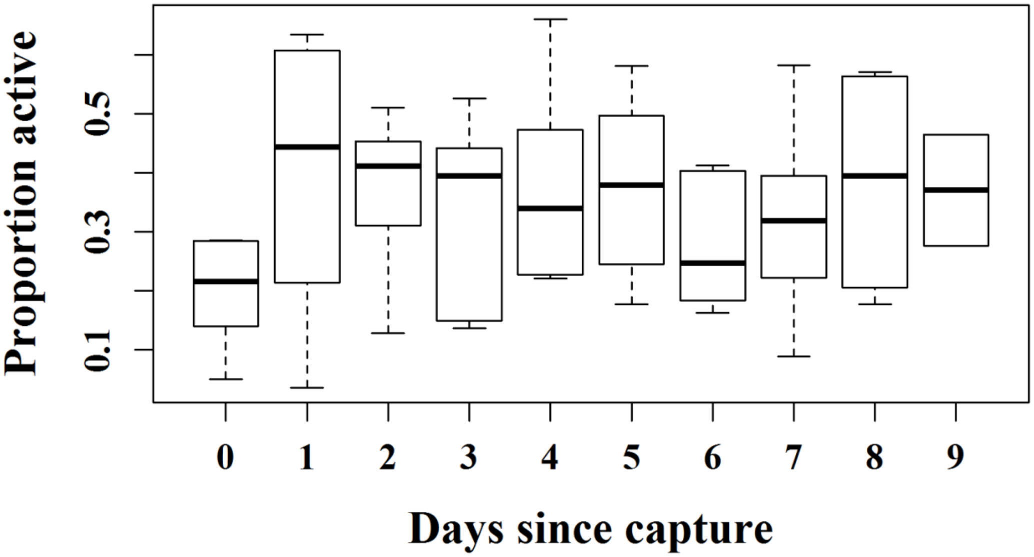

Figure 4.7. **Changes in polar bear activity post-capture**. Proportion of the time active (median, 1st and 3rd quartiles, maximum, and minimum) since capture based on accelerometer data from 6 female polar bears on the spring sea ice of the Beaufort Sea.

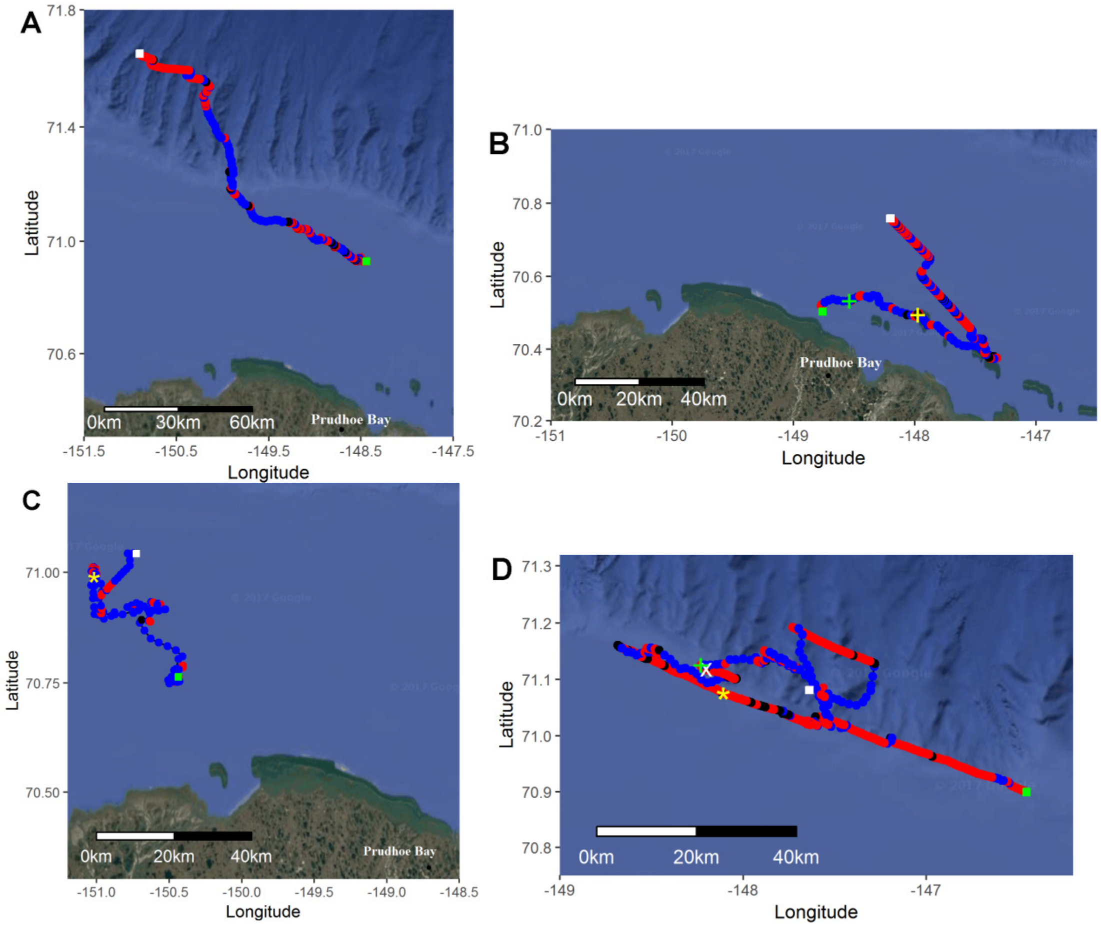

Figure 4.8. **Polar bear movement, activity, and foraging locations. A.** Movements of bear #7 over 11 days. **B.** Movements of bear #5 over 9 days. **C.** Movements of bear #6 over 10 days. **D.** Movements of bear #9 over 9 days. Figures show locations where bears were captured (green squares), recaptured (white squares), resting (red circles), walking (blue circles), exhibiting mixed behaviors (black circles), kill sites of seals (yellow asterisk), kill sites of seal pups (white crosses), scavenging sites of seal carcasses (green pluses), or scavenging sites of whale carcasses (yellow pluses).

Chapter 5

Estimating the energy expenditure of free-ranging mammals using tri-axial accelerometers: A validation with doubly-labeled water

ABSTRACT

Measures of energy expenditure can be used to inform animal conservation and management, but methods for measuring the energy expenditure of free-ranging animals have a variety of limitations. Advancements in biologging technologies have enabled the use of dynamic body acceleration derived from accelerometers as a proxy for energy expenditure. However, although dynamic body acceleration has been shown to strongly correlate with oxygen consumption in captive animals, it has been validated in only a few studies on free-ranging animals. I use relationships between oxygen consumption and overall dynamic body acceleration in resting and walking polar bears (*Ursus maritimus*) and published values of polar bear swimming costs to estimate the energy expenditure of 6 free-ranging polar bears on the sea ice of the Beaufort Sea. I compare these measures to simultaneous measures of energy expenditure on the same individuals derived from doubly-labeled water. I find accelerometer-based measures of energy expenditure averaged 30% less than measures derived from doubly labeled water. Nevertheless, accelerometer-based measures of energy expenditure strongly correlated ($r^2 = 0.70$) with measures derived from doubly labeled water. The findings from this study highlight the limitations in

dynamic body acceleration as a measure of energy expenditure while also further supporting its use as a proxy for energy expenditure in free-ranging animals.

INTRODUCTION

Energy expenditure is fundamental to animal movement ecology and influences survival and reproductive success and, hence, population dynamics (Brown et al. 2004). In particular, measures of energy expenditure can inform the mechanisms by which animals respond to environmental change (Wikelski and Cooke 2006). As a result, methods have been developed to measure animal energy expenditure in the field using electronic logging and tracking devices (Wilmers et al. 2015). For example, heart rate monitors (Boothby 1915, Krogh and Lindhard 1917, Butler et al. 1992) and more recently accelerometers have been developed as a proxy for energy expenditure (Wilson et al. 2006). Similar to heart rate monitors (Butler et al. 2004), accelerometers can be calibrated with measures of oxygen consumption as a means to quantify overall energy expenditure (e.g., Wilson et al. 2006, 2012, Halsey et al. 2009*b*, 2011*b*, Gómez Laich et al. 2011).

This method has been termed dynamic body acceleration (Wilson et al. 2006), which represents the rate of change in velocity as a result of animal body movements (Shepard et al. 2008). The method is based on the concept that dynamic body acceleration provides a measure of mechanical work performed by locomotor muscles (Wilson et al. 2006, Gleiss et al. 2011). This relies on the assumption that movement is the primary factor influencing variability in energy expenditure (Costa and Williams 1999, Wilson et al. 2006, Gleiss et al. 2011). Nevertheless, Green et al.

(2009*b*) found that dynamic body acceleration could also strongly predict energy expenditure during inactivity in birds. When dynamic body acceleration is summed across 3 dimensions it has been termed overall dynamic body acceleration (ODBA), which provides a means to quantify body movement in all directions at the center of mass (Wilson et al. 2006). The advantages of the dynamic body acceleration method are that accelerometers can be externally attached, can potentially record for extended durations, and they can provide detailed short-term measures of energetic costs (Wilson et al. 2006, Gleiss et al. 2011, Halsey et al. 2011*a*, Williams et al. 2014). This has considerable benefits in reducing the invasiveness of the device, which should reduce the potential for injury (Green et al. 2009*b*) and reduce the potential for influencing the animal's behavior or energy expenditure (but see Walker and Boveng 1995, Wilson 2011, Maresh et al. 2014, Vandenabeele et al. 2014, Chivers et al. 2016). As a result, this approach is increasingly being used as a proxy for energy expenditure in free-ranging animals (Halsey and White 2010, Wilson et al. 2012, Williams et al. 2014, 2016, Bishop et al. 2015, Enstipp et al. 2016, Scharf et al. 2016, Wang et al. 2017, Wilmers et al. 2017, Grémillet et al. 2018). Despite the potential utility of accelerometers, the validity of dynamic body acceleration for measuring energy expenditure in free-ranging animals has only been tested in a few studies (Elliott et al. 2013, Stothart et al. 2016, Jeanniard-du-dot et al. 2017).

In contrast, the doubly-labeled water (DLW) method (Lifson et al. 1955, 1966) is the most widely used technique for measuring energy expenditure in free-ranging animals (Nagy 1989, Speakman 1997, Halsey et al. 2011*a*). The DLW method provides a direct average estimate of CO_2 production over an interval of time, which can be used in place of oxygen consumption to estimate metabolic rates (Speakman 1997). The method involves injecting a dose of water containing the isotopes ^{2}H or ^{3}H and ^{18}O to determine the rate of CO_2 production over the measurement period. The difference between the turnovers of the oxygen and hydrogen isotopes provides a measure of CO_2 production because ^{18}O declines from the body as both respiratory CO_2 (efflux) and water influx while ^{2}H or ^{3}H decline solely as a result of water influx (Costa 1987, 1988, Speakman 1997). The biggest advantages of the DLW method are that it does not require calibration from captive animals and it can be used directly on animals in the field. However, the use of DLW entails a variety of assumptions (Nagy 1980, Costa 1987, Speakman 1997, Butler et al. 2004), it typically requires capturing and sampling individuals on two occasions within a specific time frame, and it only provides an average of metabolic data during the period between equilibration at initial capture and final enrichment at recapture. Hence, the DLW method is only useful over relatively short time frames and it provides a single average measure of energy expenditure making it difficult to assess the energetic costs of specific behaviors (Costa 1988, Speakman 1997, Butler et al. 2004). Furthermore, the purchase of ^{18}O can be expensive (Speakman 1997). Thus, the DLW method is often unsuitable or cost-prohibitive for most field studies of large mammals. Nevertheless, the DLW method can be used to evaluate alternative measures of energy expenditure such as the dynamic body acceleration method as a means of measuring the energy expenditure of free-ranging animals.

Studies examining energy expenditure in free-ranging thick-billed murres (*Uria lomvia*) and pelagic cormorants (*Phalacrocorax pelagicus*), found dynamic body acceleration strongly correlated ($r^2 = 0.73$ and 0.91, respectively) with energy expenditure measured by DLW, indicating accelerometers can provide accurate measures of free-ranging bird energetics (Elliott et al. 2013, Stothart et al. 2016). Yet, a study in free-ranging northern (*Callorhinus ursinus*) and Antarctic fur seals (*Arctocephalus gazelle*), found measures of dynamic body acceleration needed to be paired with time activity budgets in order to strongly predict total energy expenditure measured by DLW (Jeanniard-du-dot et al. 2017). These studies suggest that dynamic body acceleration has promise as a measure of energy expenditure in free-ranging animals, but they also suggest some potential variability among taxa or among behaviors. However, while these studies examined the relationship between dynamic body acceleration and energy expenditure, they did not first determine the relationship between dynamic body acceleration and oxygen consumption and use that relationship as a measure of energy expenditure (e.g., Wilson et al. 2006, Halsey et al. 2009*b*, 2011*b*, Williams et al. 2014) in comparison to measures derived from DLW.

I evaluate the use of ODBA from tri-axial accelerometers to measure the energy expenditure of free-ranging female polar bears (*Ursus maritimus*) on the sea ice of the Beaufort Sea based on simultaneous measures of their energy expenditure derived using DLW (Chapter 4). The behaviors and activity rates of these individuals were identified based on a previously developed random forest model using tri-axial accelerometer and conductivity sensor data (Chapter 1). A relationship between oxygen consumption and ODBA was developed based on simultaneous measures collected from captive adult female polar bears resting and walking on a treadmill (Chapter 2). Energetic costs of swimming were derived from modeled estimates from internal body temperature data from free-ranging polar bears while swimming (Griffen 2018). The ability of accelerometer-derived measures of energy expenditure were evaluated in comparison to measures derived using DLW. Measures of daily energy expenditure derived from DLW were further compared to mean ODBA, mean activity rates, mean movement rates, and mean body mass to assess whether accelerometer-derived measures of energy expenditure offer an improvement over other metrics.

METHODS

Data were collected from free-ranging subadult and adult female polar bears without dependent young on the sea ice of the Beaufort Sea as part of a previous study (Chapter 4) in April 2014, 2015, and 2016. Details of the capture methods, use of doubly-labeled water, and deployment of satellite collars with tri-axial accelerometers are described in Chapter 4. Briefly, polar bears were located from a helicopter and immobilized with a rapid-injection dart (Palmer Cap-Chur Equipment, Douglasville, GA) containing zolazepam-tiletamine (Telazol®) (Stirling et al. 1989). Following immobilization, I weighed bears using an electronic load cell suspended from an aluminum tripod. Bears that had not been previously captured were aged based on counts of cementum annuli from an extracted vestigial premolar (Calvert and Ramsay, 1998; C-D & Associates Biological Consulting, Spruce Grove, Alberta, Canada). Procedures were approved by the Animal Care and Use Committees of the University of California, Santa Cruz and the U.S. Geological Survey, Alaska Science Center. Research was authorized under U.S. Fish and Wildlife Service Marine Mammal Permit MA690038.

Following immobilization, an initial blood sample was collected to serve as a baseline measure of ^{18}O (oxygen-18) and ^{2}H (deuterium). The bear was then injected intravenously with a precisely weighed dose containing 0.12 – 0.25 g kg^{-1} of 97% enriched ^{18}O (Isoflex USA, San Francisco, CA, USA) and 0.06 – 0.10 g kg^{-1} of 99.9% enriched ^{2}H (Isotec, Inc., Miamisburg, OH, USA or Cambridge Isotope Laboratories, Inc., Tewksbury, MA, USA) with NaCl added to make it 0.9% isotonic and sterilized using a 0.2 µ Millipore filter. On injection, the syringe was back washed with blood three times to ensure all the DLW had been injected into the bear. The bear was kept immobilized for 2 hours after the injection of DLW to allow isotope equilibration (Pagano et al. 2017). I recaptured bears 8 – 11 days later to obtain a blood sample to measure final enrichment. At recapture, I weighed bears to measure changes in body mass.

Serum samples were analyzed for the concentrations of ^{18}O and ^{2}H (Metabolic Solutions, Inc., Nashua, NH, USA). I calculated CO_2 production using the plateau method and Speakman's two-pool equation (Speakman 1997), which has been shown to be best suited for large mammals [(Speakman 1997, Speakman et al. 2001, Sparling et al. 2008), but see (Dalton et al. 2014)]. I used the mean group dilution space ratio in calculating CO_2 production (Speakman 1997). I converted CO_2 production to metabolic rate using a respiratory quotient of 0.76 (26.32 kJ per liter CO_2) (Chapter 4).

I deployed GPS-equipped video camera collars (Exeye, LLC., Bristow, VA, USA) and archival loggers (TDR10-X-340D, Wildlife Computers Inc., Redmond, WA) on the same individuals dosed with DLW (see Chapter 4 for additional information). To evaluate differences in mean movement rates (km hr^{-1}) among bears, I used a continuous time correlated random walk (CRAWL) model (Johnson et al. 2008, Johnson 2016) in program R (R Core Team 2014) to predict locations on a 30 minute interval based on GPS locations. I calculated minimum distance travelled between two successive predicted locations as the great-circle distance (i.e., distance accounting for the earth's curvature), and calculated movement rate by dividing distance by the duration between predicted locations (i.e., 30 minutes) in SAS (version 9.3, SAS Institute Inc., Cary, NC, USA).

Archival loggers recorded tri-axial acceleration ($m \cdot s^{-2}$) at 16 Hz (range ±20 $m \cdot s^{-2}$), time-of-day, and wet/dry conductions at 1 Hz (via an on-board conductivity sensor) continuously from the time of deployment until recovery. Behaviors were derived from the accelerometer and conductivity data using a random forest algorithm (Breiman 2001) in R ('RandomForest' package) (Chapter 1). To calculate dynamic body acceleration, I converted accelerometer measures from $m \cdot s^{-2}$ to g ($1\ g = 9.81$ $m \cdot s^{-2}$). I used a 2 s running mean of the raw acceleration data to calculate static acceleration (gravitational acceleration) and subtracted the static acceleration from the raw acceleration data to calculate dynamic acceleration (Wilson et al. 2006, Shepard et al. 2008). I calculated ODBA as the absolute sum of dynamic acceleration across the 3 axes (Wilson et al. 2006).

Energy expenditure during non-swimming movements were based on the relationship between ODBA and oxygen consumption ($\dot{V}O_2$) derived in Chapter 2. However, I found a negative intercept between ODBA and $\dot{V}O_2$ and suggested this relationship needed to be further developed (Chapter 2). This negative intercept may have been related to head movements of the bears during resting $\dot{V}O_2$ and ODBA measurements. To correct for this, I measured the mean ODBA of 3 captive adult female polar bears while resting and motionless in their exhibits (Chapter 1) and assigned them the mean mass-specific RMR summarized in Chapter 2 from 3 separate studies (0.230 ml O_2 g^{-1} h^{-1}). I incorporated these 3 measures with the previous measures determined in Chapter 2 and found $\dot{V}O_2$ (ml O_2 g^{-1} h^{-1}) increased linearly as a function of ODBA (g) where: $\dot{V}O_2 = 0.07 + 1.90 \times \text{ODBA}$ ($r^2 = 0.71$, $p < 0.001$, $n = 21$, Figure 5.1). For swimming movements, I used the mean swimming metabolic rate determined by Griffen (2018) (2.75 ml O_2 g^{-1} h^{-1}). Measures of $\dot{V}O_2$ were converted to metabolic rate using the standard conversion factor of 20.083 J ml^{-1} O_2 (Schmidt-Nielsen 1997). These relationships were then applied to the archival logger data recovered from the same free-ranging individuals that were dosed with DLW to measure their total energy expenditure (mJ kg^{-1}) in SAS. Total energy expenditure was converted to daily energy expenditure by dividing by the total number of days each animal was studied.

Analyses

I used paired *t*-tests to compare estimates of daily energy expenditure (kJ kg^{-1} day^{-1}) measured by DLW and estimates derived from the accelerometer-based relationships. Least-squares linear regression were then used to evaluate the relationship between daily energy expenditure measured by DLW and estimates derived from the accelerometer-based relationships. Least-squares linear regression were further used to evaluate the relationships between daily energy expenditure (kJ kg^{-1} day^{-1}) derived from DLW and 1) mean ODBA (*g*), 2) mean activity rate (%), 3) mean movement rate (km hr^{-1}), and 4) mean body mass (kg). I considered differences of $P \leq 0.05$ to be significant. Lastly, I used general linear models to assess whether a combination of these variables might provide improved estimates of daily energy expenditure derived from DLW. Given the small sample size of this dataset, I limited these models to ≤ 2 explanatory variables. The small-sample extension of Akaike's Information Criterion (AIC_c) was used to rank models from best to least supported (Burnham and Anderson 2002). All analyses were conducted in program R (R Core Team, 2014)

RESULTS

I captured 4 adult female polar bears in 2014, 3 adult female and 1 subadult female polar bears in 2015, and 2 adult female polar bears in 2016. I recaptured bears 8 – 11 days later to obtain a blood sample to measure final enrichment and recover collars and archival loggers. In 2015, I was unable to recapture 1 adult female to measure her final enrichment. Additionally, three of the archival loggers deployed in

2014 failed within 12 hours of deployment. I excluded data from these 4 bears from analyses. Consequently, I had a sample of 6 female polar bears who provided simultaneous measures of energy expenditure derived from DLW and continuous measures of tri-axial acceleration (Table 5.1).

Daily energy expenditure derived from DLW ranged from 1.2 to 1.7 times greater than estimates derived from the accelerometer-based relationships ($\bar{x} = 1.4$, SE = 0.07, Table 5.1). As a result, daily energy expenditure derived from DLW differed significantly from estimates derived from the accelerometer-based relationships ($t_5 = 6.1$, $P = 0.002$). Nevertheless, daily energy expenditure estimates derived from the accelerometer-based relationships accounted for 70% of the variation in daily energy expenditure estimates derived from DLW ($P = 0.039$, $n = 6$, Figure 5.2A). Similarly, mean ODBA accounted for 70% of the variation in daily energy expenditure estimates derived from DLW ($P = 0.039$, $n = 6$, Figure 5.2B). Mean activity rate did not significantly explain variation in daily energy expenditure estimates derived from DLW ($r^2 = 0.60$, $n = 6$, $P = 0.069$). Mean movement rate accounted for 88% of the variation in daily energy expenditure estimates derived from DLW ($P = 0.005$, $n = 6$, Figure 5.2C). Mean body mass accounted for 77% of the variation in daily energy expenditure estimates derived from DLW ($P = 0.02$, $n = 6$, Figure 5.2D). The best-supported model (AIC_c weight = 0.37) included only mean movement rate as an explanatory variable and models with 2 explanatory variables received no support (Table 5.2).

DISCUSSION

An animal's energy expenditure is a function of its basal metabolism, specific dynamic action, thermoregulation, reproduction, growth, and locomotion (Fig. 6.3) (Nagy 1989, Costa and Williams 1999). A previous study using the same doubly-labeled water measures of energy expenditure found energy expenditure to be influenced by body mass, movement rate, activity, and total distance traveled (Chapter 4), which suggests that basal metabolism and movement costs were primary determinants of energy expenditure in this species. However, the discrepancies I found between energy expenditure determined via DLW and the accelerometer-based relationships suggest the potential influence of other costs on energy expenditure, such as specific dynamic action, thermoregulation, growth, and reproduction (Fig. 6.3). These costs are inherently incorporated within DLW estimates, but variability in these costs could not be accounted for with the methods I used in the estimates derived from the accelerometer-based relationships (Fig. 6.3). Five of the 6 bears in this study were adults and all of the bears were independent females without cubs. Hence, growth and reproduction likely had minimal impacts on energy expenditure. Conversely, specific dynamic action was likely an important factor as 5 of the bears in this study either scavenged from seal and bowhead whale (*Balaena mysticetus*) carcasses or caught and ate adult/subadult ringed seals (*Pusa hispida*) and only 1 bear fasted for the duration of the study (Chapter 4). Yet, even the bear that fasted was estimated to have 1.4 times greater energy expenditure based on DLW than estimates derived from the accelerometer-based relationships. Ambient temperatures during the period of this study ranged from 1.7 – -33.9 °C. Best (1976) estimated that the thermoneutral zone for a 200 kg polar bear may range from 37 – -50 °C while resting, which suggests that the effect of thermoregulation on the energy expenditure of the bears in this study would be expected to be minimal. Furthermore, the bears in this study spent only 0.3% of the time in the water (Chapter 4) (where thermoregulation costs may be greater). Thus, other potential factors appear to be contributing to the discrepancies I found in measuring energy expenditure between the two methods.

The relationship between $\dot{V}O_2$ and ODBA that I developed on a treadmill was limited to a maximum speed of 3 km hr^{-1}, which may have limited the ability to predict energy expenditure at greater speeds. However, in polar bears, $\dot{V}O_2$ has been shown to increase linearly at speeds up to 5.4 km hr^{-1} (Chapter 2) and free-ranging polar bears, including the bears in this study, rarely exceed this speed (Whiteman et al. 2015, Chapter 2). However, the relationship between ODBA and $\dot{V}O_2$ is known to differ depending upon the incline an animal is moving on (Halsey et al. 2008), which would require further calibration at varying inclines and determination of the slope at which animals are moving in the field (Gleiss et al. 2011). Additionally, it is assumed that the relationship between $\dot{V}O_2$ and ODBA derived on a treadmill will follow similar trends in the field. Yet, field movements are known to impose greater energetic costs relative to movements on a treadmill and in humans dynamic body acceleration has been shown to underestimate field measurements of $\dot{V}O_2$ (Bidder et al. 2017). The results of this study further suggest that dynamic body acceleration may underestimate field measurements. The disparity I found in energy expenditure derived from the accelerometer-based relationships reinforces some of the potential limitations in using dynamic body acceleration as a measure of energy expenditure in free-ranging animals (Green et al. 2009*a*, Halsey et al. 2011*a*, Adachi et al. 2014, Dalton et al. 2014, Bidder et al. 2017, Jeanniard-du-dot et al. 2017).

Nevertheless, measures of energy expenditure derived from the accelerometer-based relationships and mean ODBA both strongly correlated with energy expenditure derived from DLW. This highlights the potential value of dynamic body acceleration as a proxy of energy expenditure because locomotion costs typically account for most of the variability in energy expenditures in free-ranging animals (Costa and Williams 1999, Wilson et al. 2006, Gleiss et al. 2011). Although mean movement rate and body mass provided even stronger correlations with energy expenditure, these metrics have their own limitations. To measure potential changes in energy expenditure, measures of body mass requires repeated sampling of individuals, which is one of the limitations in the use of DLW itself. Movement rates can be calculated from satellite telemetry location data, but for polar bears, movement rates derived by satellite telemetry can be biased by sea ice drift (Mauritzen et al. 2003*b*, Platonov et al. 2014, Auger-Méthé et al. 2016, Durner et al. 2017). Although such effects were likely minimal in the region and month of this study (Durner et al. 2017), research indicates such bias would be more prevalent in other regions and months (Durner et al. 2017). Furthermore, movement rates are typically calculated from infrequent location data and can underestimate true movement paths and rates (Kramer and McLaughlin 2001, Rowcliffe et al. 2012, Prichard et al. 2014, Bidder et al. 2015). Conversely, measures of dynamic body acceleration are typically recorded at high frequencies and, hence, should better reflect an animal's true movements (Wilson et al. 2013, Bidder et al. 2015). Measures of tri-axial acceleration can also be used to simultaneously determine animal behavior, which can provide additional insight into animal movement ecology and conservation (Cooke et al. 2014).

Although I highlight some potential limitations in the use of dynamic body acceleration as a measure of energy expenditure, I recommend future research further explore the potential for dynamic body acceleration to measure energy expenditure in free-ranging animals. Due to the expense of DLW isotopes and the logistical constraints of working with large carnivorous mammals in the Arctic, the sample size in this study was limited. Furthermore, although the bears in this study spent <1% of the time swimming, the energetic costs of swimming in polar bears has yet to be directly measured. The use of ODBA as a measure of energy expenditure relies on the premise that measures of acceleration represent movements at the animal's center of mass (Wilson et al. 2006, Gleiss et al. 2011). Similar to other studies, I used tri-axial accelerometers mounted to collars at the neck to measure ODBA (e.g., Halsey et al. 2008, 2009*b*, Qasem et al. 2012, Williams et al. 2014). However, it is unknown whether the relationships I derived might have been influenced by attachment on the collar and if I would have found improved relationships with the accelerometer mounted directly on the animal's trunk. Additionally, DLW measures of energy expenditure themselves are known to contain some error. Nagy (1989) and Speakman (1997) reported this error to average 4% and 3.1% in mammals, respectively.

However, individual error may be as high as 44% (Butler et al. 2004, Sparling et al. 2008, Dalton et al. 2014). Hence, the discrepancies I found in correlations with energy expenditure derived from accelerometer-based relationships may in part be due to errors in the DLW estimates themselves. Future research exploring these topics would help to improve the accuracy and reliability of measures of energy expenditure in free-ranging mammals. Nevertheless, the findings from this study indicate that while relationships between dynamic body acceleration and $\dot{V}O_2$ underestimate the energy expenditure of free-ranging polar bears, dynamic body acceleration can provide a reasonable proxy for the energy expenditure of free-ranging mammals. However, given the lack of current methods using dynamic body acceleration to account for changes in non-activity related costs, I recommend future research explore the potential for dynamic body acceleration to quantify such costs. Alternatively, dynamic body acceleration could be used solely as a measure of activity costs, excluding other energetic costs, which would provide more representative measures of activity-related energy expenditure.

Table 5.1. Polar bear age, duration studied, mean body mass, field metabolic rates (FMRs) derived from doubly-labeled water (DLW), FMRs derived from accelerometer-based relationships (ACC), and mean measures of overall dynamic body acceleration (ODBA).

Bear	Age (years)	Duration (days)	Mean mass (kg)	DLW - FMR (kJ kg^{-1} day^{-1})	ACC - FMR (kJ kg^{-1} day^{-1})	Mean ODBA (*g*)
1	6	9.1	184.4	363.6	282.7	0.274
2	4	9.2	189.2	290.1	243.1	0.231
3	5	10.0	171.3	274.0	182.4	0.168
4	3	10.6	133.6	214.1	155.1	0.135
5	6	8.0	209.1	402.1	269.7	0.256
6	22	8.9	205.3	337.4	199.1	0.186

Table 5.2. Model comparisons of mean movement rate (Rate), mean body mass (Mass), daily energy expenditure estimates derived from tri-axial accelerometer data (AccelerometerEnergy), mean overall dynamic body acceleration (ODBA), and mean activity rate (Activity) to explain the daily energy expenditure of free-ranging female polar bears based on measurements from DLW. Results are presented for all models with AIC_c weight > 0.

Model	ΔAIC_c	AIC_c weight
Rate	0.00	0.37
Mass	0.32	0.32
AccelerometerEnergy	2.08	0.13
ODBA	2.09	0.13
Activity	4.06	0.05

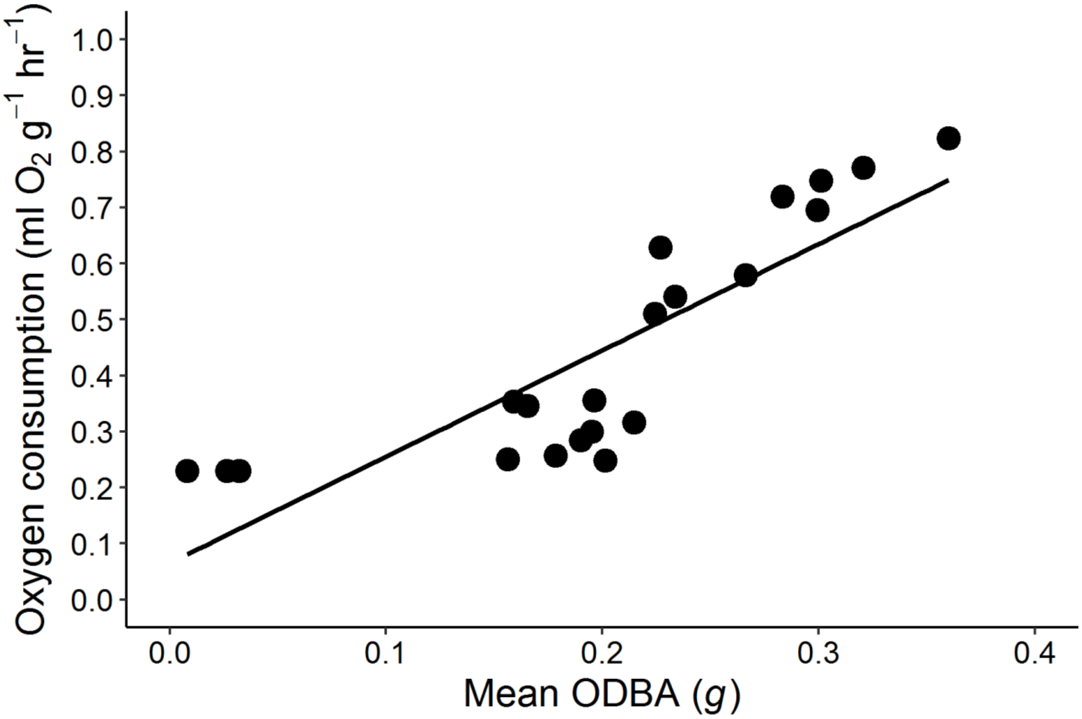

Figure 5.1. Least-squares regression of mass-specific oxygen consumption and mean overall dynamic body acceleration (ODBA) from 2 adult female polar bears resting and walking on a treadmill and 3 adult female polar bears resting on exhibit. Regression statistics are provided in the main text.

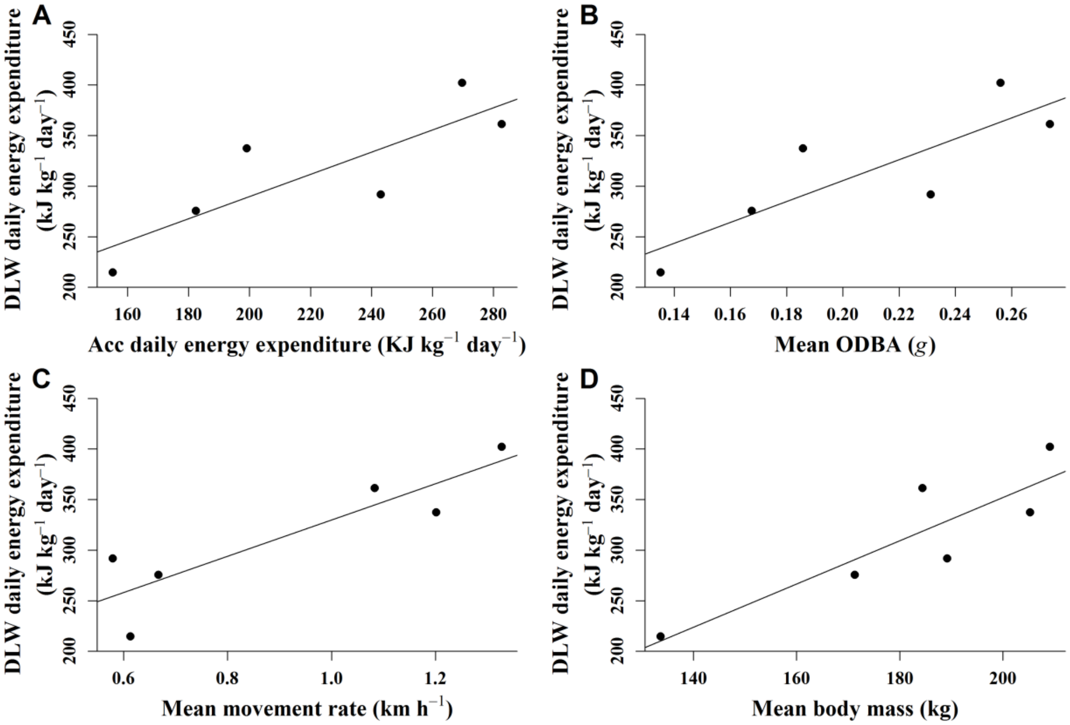

Figure 5.2. Mass-specific energy expenditure in relation to accelerometer-derived estimates, overall dynamic body acceleration (ODBA), movement, and body mass of polar bears. **A.** Least squares regression (solid line) of mean daily mass-specific energy expenditure of female polar bears on the sea ice measured by DLW in comparison to mean daily mass-specific energy expenditure of the same individuals from accelerometer-derived relationships (Acc). **B.** Least squares regression (solid line) of mean daily mass-specific energy expenditure of female polar bears on the sea ice measured by DLW in comparison to mean ODBA. **C.** Least squares regression (solid line) of mean daily mass-specific energy expenditure of female polar bears on the sea ice measured by DLW in comparison to mean movement rate. **D.** Least squares regression (solid line) of mean daily mass-specific energy expenditure of female polar bears on the sea ice measured by DLW in comparison to mean body mass. Regression statistics are provided in the main text. Each point represents a single value for one bear.

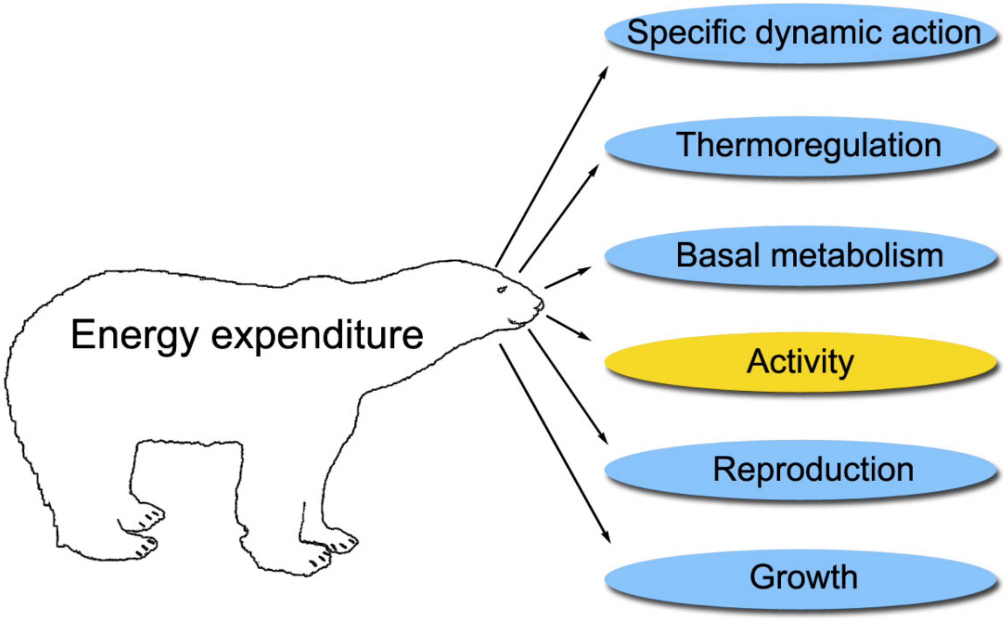

Figure 5.3. Conceptual chart showing the energetic pathways making up an animal's overall energy expenditure. The DLW method measures potential changes in energy expenditure across all of these pathways. Conversely, the accelerometer method only accounts for potential changes in energy expenditure that result from changes in activity.

SYNTHESIS

Polar bears exhibit high energy demands typical of large mammalian carnivores (Chapter 4). This high energy demand has imposed a diet specialization, making polar bears reliant on energy-dense pagophilic seal prey (Chapter 4). As the largest walking carnivore, this high energy demand makes them more vulnerable to environmental perturbations than smaller carnivores (Van Valkenburgh 1999, Van Valkenburgh et al. 2004, Carbone et al. 2007). Other species of carnivores that have displayed selection for large body size and hypercarnivory have exhibited increased risk of extinction due to environmental change (Van Valkenburgh 1999, Van Valkenburgh et al. 2004). Van Valkenburgh (1999:487) describes the risk in such specialization, "Natural selection is not prescient, and adaptations for current conditions may prove detrimental when the environment changes, particularly if those adaptations involve significant specialization."

The Arctic is undergoing rapid environmental change (Overpeck et al. 1997, Walsh 2008, Kaufman et al. 2009). Spring break-up of sea ice is occurring earlier, fall freeze-up is occurring later, and the sea ice minimum extent in September is decreasing at a rate of 14% per decade, which is twice the rate it decreased from 1979–2001 (Stroeve et al. 2014). The Arctic sea ice is also exhibiting increases in fragmentation (Sahanatien and Derocher 2012) and increases in sea ice drift (Durner et al. 2017). In some regions, these habitat changes have been linked with increases in activity, movements, land use, and long-distance swims in polar bears (Pagano et al.

2012, Atwood et al. 2016*b*, Durner et al. 2017, Pilfold et al. 2017). Although polar bears exhibit walking costs that are commensurate with other quadrupedal mammals, they have high costs of activity (Chapter 2) and appear to have high energetic costs of swimming (Chapter 3). Hence, increases in activity and swimming rates could greatly increase their energy expenditure (Chapter 4). Similar to extinct large bodied hypercarnivores (Van Valkenburgh 1999, Van Valkenburgh et al. 2004), polar bears appear physiologically-constrained in their ability to cope with forecasted declines in Arctic sea ice (Amstrup et al. 2008, Atwood et al. 2016*a*, Chapter 4).

Yet, sea ice dynamics and polar bear responses to sea ice conditions are not uniform (Amstrup et al. 2008, Rode et al. 2012, 2014*b*, Ware et al. 2017). Polar bears are managed as 19 subpopulations across the Arctic (Obbard et al. 2010). Genetic analyses indicate 4 discrete clusters of polar bears (Peacock et al. 2015), which are similar to the 4 polar bear ecoregions that were defined by Amstrup et al. (2008): the divergent ice, seasonal ice, archipelago, and convergent ice ecoregions. In the summer in the divergent ice ecoregion, the sea ice recedes to the north toward the polar basin and away from the continental shelf before refreezing again in the fall. This differs from other areas in the Arctic where the sea ice melts completely in the summer (seasonal ice ecoregion) or persists over the continental shelf throughout the summer (archipelago, convergent ice ecoregion) (Amstrup et al. 2008). Given this variability throughout the Arctic, data are needed at regional scales to understand how polar bears in different regions are responding to changes in sea ice conditions and changes in marine productivity (Arrigo et al. 2008, Rode et al. 2018).

This dissertation was conceived with the intent to develop metrics to quantify the energy expenditure of free-ranging polar bears to better understand the implications of ongoing declines in Arctic sea ice. The results from this dissertation will be used by the US Geological Survey to inform projections of future polar bear populations under scenarios of a changing climate (e.g., Amstrup et al. 2008, Atwood 2016*a*) and to inform polar bear conservation and management decisions (US Fish and Wildlife Service 2015). I provide a framework using tri-axial accelerometers to quantify polar bear behaviors and index their energy expenditure. Given their relatively small size and ability to collect data for extended durations, tri-axial accelerometers offer a tool to measure such parameters across multiple seasons. This has particular value given that bears are exhibiting divergent movement strategies in the summer and fall in which some bears are moving to land while others remain on the sea ice. Yet the energetic costs or benefits of remaining on the sea ice compared to moving to land remain unexplored. Additionally, little is known about the seasonal energy expenditure of these animals. The metrics used in this dissertation would enable such evaluations to assess the implications of declines in Arctic sea ice on polar bear behavior, energy expenditure, body condition, and ultimately their recruitment and survival. The results from this dissertation reinforce a reliance on a diet of energy-dense seal prey and suggest any potential disruptions in spring foraging success could dramatically reduce polar bear body condition leading to reduced reproductive success. Ultimately, access and abundance of seal prey will determine the ability of polar bears to compensate for declines in Arctic sea ice.

BIBLIOGRAPHY

Aars, J., and A. Plumb. 2010. Polar bear cubs may reduce chilling from icy water by sitting on mother's back. Polar Biology 33:557–559.

Aarseth, J. J., E. S. Nordøy, and A. S. Blix. 1999. The effect of body fat on basal metabolic rate in adult harp seals (*Phoca groenlandica*). Comparative Biochemistry and Physiology, Part A 124:69–72.

Adachi, T., J. L. Maresh, P. W. Robinson, S. H. Peterson, D. P. Costa, Y. Naito, Y. Y. Watanabe, and A. Takahashi. 2014. The foraging benefits of being fat in a highly migratory marine mammal. Proceedings of the Royal Society B: Biological Sciences 281:20142120.

Alvarenga, F. A. P., I. Borges, L. Palkovič, J. Rodina, V. H. Oddy, and R. C. Dobos. 2016. Using a three-axis accelerometer to identify and classify sheep behaviour at pasture. Applied Animal Behaviour Science 181:91–99.

Amstrup, S. C., B. G. Marcot, and D. C. Douglas. 2008. A Bayesian network modeling approach to forecasting the 21st century worldwide status of polar bears. Pages 213–268 *in* E. T. DeWeaver, C. M. Blitz, and L.-B. Tremblay, editors. Arctic sea ice decline: observations, projections, mechanisms, and implications. Geophysics monograph series 180. American Geophysical Union, Washington, D.C., USA.

Arnould, J. P. Y. 1990. The energetics of lactation in polar bears. Thesis, University of Saskatchewan, Saskatoon, Canada.

Arrigo, K. R., G. van Dijken, and S. Pabi. 2008. Impact of a shrinking Arctic ice cover on marine primary production. Geophysical Research Letters 35:L19603.

Atkinson, S. N., R. A. Nelson, and M. A. Ramsay. 1996. Changes in the body composition of fasting polar bears (*Ursus maritimus*): the effect of relative fatness on protein conservation. Physiological Zoology 69:304–316.

Atkinson, S. N., and M. A. Ramsay. 1995. The effects of prolonged fasting on the body composition and reproductive success of female polar bears (*Ursus maritimus*). Functional Ecology 9:559–567.

Atwood, T. C., B. G. Marcot, D. C. Douglas, S. C. Amstrup, K. D. Rode, G. M. Durner, and J. F. Bromaghin. 2016*a*. Forecasting the relative influence of environmental and anthropogenic stressors on polar bears. Ecosphere 7:1–22.

Atwood, T. C., E. Peacock, M. A. McKinney, K. Lillie, R. Wilson, D. C. Douglas, S. Miller, and P. Terletzky. 2016*b*. Rapid environmental change drives increased land use by an Arctic marine predator. PLoS ONE 11:e0155932.

Auger-Méthé, M., M. A. Lewis, and A. E. Derocher. 2016. Home ranges in moving habitats: polar bears and sea ice. Ecography 39:26–35.

Basu, I., D. Graupe, D. Tuninetti, P. Shukla, K. V. Slavin, L. V. Metman, and D. M. Corcos. 2013. Pathological tremor prediction using surface electromyogram and acceleration: potential use in “ON-OFF” demand driven deep brain stimulator design. Journal of Neural Engineering 10:36019.

Berta, A. 2012. Return to the sea: the life and evolutionary times of marine mammals. University of California Press, Berkeley, California, USA.

Best, R. C. 1976. Ecological energetics of the polar bear (*Ursus maritimus* Phipps

1774). Thesis, University of Guelph, Ontario, Canada.

Best, R. C. 1985. Digestibility of ringed seals by the polar bear. Canadian Journal of Zoology 63:1033–1036.

Bidder, O. R., C. Goulding, A. Toledo, T. A. Van Walsum, U. Siebert, and L. G. Halsey. 2017. Does the treadmill support valid energetics estimates of field locomotion? Integrative and Comparative Biology 57:301–319.

Bidder, O. R., L. A. Qasem, and R. P. Wilson. 2012. On higher ground: how well can dynamic body acceleration determine speed in variable terrain? PLoS ONE 7:e50556.

Bidder, O. R., J. S. Walker, M. W. Jones, M. D. Holton, P. Urge, D. M. Scantlebury, N. J. Marks, E. A. Magowan, I. E. Maguire, and R. P. Wilson. 2015. Step by step: reconstruction of terrestrial animal movement paths by dead-reckoning. Movement Ecology 3:23.

Biewener, A. A. 1989. Scaling body support in mammals: limb posture and muscle mechanics. Science 245:45–48.

Bishop, C. M., R. J. Spivey, L. A. Hawkes, N. Batbayar, B. Chua, P. B. Frappell, W. K. Milsom, T. Natsagdorj, S. H. Newman, G. R. Scott, J. Y. Takekawa, M. Wikelski, and P. J. Butler. 2015. The roller coaster flight strategy of bar-headed geese conserves energy during Himalayan migrations. Science 347:250–254.

Bivand, R., and N. Lewin-Koh. 2017. maptools: Tools for reading and handling spatial objects. R package.

Bograd, S. J., B. A. Block, D. P. Costa, and B. J. Godley. 2010. Biologging technologies: new tools for conservation. Introduction. Endangered Species Research 10:1–7.

Boothby, W. M. 1915. A determination of the circulation rate in man at rest and at work. American Journal of Physiology 37:383–417.

Breiman, L. 2001. Random forests. Machine Learning 45:5–32.

Brody, S. 1945. Bioenergetics and growth. Reinhold Publishing Corporation, New York, New York, USA.

Broell, F., T. Noda, S. Wright, P. Domenici, J. F. Steffensen, J.-P. Auclair, and C. T. Taggart. 2013. Accelerometer tags: detecting and identifying activities in fish and the effect of sampling frequency. Journal of Experimental Biology 216:1255–1264.

Bromaghin, J. F., T. L. McDonald, I. Stirling, A. E. Derocher, E. S. Richardson, E. V. Regehr, D. C. Douglas, G. M. Durner, T. Atwood, and S. C. Amstrup. 2015. Polar bear population dynamics in the southern Beaufort Sea during a period of sea ice decline. Ecological Applications 25:634–651.

Brown, D. D., R. Kays, M. Wikelski, R. Wilson, and A. P. Klimley. 2013. Observing the unwatchable through acceleration logging of animal behavior. Animal Biotelemetry 1:20.

Brown, J. C., and D. W. Yalden. 1973. The description of mammals - 2 Limbs and locomotion of terrestrial mammals. Mammal Review 3:107–134.

Brown, J. H., J. F. Gillooly, A. P. Allen, V. M. Savage, and G. B. West. 2004. Toward a metabolic theory of ecology. Ecology 85:1771–1789.

Bryce, C. M. 2017. Movement energetics across landscapes: a canid case study. Thesis, University of California, Santa Cruz, USA.

Bryce, C. M., and T. M. Williams. 2017. Comparative locomotor costs of domestic dogs reveal energetic economy of wolf-like breeds. Journal of Experimental Biology 220:312–321.

Burnham, K. P., and D. R. Anderson. 2002. Model selection and multimodel inference: a practical information-theoretic approach. 2nd edition. Springer, New York, New York, USA.

Butler, P. J. 2000. Energetic costs of surface swimming and diving of birds. Physiological and Biochemical Zoology 73:699–705.

Butler, P. J., J. A. Green, I. L. Boyd, and J. R. Speakman. 2004. Measuring meatabolic rate in the field: the pros and cons of the doubly labelled water and heart rate methods. Functional Ecology 18:168–183.

Butler, P. J., A. J. Woakes, I. L. Boyd, and S. Kanatous. 1992. Relationship between heart rate and oxygen consumption during steady-state swimming in California sea lions. Journal of Experimental Biology 170:35–42.

Calvert, W., and M. A. Ramsay. 1998. Evaluation of age determination of polar bears by counts of cementum growth layer groups. Ursus 10:449–453.

Campbell, H. A., L. Gao, O. R. Bidder, J. Hunter, and C. E. Franklin. 2013. Creating a behavioural classification module for acceleration data: using a captive surrogate for difficult to observe species. Journal of Experimental Biology 216:4501–4506.

Carbone, C., A. Teacher, and J. M. Rowcliffe. 2007. The costs of carnivory. PLoS Biology 5:e22.

Caro, T. 1999. The behaviour – conservation interface. TRENDS in Ecology & Evolution 14:366–369.

Carrier, D. R. 2016. The fight or flight dichotomy: functional trade-off in specialization for aggression versus locomotion. Pages 325–348 *in* J. E. A. Bertram, editor. Understanding mammalian locomotion: concepts and applications. John Wiley & Sons, Inc, Hoboken, New Jersey, USA.

Cattet, M. R. L., N. A. Caulkett, S. C. Polischuk, and M. A. Ramsay. 1997. Reversible immobilization of free-ranging polars with medetomidine-zolazepam-tiletamine and atipamezole. Journal of Wildlife Diseases 33:611–617.

Cavagna, G. A., N. C. Heglund, and C. R. Taylor. 1977. Mechanical work basic mechanisms in terrestrial locomotion: two basic mechanisms for minimizing energy expenditure. Journal of Physiology 268:467–481.

Chen, C., A. Liaw, and L. Breiman. 2004. Using random forest to learn imbalanced data. Technical Report 666. University of California, Berkeley, USA.

Chivers, L. S., S. A. Hatch, and K. H. Elliott. 2016. Accelerometry reveals an impact of short-term tagging on seabird activity budgets. Condor 118:159–168.

Cooke, S. J. 2008. Biotelemetry and biologging in endangered species research and animal conservation: relevance to regional, national, and IUCN Red List threat assessments. Endangered Species Research 4:165–185.

Cooke, S. J., D. T. Blumstein, R. Buchholz, T. Caro, E. Fernández-Juricic, C. E. Franklin, J. Metcalfe, C. M. O'Connor, C. C. St. Clair, W. J. Sutherland, and M. Wikelski. 2014. Physiology, behavior, and conservation. Physiological and Biochemical Zoology 87:1–14.

Costa, D. P. 1987. Isotopic methods for quantifying material and energy intake of free-ranging marine mammals. Pages 43–66 *in* A. C. Huntley, D. P. Costa, G. A. J. Worthy, and M. A. Castellini, editors. Approaches to marine mammal energetics. Allen Press, Lawrence, Kansas, USA.

Costa, D. P. 1988. Methods for studying the energetics of freely diving animals. Canadian Journal of Zoology 66:45–52.

Costa, D. P., L. A. Huckstadt, D. E. Crocker, B. I. McDonald, M. E. Goebel, and M. A. Fedak. 2010. Approaches to studying climatic change and its role on the habitat selection of antarctic pinnipeds. Integrative and Comparative Biology 50:1018–1030.

Costa, D. P., and T. M. Williams. 1999. Marine mammal energetics. Pages 176–217 *in* J. E. Reynolds and S. A. Rommel, editors. Biology of marine mammals. Smithsonian Institution Press, Washington, D.C., USA.

Cunningham, C. B., N. Schilling, C. Anders, and D. R. Carrier. 2010. The influence of foot posture on the cost of transport in humans. Journal of Experimental Biology 213:790–797.

Dalton, A. J. M., D. A. S. Rosen, and A. W. Trites. 2014. Season and time of day affect the ability of accelerometry and the doubly labeled water methods to measure energy expenditure in northern fur seals (*Callorhinus ursinus*). Journal of Experimental Marine Biology and Ecology 452:125–136.

DeMaster, D. P., and I. Stirling. 1981. *Ursus maritimus*. Mammalian Species 145:1–7.

Derocher, A. E. 2012. Polar bears: a complete guide to their biology and behavior. Johns Hopkins University Press, Baltimore, Maryland, USA.

Derocher, A. E., N. J. Lunn, and I. Stirling. 2004. Polar bears in a warming climate. Integrative and Comparative Biology 44:163–176.

Derocher, A. E., R. A. Nelson, I. Stirling, and M. A. Ramsay. 1990. Effects of fasting and feeding on serum urea and serum creatinine levels in polar bears. Marine Mammal Science 6:196–203.

Douglas, D. C. 2010. Arctic sea ice decline: projected changes in timing and extent of sea ice in the Bering and Chukchi Seas. Open-File Report 2010-1176. US Geological Survey, Reston, Virginia, USA.

Durner, G. M., D. C. Douglas, S. E. Albeke, J. P. Whiteman, M. Ben-david, S. C. Amstrup, E. Richardson, and R. R. Wilson. 2017. Increased Arctic sea ice drift alters adult female polar bear movements and energetics. Global Change Biology 23:3460–3473.

Durner, G. M., D. C. Douglas, R. M. Nielson, S. C. Amstrup, T. L. McDonald, I. Stirling, M. Mauritzen, E. W. Born, Ø. Wiig, E. DeWeaver, M. C. Serreze, S. E. Belikov, M. M. Holland, J. Maslanik, J. Aars, D. A. Bailey, and A. E. Derocher. 2009. Predicting 21st-century polar bear habitat distribution from global climate models. Ecological Monographs 79:25–58.

Durner, G. M., J. P. Whiteman, H. J. Harlow, S. C. Amstrup, E. V. Regehr, and M. Ben-David. 2011. Consequences of long-distance swimming and travel over deep-water pack ice for a female polar bear during a year of extreme sea ice retreat. Polar Biology 34:975–984.

Dyck, M. G., and S. Romberg. 2007. Observations of a wild polar bear (*Ursus maritimus*) successfully fishing Arctic charr (*Salvelinus alpinus*) and Fourhorn sculpin (*Myoxocephalus quadricornis*). Polar Biology 30:1625–1628.

Elliott, K. H., M. Le Vaillant, A. Kato, J. R. Speakman, and Y. Ropert-Coudert. 2013. Accelerometry predicts daily energy expenditure in a bird with high activity levels. Biology Letters 9:20120919.

Enstipp, M. R., K. Ballorain, S. Ciccione, T. Narazaki, K. Sato, and J. Y. Georges. 2016. Energy expenditure of adult green turtles (*Chelonia mydas*) at their foraging grounds and during simulated oceanic migration. Functional Ecology 30:1810–1825.

Farley, D., and T. Robbins. 1994. Development of two methods to estimate body composition of bears. Canadian Journal of Zoology 72:220–226.

Fedak, M. A., L. Rome, and H. J. Seeherman. 1981. One-step N_2-dilution technique for calibrating open-circuit VO_2 measuring systems. Journal of Applied Physiology 51:772–776.

Fei, Y., R. Hou, J. R. Spotila, F. V. Paladino, D. Qi, Z. Zhang, Z. Zhang, D. Wildt, A. Zhang, H. Zhang, D. Janssen, S. Ellius, F. Wei, Z. Wang, Z. Feng, M. N.

Tuanmu, L. He, L. O. Schulz, S. Alger, I. Harper, J. H. Wilmore, E. Ravussin, G. Walsberg, T. Hoffman, S. J. O'Brien, W. G. Nash, D. E. Wildt, M. E. Bush, R. E. Benveniste, J. Hu, S. Ellis, W. Pan, Z. Xie, D. E. Wildt, A. Zhang, H. Zhang, D. L. Janssen, R. Li, B. K. McNab, G. G. Montgomery, P. D. Watts, N. A. Øritsland, R. J. Hurst, P. Watts, C. Cuyler, P. D. Watts, C. Jonkel, B. K. McNab, A. E. Sieg, Y. Nie, B. K. McNab, C. Henry, A. E. Black, W. A. Coward, T. J. Cole, A. M. Prentice, D. Liu, D. Qi, G. Livesey, M. Elia, J. R. King, R. A. Nelson, H. W. Wahner, J. D. Jones, R. D. Ellefson, P. E. Zollman, G. Thorbek, K. H. Menke, H.-J. Lantzsch, J. Reichel, A. Chwalibog, A.-H. Tauson, G. Thorbek, L. C. H. Wang, R. E. Peter, D. C. Jackson, O. E. Owen, K. L. Smalley, D. A. D'Alessio, M. A. Mozzoli, E. K. Dawson, G. E. Walsberg, B. O. Wolf, Y. Schutz, E. Ravussin, J. R. Spotila, R. D. K. Thomas, E. C. Olson, P. J. Waddell, Y. Cao, J. Hauf, M. Hasegawa, M. S. Springer, W. J. Murphy, E. Eizirik, S. J. O'Brien, K. D. Rose, J. D. Archibald, C. R. White, R. S. Seymour, T. Li, L. N. Hudson, N. J. B. Isaac, D. C. Reuman, V. Hull, J. Liu, M. Linderman., J. R. Speakman, R. M. McDevitt, and K. R. Cole. 2016. Metabolic rates of giant pandas inform conservation strategies. Scientific Reports 6:27248.

Ferguson, S. H., K. Mitchell, E. W. BORN, A. Rosing-Asvid, F. Messier, M. K. TAYLOR, E. W. BORN, A. Rosing-Asvid, and F. Messier. 1999. Determinants of home range size for polar bears (*Ursus maritimus*). Ecology Letters 2:311–318.

Ferguson, S. H., M. K. Taylor, and F. Messier. 2000. Influence of sea ice dynamics on habitat selection by polar bears. Ecology 81:761–772.

Fish, F. E. 1982. Aerobic energetics of surface swimming in the muskrat *Ondatra zibethicus*. Physiological Zoology 55:180–189.

Fish, F. E. 1984. Mechanics, power output and efficiency of the swimming muskrat (*Ondatra zibethicus*). Journal of Experimental Biology 110:183–201.

Fish, F. E. 1992. Aquatic locomotion. Pages 34–63 *in* T. E. Tomasi and T. H. Horton, editors. Mammalian energetics: interdisciplinary views of metabolism and reproduction. Cornell University Press, Ithaca, New York, USA.

Fish, F. E. 2000. Biomechanics and energetics in aquatic and semiaquatic mammals: platypus to whale. Physiological and Biochemical Zoology 73:683–698.

Fish, F. E., and R. V Baudinette. 1999. Energetics of locomotion by the Australian water rat (*Hydromys chrysogaster*): a comparison of swimming and running in a semi-aquatic mammal. Journal of Experimental Biology 202:353–363.

Fish, F. E., and R. V Baudinette. 2008. Energetics of swimming by the ferret: consequences of forelimb paddling. Comparative Biochemistry and Physiology, Part A 150:136–143.

Fish, F. E., R. V Baudinette, P. B. Frappell, and M. P. Sarre. 1997. Energetics of swimming by the platypus *Ornithorhynchus anatinus*: metabolic effort associated with rowing. Journal of Experimental Biology 200:2647–2652.

Fish, F. E., J. Smelstoys, R. V Baudinette, and P. S. Reynolds. 2002. Fur doesn’t fly, it floats: buoyancy of pelage in semi-aquatic mammals. Aquatic Mammals 28:103–112.

Frair, J. L., J. Fieberg, M. Hebblewhite, F. Cagnacci, N. J. DeCesare, and L. Pedrotti. 2010. Resolving issues of imprecise and habitat-biased locations in ecological analyses using GPS telemetry data. Philosophical Transactions of the Royal Society B: Biological Sciences 365:2187–2200.

Furnell, D. J., and D. Oolooyuk. 1980. Polar bear predation on ringed seals in ice-free water. Canadian Field-Naturalist 94:88–89.

Garneau, D. E., E. Post, T. Boudreau, M. Keech, and P. Valkenburg. 2007. Spatio-temporal patterns of predation among three sympatric predators in a single-prey system. Wildlife Biology 13:186–194.

Geffen, E., A. A. Degen, M. Kam, R. Hefner, and K. A. Nagy. 1992. Daily energy expediture and water flux of free-living Blandford's foxes (*Vulpes cana*), a small desert carnivore. The Journal of Animal Ecology 61:611–617.

Gervasi, V., S. Brunberg, and J. O. N. E. Swenson. 2006. An individual-based method to measure animal activity levels: a test on brown bears. Wildlife Society Bulletin 34:1314–1319.

Gese, E. M., R. L. Ruff, and R. L. Crabtree. 1996. Foraging ecology of coyotes (*Canis latrans*): the influence of extrinsic factors and a dominance hierarchy. Canadian Journal of Zoology 74:769–783.

Gleiss, A. C., R. P. Wilson, and E. L. C. Shepard. 2011. Making overall dynamic body acceleration work: on the theory of acceleration as a proxy for energy expenditure. Methods in Ecology and Evolution 2:23–33.

Gómez Laich, A., R. P. Wilson, A. C. Gleiss, E. L. C. Shepard, and F. Quintana.

2011. Use of overall dynamic body acceleration for estimating energy expenditure in cormorants. Does locomotion in different media affect relationships? Journal of Experimental Marine Biology and Ecology 399:151–155.

Gormezano, L. J., S. R. Mcwilliams, D. T. Iles, and R. F. Rockwell. 2016. Costs of locomotion in polar bears: when do the costs outweigh the benefits of chasing down terrestrial prey? Conservation Physiology 4:cow045.

Graf, P. M., R. P. Wilson, L. Qasem, K. Hackländer, and F. Rosell. 2015. The use of acceleration to code for animal behaviours; a case study in free-ranging Eurasian beavers *Castor fiber*. PLoS ONE 10:e0136751.

Green, J. A., L. G. Halsey, R. P. Wilson, and P. B. Frappell. 2009*a*. Estimating energy expenditure of animals using the accelerometry technique: activity, inactivity and comparison with the heart-rate technique. Journal of Experimental Biology 212:471–482.

Green, J. A., M. Haulena, I. L. Boyd, D. Calkins, F. Gulland, A. J. Woakes, and P. J. Butler. 2009*b*. Trial implantation of heart rate data loggers in pinnipeds. Journal of Wildlife Management 73:115–121.

Grémillet, D., A. Lescroel, G. Ballard, K. M. Dugger, M. Massaro, E. L. Porzig, and D. G. Ainley. 2018. Energetic fitness: field metabolic rates assessed via 3D accelerometry complement conventional fitness metrics. Functional Ecology 32:1203–1213.

Griffen, B. D. 2018. Modeling the metabolic costs of swimming in polar bears (*Ursus* *maritimus*). Polar Biology 41:491–503.

Halsey, L. G., J. A. Green, R. P. Wilson, and P. B. Frappell. 2009*a*. Accelerometry to estimate energy expenditure during activity: best practice with data loggers. Physiological and Biochemical Zoology 82:396–404.

Halsey, L. G., E. L. C. Shepard, C. J. Hulston, M. C. Venables, C. R. White, A. E. Jeukendrup, and R. P. Wilson. 2008. Acceleration versus heart rate for estimating energy expenditure and speed during locomotion in animals: tests with an easy model species, *Homo sapiens*. Zoology 111:231–241.

Halsey, L. G., E. L. C. Shepard, F. Quintana, A. Gomez Laich, J. A. Green, and R. P. Wilson. 2009*b*. The relationship between oxygen consumption and body acceleration in a range of species. Comparative Biochemistry and Physiology - A Molecular and Integrative Physiology 152:197–202.

Halsey, L. G., E. L. C. Shepard, and R. P. Wilson. 2011*a*. Assessing the development and application of the accelerometry technique for estimating energy expenditure. Comparative Biochemistry and Physiology - A Molecular and Integrative Physiology 158:305–314.

Halsey, L. G., and C. R. White. 2010. Measuring energetics and behaviour using accelerometry in cane toads *Bufo marinus*. PLoS ONE 5:e10170.

Halsey, L. G., C. R. White, M. R. Enstipp, R. P. Wilson, P. J. Butler, G. R. Martin, D. Grémillet, and D. R. Jones. 2011*b*. Assessing the validity of the accelerometry technique for estimating the energy expenditure of diving double-crested cormorants *Phalacrocorax auritus*. Physiological and Biochemical Zoology

84:230–237.

Hammond, T. T., D. Springthorpe, R. E. Walsh, and T. Berg-Kirkpatrick. 2016. Using accelerometers to remotely and automatically characterize behavior in small animals. Journal of Experimental Biology 219:1618–1624.

Hansson, R., and J. Thomassen. 1983. Behavior of polar bears with cubs in the denning area. International Conference on Bear Research and Management 5:246–254.

Harrington, C. R. 1965. The life and status of the polar bear. Oryx 8:169–176.

Hayward, M. W., and G. J. Hayward. 2007. Activity patterns of reintroduced lion *Panthera leo* and spotted hyaena *Crocuta crocuta* in the Addo Elephant National Park, South Africa. African Journal of Ecology 45:135–141.

Heglund, N. C., and C. R. Taylor. 1988. Speed, stride frequency and energy cost per stride: how do they change with body size and gait? Journal of Experimental Biology 138:301–318.

Hertel, H. 1966. Structure, form, movement. Reinhold, New York, New York, USA.

Hilderbrand, G. V, S. D. Farley, and C. T. Robbins. 1998. Predicting body condition of bears via two field methods. Journal of Wildlife Management 62:406–409.

Hilderbrand, G. V., C. C. Schwartz, C. T. Robbins, and T. A. Hanley. 2000. Effect of hibernation and reproductive status on body mass and condition of coastal brown bears. Journal of Wildlife Management 64:178–183.

Hunter, C. M., H. Caswell, M. C. Runge, E. V Regehr, S. C. Amstrup, and I. Stirling. 2010. Climate change threatens polar bear populations: a stochastic demographic analysis. Ecology 91:2883–2897.

Hurst, R. J. 1981. Thermal and energetic consequences of oil contamination in polar bears. Thesis, University of Ottawa, Ontario, Canada.

Hurst, R. J., M. L. Leonard, P. D. Watts, P. Beckerton, and N. A. Øritsland. 1982*a*. Polar bear locomotion: body temperature and energetic cost. Canadian Journal of Zoology 60:40–44.

Hurst, R. J., N. A. Øritsland, and P. D. Watts. 1982*b*. Body mass, temperature and cost of walking in polar bears. Acta Physiologica Scandinavica 115:391–395.

Hurst, R. J., P. D. Watts, and N. A. Øritsland. 1991. Metabolic compensation in oil-exposed polar bears. Journal of Thermal Biology 16:53–56.

Iles, D. T., S. L. Peterson, L. J. Gormezano, D. N. Koons, and R. F. Rockwell. 2013. Terrestrial predation by polar bears: not just a wild goose chase. Polar Biology 36:1373–1379.

Iwaniuk, A. N., S. M. Pellis, and I. Q. Whishaw. 2000. The relative importance of body size, phylogeny, locomotion, and diet in the evolution of forelimb dexterity in fissiped carnivores (Carnivora). Canadian Journal of Zoology 78:1110–1125.

Jeanniard-du-dot, T., C. Guinet, J. P. Y. Arnould, J. R. Speakman, and A. W. Trites. 2017. Accelerometers can measure total and activity-specific energy expenditures in free-ranging marine mammals only if linked to time-activity budgets. Functional Ecology 31:377–386.

Johnson, D. S. 2016. Crawl: fit continuous-time correlated random walk models to animal movement data. R package.

Johnson, D. S., J. M. London, M.-A. Lea, and J. W. Durban. 2008. Continous-time correlated random walk model for animal telemetry data. Ecology 89:1208–1215.

Joly, S., S. Senneville, D. Caya, and F. J. Saucier. 2011. Sensitivity of Hudson Bay Sea ice and ocean climate to atmospheric temperature forcing. Climate Dynamics 36:1835–1849.

Jonkel, C. J. 1967. Life history, ecology and biology of the polar bear, autumn 1966 studies. Canadian Wildlife Service Progress Notes, Ottawa, Ontario, Canada.

Kahle, D., and H. Wickham. 2013. ggmap: spatial visualization with ggplot2. The R Journal 5:144–161.

Kalxdorff, S. 1997. Collection of local knowledge regarding polar bear habitat use in Alaska. US Fish and Wildlife Service Technical Report MMM 97-2. US Fish and Wildlife Service. Anchorage, Alaska, USA.

Kaufman, D. S., D. P. Schneider, N. P. Mckay, C. M. Ammann, R. S. Bradley, K. R. Briffa, G. H. Miller, B. L. Otto-bliesner, J. T. Overpeck, and B. M. Vinther. 2009. Recent warming reverses long-term Arctic cooling. Science 325:1236–1239.

Kelly, B. P., and L. T. Quakenbush. 1990. Spatiotemporal use of lairs by ringed seals (*Phoca hispida*). Canadian Journal of Zoology 68:2503–2512.

Kingsley, M. C. S. 1998. The number of ringed seals (*Phoca hispida*) in Baffin Bay and associated waters. Pages 181–196 *in* M.-P. Heide-Jorgensen and C. Lydersen, editors. Ringed seals in the North Atlantic. Volume 1. The North

Atlantic Marine Mammal Commission, Tromsø, Norway.

Kleiber, M. 1975. The fire of life: an introduction to animal energetics. John Wiley & Sons, Inc., New York, New York, USA.

Knudsen, B. 1978. Time budgets of polar bears (*Ursus maritimus*) on North Twin Island, James Bay, during summer. Canadian Journal of Zoology 56:1627–1628.

Kochnev, A. A., V. M. Etylin, V. I. Kavry, S.-S. E. B., and I. V. Tanko. 2003. Traditional knowledge of Chukotka native peoples regarding polar bear habitat use. Final Report. US National Park Service. Anchorage, Alaska, USA.

Kolenosky, G. B., and R. O. Standfield. 1966. Polar bears of Canada. Animals 8:528–531.

Kolowski, J. M., D. Katan, K. R. Theis, and K. E. Holekamp. 2007. Daily patterns of activity in the spotted hyena. Journal of Mammalogy 88:1017–1028.

Kramer, D. L., and R. L. McLaughlin. 2001. The behavioral ecology of intermittent locomotion. American Zoologist 41:137–153.

Krogh, A., and J. Lindhard. 1917. A comparison between voluntary and electrically induced muscular work in man. Journal of Physiology 51:182–201.

Laforest, B. J., J. S. Hébert, M. E. Obbard, and G. W. Thiemann. 2018. Traditional ecological knowledge of polar bears in the Northern Eeyou Marine Region, Québec, Canada. Arctic 71:40–58.

Laidre, K. L., I. Stirling, L. F. Lowry, Ø. Wiig, M. P. Heide-Jørgensen, and S. H. Ferguson. 2008. Quantifying the sensitivity of Arctic marine mammals to climate-induced habitat change. Ecological Applications 18:S97–S125.

Langman, V. A., M. F. Rowe, T. J. Roberts, N. V Langman, and C. R. Taylor. 2012. Minimum cost of transport in Asian elephants: do we really need a bigger elephant? Journal of Experimental Biology 215:1509–1514.

Larsen, T. 1968. Ecological investigations of the polar bear in Svalbard. Norsk Polarinstitutt, Oslo, Norway.

Larsen, T. 1971. Capturing, handling, and marking polar bears in Svalbard. Journal of Wildlife Management 35:27–36.

Latour, P. B. 1981. Interactions between free-ranging, adult male polar bears (*Ursus maritimus* Phipps): a case of adult social play. Canadian Journal of Zoology 59:1775–1783.

Lavigne, D. M., S. Innes, G. A. J. Worthy, K. M. Kovacs, O. J. Schmitz, and J. P. Hickie. 1986. Metabolic rates of seals and whales. Canadian Journal of Zoology 64:279–284.

Lentfer, J. W. 1968. A technique for immobilizing and marking polar bears. Journal of Wildlife Management 32:317–321.

Liaw, A., and M. Wiener. 2002. Classification and regression by randomForest. R News 2:18–22.

Lifson, N., G. B. Gordon, and R. McClintock. 1955. Measurement of total carbon dioxide production by means of D_2O^{18}. Journal of Applied Physiology 7:704–710.

Lifson, N., McClintock, and R. McClintock. 1966. Theory of use of the turnover rates of body water for measuring energy and material balance. Journal of Theoretical

Biology 12:46–74.

Lønø, O. 1970. The polar bear (*Ursus maritimus* Phipps) in the Svalbard area. Norsk Polarinstitutt SKRIFTER NR. 149, Oslo, Norway.

Lovegrove, B. G., and L. Haines. 2004. The evolution of placental mammal body sizes: evolutionary history, form, and function. Oecologia 138:13–27.

Lunn, N. J., S. Servanty, E. V. Regehr, S. J. Converse, E. Richardson, and I. Stirling. 2016. Demography of an apex predator at the edge of its range – impacts of changing sea ice on polar bears in Hudson Bay. Ecological Applications 26:1302–1320.

Lunn, N. J., and I. Stirling. 1985. The significance of supplemental food to polar bears during the ice-free period of Hudson Bay. Canadian Journal of Zoology 63:2291–2297.

Lush, L., S. Ellwood, A. Markham, A. I. Ward, and P. Wheeler. 2016. Use of tri-axial accelerometers to assess terrestrial mammal behaviour in the wild. Journal of Zoology 298:257–265.

Maresh, J. L., S. E. Simmons, D. E. Crocker, B. I. McDonald, T. M. Williams, and D. P. Costa. 2014. Free-swimming northern elephant seals have low field metabolic rates that are sensitive to an increased cost of transport. Journal of Experimental Biology 217:1485–1495.

Markus, T., J. C. Stroeve, and J. Miller. 2009. Recent changes in Arctic sea ice melt onset, freezeup, and melt season length. Journal of Geophysical Research 114:C12024.

Martins, M., C. Santos, L. Costa, and A. Frizera. 2016. Feature reduction and multi-classification of different assistive devices according to the gait pattern. Disability and Rehabilitation: Assistive Technology 11:202–218.

Martiskainen, P., M. Järvinen, J. P. Skön, J. Tiirikainen, M. Kolehmainen, and J. Mononen. 2009. Cow behaviour pattern recognition using a three-dimensional accelerometer and support vector machines. Applied Animal Behaviour Science 119:32–38.

Matthews, B. W. 1975. Comparison of the predicted and observed secondary structure of T4 phage lysozyme. Biochimica et Biophysica Acta 405:442–451.

Mauritzen, M., S. E. Belikov, A. N. Boltunov, A. E. Derocher, E. Hansen, R. A. Ims, Ø. Wiig, and N. Yoccoz. 2003*a*. Functional responses in polar bear habitat selection. Oikos 100:112–124.

Mauritzen, M., A. E. Derocher, O. Pavlova, and Ø. Wiig. 2003*b*. Female polar bears, *Ursus maritimus*, on the Barents Sea drift ice: walking the treadmill. Animal Behaviour 66:107–113.

McClune, D. W., N. J. Marks, R. J. Delahay, W. I. Montgomery, and D. M. Scantlebury. 2015. Behaviour-time budget and functional habitat use of a free-ranging European badger (*Meles meles*). Animal Biotelemetry 3:7.

McClune, D. W., N. J. Marks, R. P. Wilson, J. D. Houghton, I. W. Montgomery, N. E. McGowan, E. Gormley, and M. Scantlebury. 2014. Tri-axial accelerometers quantify behaviour in the Eurasian badger (*Meles meles*): towards an automated interpretation of field data. Animal Biotelemetry 2:5.

McKinney, M. A., T. C. Atwood, S. J. Iverson, and E. Peacock. 2017. Temporal complexity of southern Beaufort Sea polar bear diets during a period of increasing land use. Ecosphere 8:e01633.

McLellan, B., and D. C. Reiner. 1994. A review of bear evolution. International Conference on Bear Research and Management 9:85–96.

McLoughlin, P. D., R. L. Case, R. J. Gau, S. H. Ferguson, and F. Messier. 1999. Annual and seasonal movement patterns of barren-ground grizzly bears in the central Northwest Territories. Ursus 11:79–86.

McLoughlin, P. D., and S. H. Ferguson. 2000. A hierarchical pattern of limiting factors helps explain variation in home range size. Ecoscience 7:123–130.

McNab, B. K. 1986. The influence of food habits on the energetics of eutherian mammals. Ecological Monographs 56:1–19.

McNab, B. K. 1988. Complications inherent in scaling the basal rate of metabolism in mammals. The Quarterly Review of Biology 63:25–54.

McNab, B. K. 1992. Rate of metabolism in the termite-eating sloth bear (*Ursus ursinus*). Journal of Mammalogy 73:168–172.

Mcphee, M. E., and K. Carlstead. 2010. The importance of maintaining natural behaviors in captive mammals. Pages 303–313 *in* D. G. Kleiman, K. V. Thompson, and C. K. Baer, editors. Wild mammals in captivity: principles and techniques for zoo management. 2nd edition. University of Chicago Press, Chicago, Illinois, USA.

Messier, F., M. K. Taylor, and M. A. Ramsay. 1992. Seasonal activity patterns of female polar bears (*Ursus maritimus*) in the Canadian Arctic as revealed by satellite telemetry. Journal of Zoology 226:219–229.

Mogensen, N. L., J. O. Ogutu, and T. Dabelsteen. 2011. The effects of pastoralism and protection on lion behaviour, demography and space use in the Mara Region of Kenya. African Zoology 46:78–87.

Moll, R. J., J. J. Millspaugh, J. Beringer, J. Sartwell, and Z. He. 2007. A new "view" of ecology and conservation through animal-borne video systems. Trends in Ecology and Evolution 22:660–668.

Molnár, P. K., A. E. Derocher, G. W. Thiemann, and M. A. Lewis. 2010. Predicting survival, reproduction and abundance of polar bears under climate change. Biological Conservation 143:1612–1622.

Molnár, P. K., T. Klanjscek, A. E. Derocher, M. E. Obbard, and M. A. Lewis. 2009. A body composition model to estimate mammalian energy stores and metabolic rates from body mass and body length, with application to polar bears. Journal of Experimental Biology 212:2313–2323.

Morris, K. S., M. A. Osborne, M. E. Shephard, D. G. Jenkins, and T. L. Skinner. 2017. Velocity, oxygen uptake, and metabolic cost of pull, kick, and whole-body swimming. International Journal of Sports Physiology and Performance 12:1046–1051.

Nagy, K. A. 1980. CO_2 production in animals: analysis of potential errors in the doubly labeled water method. American Journal of Physiology 238:R466–R473.

Nagy, K. A. 1989. Field bioenergetics: accuracy of models and methods.

Physiological Zoology 62:237–252.

Nagy, K. A. 2005. Field metabolic rate and body size. Journal of Experimental Biology 208:1621–1625.

Nagy, K. A., I. A. Girard, and T. K. Brown. 1999. Energetics of free-ranging mammals, reptiles, and birds. Annual Review of Nutrition 19:247–77.

Nakamura, I., Y. Goto, and K. Sato. 2015. Ocean sunfish rewarm at the surface after deep excursions to forage for siphonophores. Journal of Animal Ecology 84:590–603.

Nathan, R., O. Spiegel, S. Fortmann-Roe, R. Harel, M. Wikelski, and W. M. Getz. 2012. Using tri-axial acceleration data to identify behavioral modes of free-ranging animals: general concepts and tools illustrated for griffon vultures. Journal of Experimental Biology 215:986–96.

Nelson, R. A., T. D. I. Beck, and D. L. Steiger. 1984. Ratio of serum urea to serum creatinine in wild black bears. Science 226:841–842.

Nelson, R. A., G. E. J. Folk, E. W. Pfeiffer, J. J. Craighead, C. J. Jonkel, and D. L. Steiger. 1983. Behavior, biochemistry, and hibernation in black, grizzly, and polar bears. International Conference on Bear Research and Management 5:284–290.

Nelson, R. K. 1966. Alaskan eskimo exploitation of the sea ice environment. Report AAL-TR-65-19. Arctic Aeromedical Laboratory, Arctic Aeromedical Laboratory. Fort Wainwright, Alaska, USA.

Obbard, M. E., G. W. Thiemann, E. Peacock, and T. D. BeBruyn, editors. 2010. Polar bears: Proceedings of the 15th working meeting of the IUCN/SSC Polar Bear Specialist Group, Copenhagen, Denmark, 29 June – 3 July 2009. Gland, Switzerland and Cambridge, United Kingdom.

Obbard, M. E., M. R. L. Cattet, E. J. Howe, K. R. Middel, E. J. Newton, G. B. Kolenosky, K. F. Abraham, and C. J. Greenwood. 2016. Trends in body condition in polar bears (*Ursus maritimus*) from the Southern Hudson Bay subpopulation in relation to changes in sea ice. Arctic Science 32:15–32.

Obbard, M. E., S. Stapleton, G. Szor, K. R. Middel, C. Jutras, and M. Dyck. 2018. Re-assessing abundance of Southern Hudson Bay polar bears by aerial survey: effects of climate change at the southern edge of the range. Arctic Science https://doi.org/10.1139/AS-2018-0004.

Øritsland, N. A. 1969. Deep body temperatures of swimming and walking polar bear cubs. Journal of Mammalogy 50:380–382.

Øritsland, N. A. 1970. Temperature regulation of the polar bear (*Thalarctos maritimus*). Comparative Biochemistry and Physiology 37:225–233.

Øritsland, N. A., C. Jonkel, and K. Ronald. 1976. A respiration chamber for exercising polar bears. Norwegian Journal of Zoology 24:65–67.

Overpeck, J., K. Hughen, D. Hardy, R. Bradley, R. Case, M. Douglas, B. Finney, K. Gajewski, G. Jacoby, A. Jennings, S. Lamoureux, A. Lasca, G. MacDonald, J. Moore, M. Retelle, S. Smith, A. Wolfe, and G. Zielinski. 1997. Arctic environmental change of the last four centuries. Science 278:1251–1256.

Pagano, A. M., G. M. Durner, S. C. Amstrup, K. S. Simac, and G. S. York. 2012.

Long-distance swimming by polar bears (*Ursus maritimus*) of the southern Beaufort Sea during years of extensive open water. Canadian Journal of Zoology 90:663–676.

Pagano, A. M., K. D. Rode, and S. N. Atkinson. 2017. Evaluating methods to assess the body condition of female polar bears. Ursus 28:171–181.

Paisley, S., and D. L. Garshelis. 2006. Activity patterns and time budgets of Andean bears (*Tremarctos ornatus*) in the Apolobamba Range of Bolivia. Journal of Zoology 268:25–34.

Peacock, E., S. A. Sonsthagen, M. E. Obbard, A. Boltunov, E. V. Regehr, N. Ovsyanikov, J. Aars, S. N. Atkinson, G. K. Sage, A. G. Hope, E. Zeyl, L. Bachmann, D. Ehrich, K. T. Scribner, S. C. Amstrup, S. Belikov, E. W. Born, A. E. Derocher, I. Stirling, M. K. Taylor, Ø Wiig, D. Paetkau, and S. L. Talbot. 2015. Implications of the circumpolar genetic structure of polar bears for their conservation in a rapidly warming Arctic. PLoS ONE 10:e112021.

Pilfold, N. W., A. E. Derocher, I. Stirling, and E. Richardson. 2015. Multi-temporal factors influence predation for polar bears in a changing climate. Oikos 124:1098–1107.

Pilfold, N. W., A. E. Derocher, I. Stirling, E. Richardson, and D. Andriashek. 2012. Age and sex composition of seals killed by polar bears in the Eastern Beaufort Sea. PLoS ONE 7:e41429.

Pilfold, N. W., A. Mccall, A. E. Derocher, N. J. Lunn, and E. Richardson. 2017. Migratory response of polar bears to sea ice loss: to swim or not to swim.

Ecography 40:189–199.

Platonov, N. G., V. V Rozhnov, I. V Alpatsky, I. N. Mordvintsev, E. A. Ivanov, and S. V Naidenko. 2014. Evaluation of polar bear movement patterns in relation to sea ice drift. Doklady Biological Sciences 456:191–194.

Pond, C. M., C. A. Mattacks, R. H. Colby, and M. A. Ramsay. 1992. The anatomy, chemical composition, and metabolism of adipose tissue in wild polar bears (*Ursus maritimus*). Canadian Journal of Zoology 70:326–341.

Pond, C. M., and M. A. Ramsay. 1992. Allometry of the distribution of adipose tissue in Carnivora. Canadian Journal of Zoology 70:342–347.

Ponganis, P. J. 2015. Diving Physiology of Marine Mammals and Seabirds. Cambridge University Press, Cambridge, United Kingdom.

Prange, H. D., and K. Schmidt-Nielsen. 1970. The metabolic cost of swimming in ducks. Journal of Experimental Biology 53:763–777.

Prichard, A. K., D. A. Yokel, C. L. Rea, B. T. Person, and L. S. Parrett. 2014. The effect of frequency of telemetry locations on movement-rate calculations in arctic caribou. Wildlife Society Bulletin 38:78–88.

Qasem, L., A. Cardew, A. Wilson, I. Griffiths, L. G. Halsey, E. L. C. Shepard, A. C. Gleiss, and R. Wilson. 2012. Tri-axial dynamic acceleration as a proxy for animal energy expenditure; should we be summing values or calculating the vector? PLoS ONE 7:e31187.

R Core Team. 2014. R: A language and environment for statistical computing. R Foundation for Statistical Computing, Vienna. <http://www.r-project.org/>.

Rea, L. D., and D. P. Costa. 1992. Changes in standard metabolism during long-term fasting in northern elephant seal pups (*Mirounga angustirostris*). Physiological Zoology 65:97–111.

Regehr, E. V., N. J. Lunn, S. C. Amstrup, and I. Stirling. 2007. Effects of earlier sea ice breakup on survival and population size of polar bears in Western Hudson Bay. Journal of Wildlife Management 71:2673–2683.

Regehr, E. V, C. M. Hunter, H. Caswell, S. C. Amstrup, and I. Stirling. 2010. Survival and breeding of polar bears in the southern Beaufort Sea in relation to sea ice. Journal of Animal Ecology 79:117–127.

Regehr, E. V, K. L. Laidre, H. R. Akcakaya, S. C. Amstrup, T. C. Atwood, N. J. Lunn, M. Obbard, H. Stern, G. W. Thiemann, and Ø. Wiig. 2016. Conservation status of polar bears (*Ursus maritimus*) in relation to projected sea-ice declines. Biology Letters 12:20160556.

Reilly, S. M., E. J. MeElroy, and A. R. Biknevicius. 2007. Posture, gait and the ecological relevance of locomotor costs and energy-saving mechanisms in tetrapods. Zoology 110:271–289.

Rekvik, G. E. S. 2015. Identification of five brown bear (*Ursus arctos*) behaviors using tri-axial accelerometers. Thesis, Telemark University College, Bø, Norway.

Renous, S., J.-P. Gasc, and A. Abourachid. 1988. Kinematic analysis of the locomotion of the polar bear (*Ursus maritimus*, Phipps, 1774) in natural and experimental conditions. Netherlands Journal of Zoology 48:145–167.

Resheff, Y. S., S. Rotics, R. Harel, O. Spiegel, and R. Nathan. 2014. AcceleRater: a web application for supervised learning of behavioral modes from acceleration measurements. Movement Ecology 2:27.

Rigano, K. S., J. L. Gehring, B. D. Evans Hutzenbiler, A. V. Chen, O. L. Nelson, C. A. Vella, C. T. Robbins, and H. T. Jansen. 2017. Life in the fat lane: seasonal regulation of insulin sensitivity, food intake, and adipose biology in brown bears. Journal of Comparative Physiology B 187:649–676.

Robbins, C. T., C. Lopez-Alfaro, K. D. Rode, Ø. Tøien, and O. L. Nelson. 2012. Hibernation and seasonal fasting in bears: the energetic costs and consequences for polar bears. Journal of Mammalogy 93:1493–1503.

Rode, K. D., S. C. Amstrup, and E. V. Regehr. 2010. Reduced body size and cub recruitment in polar bears associated with sea ice decline. Ecological Applications 20:768–782.

Rode, K. D., A. M. Pagano, J. F. Bromaghin, T. C. Atwood, G. M. Durner, K. S. Simac, and S. C. Amstrup. 2014*a*. Effects of capturing and collaring on polar bears: findings from long-term research on the southern Beaufort Sea population. Wildlife Research 41:311–322.

Rode, K. D., E. Peacock, M. Taylor, I. Stirling, E. W. Born, K. L. Laidre, and Ø. Wiig. 2012. A tale of two polar bear populations: ice habitat, harvest, and body condition. Population Ecology 54:3–18.

Rode, K. D., E. V Regehr, D. C. Douglas, G. Durner, A. E. Derocher, G. W. Thiemann, and S. M. Budge. 2014*b*. Variation in the response of an Arctic top predator experiencing habitat loss: feeding and reproductive ecology of two polar bear populations. Global Change Biology 20:76–88.

Rode, K. D., R. R. Wilson, D. C. Douglas, V. Muhlenbruch, T. C. Atwood, E. V. Regehr, E. S. Richardson, N. W. Pilfold, A. E. Derocher, G. M. Durner, I. Stirling, S. C. Amstrup, M. St. Martin, A. M. Pagano, and K. S. Simac. 2018. Spring fasting behavior in a marine apex predator provides an index of ecosystem productivity. Global Change Biology 24:410–423.

Rogers, M. C., E. Peacock, K. Simac, M. B. O'Dell, and J. M. Welker. 2015. Diet of female polar bears in the southern Beaufort Sea of Alaska: evidence for an emerging alternative foraging strategy in response to environmental change. Polar Biology 38:1035–1047.

Ropert-Coudert, Y., and R. Wilson. 2005. Trends and perspectives in animal-attached remote sensing. Frontiers in Ecology and the Environment 3:437–444.

Rowcliffe, J. M., C. Carbone, R. Kays, B. Kranstauber, and P. A. Jansen. 2012. Bias in estimating animal travel distance: the effect of sampling frequency. Methods in Ecology and Evolution 3:653–662.

Russell, R. H. 1975. The food habits of polar bears of James Bay and southwest Hudson Bay in summer and autumn. Arctic 28:117–129.

Sahanatien, V., and A. E. Derocher. 2012. Monitoring sea ice habitat fragmentation for polar bear conservation. Animal Conservation 15:397–406.

Scharf, A. K., S. LaPoint, M. Wikelski, and K. Safi. 2016. Acceleration data reveal highly individually structured energetic landscapes in free-ranging fishers

(*Pekania pennanti*). PLoS ONE 11:e0145732.

Schmidt-Nielsen, K. 1972. Locomotion: energy cost of swimming, flying, and running. Science 177:222–228.

Schmidt-Nielsen, K. 1984. Scaling. Why is animal size so important? Cambridge University Press, New York, New York, USA.

Schmidt-Nielsen, K. 1997. Animal physiology: adaptation and environment. 5th edition. Cambridge University Press, Cambridge, United Kingdom.

Scholander, P. F., V. Walters, R. Hock, and L. Irving. 1950. Body insulation of some Arctic and tropical mammals and birds. Biological Bulletin 99:225–236.

Schweinsburg, R. E., and L. J. Lee. 1982. Movement of four satellite-monitored polar bears in Lancaster Sound, Northwest Territories. Arctic 35:504–511.

Scott, R. F., K. W. Kenyon, J. L. Buckley, and S. T. Olson. 1959. Status and management of the polar bear and Pacific walrus. Transactions of the North American Wildlife Conference 24:366–374.

Segal, K. R., I. Lacayanga, A. Dunaif, B. Gutin, and F. X. Pi-Sunyer. 1989. Impact of body fat mass and percent fat on metabolic rate and thermogenesis in men. American Journal of Physiology - Endocrinology and Metabolism 256:E573–E579.

Seidensticker, J. C., M. G. Hornocker, W. V. Wiles, and J. P. Messick. 1973. Mountain lion social organization in the Idaho primitive area. Wildlife Monographs 35:3–60.

Shamoun-Baranes, J., R. Bom, E. E. van Loon, B. J. Ens, K. Oosterbeek, and W.

Bouten. 2012. From sensor data to animal behaviour: an oystercatcher example. PLoS ONE 7:e37997.

Shepard, E. L. C., R. P. Wilson, F. Quintana, A. G. Laich, N. Liebsch, D. A. Albareda, L. G. Halsey, A. Gleiss, D. T. Morgan, A. E. Myers, C. Newman, and D. W. Macdonald. 2008. Identification of animal movement patterns using tri-axial accelerometry. Endangered Species Research 10:47–60.

Shepard, E. L. C., R. P. Wilson, W. G. Rees, E. Grundy, S. A. Lambertucci, and S. B. Vosper. 2013. Energy landscapes shape animal movement ecology. American Naturalist 182:298–312.

Shine, C. L., S. Penberthy, C. T. Robbins, O. L. Nelson, and C. P. McGowan. 2015. Grizzly bear (*Ursus arctos horribilis*) locomotion: gaits and ground reaction forces. Journal of Experimental Biology 218:3102–3109.

Soltis, J., R. P. Wilson, I. Douglas-Hamilton, F. Vollrath, L. E. King, and A. Savage. 2012. Accelerometers in collars identify behavioral states in captive African elephants *Loxodonta africana*. Endangered Species Research 18:255–263.

Sparling, C. E., D. Thompson, M. A. Fedak, S. L. Gallon, and J. R. Speakman. 2008. Estimating field metabolic rates of pinnipeds: doubly labelled water gets the seal of approval. Functional Ecology 22:245–254.

Speakman, J. R. 1997. Doubly labelled water: theory and practice. Chapman and Hall, London, United Kingdom.

Speakman, J. R., G. Perez-Camargo, T. McCappin, T. Frankel, P. Thomson, and V. Legrand-Defretin. 2001. Validation of the doubly-labelled water technique in the domestic dog (*Canis familiaris*). British Journal of Nutrition 85:75–87.

Speakman, J. R., A. Van Acker, and E. J. Harper. 2003. Age-related changes in the metabolism and body composition of three dog breeds and their relationship to life expectancy. Aging Cell 2:265–275.

Stern, H. L., and K. L. Laidre. 2016. Sea-ice indicators of polar bear habitat. Cryosphere 10:2027–2041.

Stirling, I. 1974. Midsummer observations on the behavior of wild polar bears (*Ursus maritimus*). Canadian Journal of Zoology 52:1191–1198.

Stirling, I. 1988. Polar bears. University of Michigan Press, Ann Arbor, Michigan, USA.

Stirling, I., and W. R. Archibald. 1977. Aspects of predation of seals by polar bears. Journal of the Fisheries Research Board of Canada 34:1126–1129.

Stirling, I., W. R. Archibald, and D. P. DeMaster. 1977. Distribution and abundance of seals in the eastern Beaufort Sea. Journal of the Fisheries Research Board of Canada 34:976–988.

Stirling, I., and A. E. Derocher. 1990. Factors affecting the evolution and behavioral ecology of the modern bears. International Conference on Bear Research and Management 8:189–204.

Stirling, I., and A. E. Derocher. 1993. Possible impacts of climatic warming on polar bears. Arctic 46:240–245.

Stirling, I., and P. B. Latour. 1978. Comparative hunting abilities of polar bear cubs of different ages. Canadian Journal of Zoology 56:1768–1772.

Stirling, I., N. J. Lunn, and J. Iacozza. 1999. Long-term trends in the population ecology of polar bears in western Hudson Bay in relation to climatic change. Arctic 52:294–306.

Stirling, I., and E. H. McEwan. 1975. The caloric value of whole ringed seals (*Phoca hispida*) in relation to polar bear (*Ursus maritimus*) ecology and hunting behavior. Canadian Journal of Zoology 53:1021–1027.

Stirling, I., and R. van Meurs. 2015. Longest recorded underwater dive by a polar bear. Polar Biology 38:1301–1304.

Stirling, I., and N. A. Øritsland. 1995. Relationships between estimates of ringed seal (*Phoca hispida*) and polar bear (*Ursus maritimus*) populations in the Canadian Arctic. Canadian Journal of Fisheries and Aquatic Sciences 52:2594–2612.

Stirling, I., C. Spencer, and D. Andriashek. 1989. Immobilization of polar bears (*Ursus maritimus*) with Telazol® in the Canadian Arctic. Journal of Wildlife Diseases 25:159–168.

Stirling, I., C. Spencer, and D. Andriashek. 2016. Behavior and activity budgets of wild breeding polar bears (*Ursus maritimus*). Marine Mammal Science 32:13–37.

Stothart, M. R., K. H. Elliott, T. Wood, S. A. Hatch, and J. R. Speakman. 2016. Counting calories in cormorants: dynamic body acceleration predicts daily energy expenditure measured in pelagic cormorants. Journal of Experimental Biology 219:2192–2200.

Stroeve, J. C., T. Markus, L. Boisvert, J. Miller, and A. Barrett. 2014. Changes in

Arctic melt season and implications for sea ice loss. Geophysical Research Letters 41:1216–1225.

Stroeve, J., T. Markus, W. N. Meier, and J. Miller. 2006. Recent changes in the Arctic melt season. Annals of Glaciology 44:367–374.

Sutherland, W. J. 1998. The importance of behavioural studies in conservation biology. Animal Behaviour 56:801–809.

Talbot, S. L., and G. F. Shields. 1996. A phylogeny of the bears (Ursidae) inferred from complete sequences of three mitochondrial genes. Molecular Phylogenetics and Evolution 5:567–75.

Taylor, C. R., N. C. Heglund, and G. M. Maloiy. 1982. Energetics and mechanics of terrestrial locomotion. I. Metabolic energy consumption as a function of speed and body size in birds and mammals. Journal of Experimental Biology 97:1–21.

Taylor, C. R., K. Schmidt-Nielsen, and J. L. Raab. 1970. Scaling of energetic cost of running to body size in mammals. American Journal of Physiology 219:1104–1107.

Taylor, M. K. 1986. Movements of Alaskan polar bears instrumented with satellite transmitters. International Conference on Bear Research and Management 6:103–104.

Teisberg, J. E., S. D. Farley, O. L. Nelson, G. V Hilderbrand, M. J. Madel, P. A. Owen, J. A. Erlenbach, and C. T. Robbins. 2014. Immobilization of grizzly bears (*Ursus arctos*) with dexmedetomidine, tiletamine, and zolazepam. Journal of Wildlife Diseases 50:74–83.

Theuerkauf, J., W. Jędrzejewski, K. Schmidt, H. Okarma, I. Ruczyński, S. Śnieżko, and R. Gula. 2003. Daily patterns and duration of wolf activity in the Białowieża forest, Poland. Journal of Mammalogy 84:243–253.

Thiemann, G. W., S. J. Iverson, and I. Stirling. 2008. Polar bear diets and arctic marine food webs: insights from fatty acid analysis. Ecological Monographs 78:591–613.

Tøien, Ø., J. Blake, D. M. Edgar, D. A. Grahn, H. Heller Craig, B. M. Barnes, H. C. Heller, and M. Brian. 2011. Hibernation in black bears: independence of metabolic suppression from body temperature. Science 331:906–909.

US Fish and Wildlife Service. 2015. Polar Bear (*Ursus maritimus*) Conservation Management Plan, Draft. Anchorage, Alaska, USA.

Van Valkenburgh, B. 1999. Major patterns in the history of carnivorous mammals. Annual Review of Earth and Planetary Sciences 27:463–493.

Van Valkenburgh, B., X. Wang, and J. Damuth. 2004. Cope's rule, hypercarnivory, and extinction in North American canids. Science 306:101–104.

Vandenabeele, S. P., E. Grundy, M. I. Friswell, A. Grogan, S. C. Votier, and R. P. Wilson. 2014. Excess baggage for birds: inappropriate placement of tags on gannets changes flight patterns. PLoS ONE 9:e92657.

Volpov, B. L., A. J. Hoskins, B. C. Battaile, M. Viviant, K. E. Wheatley, G. Marshall, K. Abernathy, and J. P. Y. Arnould. 2015. Identification of prey captures in Australian fur seals (*Arctocephalus pusillus doriferus*) using head-mounted accelerometers: field validation with animal-borne video cameras. PloS one

10:e0128789.

Vongraven, D., J. Aars, S. Amstrup, S. N. Atkinson, S. Belikov, E. W. Born, T. D. Debruyn, A. E. Derocher, G. Durner, M. Gill, N. Lunn, M. E. Obbard, J. Omelak, N. Ovsyanikov, E. Peacock, E. Richardson, V. Sahanatien, I. Stirling, and Ø. Wiig. 2012. A circumpolar monitoring framework for polar bears. Ursus Monograph Series 5:1–66.

Voorhees, H., R. Sparks, H. P. Huntington, and K. D. Rode. 2014. Traditional knowledge about polar bears (*Ursus maritimus*) in northwestern Alaska. Arctic 67:523–536.

Walker, B. G., and P. L. Boveng. 1995. Effects of time-depth recorders on maternal foraging and attendance behavior of Antarctic fur seals (*Arctocephalus gazella*). Canadian Journal of Zoology 73:1538–1544.

Walsh, J. E. 2008. Climate of the Arctic marine environment. Ecological Applications 18:S3–S22.

Wang, Y., B. Nickel, M. Rutishauser, C. Bryce, T. Williams, G. Elkaim, and C. Wilmers. 2015. Movement, resting, and attack behaviors of wild pumas are revealed by tri-axial accelerometer measurements. Movement Ecology 3:2.

Wang, Y., J. A. Smith, and C. C. Wilmers. 2017. Residential development alters behavior, movement, and energetics in an apex predator, the puma. PLoS ONE 12:e0184687.

Ware, J. V., K. D. Rode, J. F. Bromaghin, D. C. Douglas, R. R. Wilson, E. V. Regehr, S. C. Amstrup, G. M. Durner, A. M. Pagano, J. Olson, C. T. Robbins, and H. T.

Jansen. 2017. Habitat degradation affects the summer activity of polar bears. Oecologia 184:87–99.

Ware, J. V, K. D. Rode, A. M. Pagano, J. Bromaghin, C. T. Robbins, J. Erlenbach, S. Jensen, A. Cutting, N. Nicassio-Hiskey, A. Hash, M. Owen, and H. T. Jansen. 2015. Validation of mercury tip-switch and accelerometer activity sensors for identifying resting and active behavior in bears. Ursus 26:8–18.

Watanabe, S., M. Izawa, A. Kato, Y. Ropert-Coudert, and Y. Naito. 2005. A new technique for monitoring the detailed behaviour of terrestrial animals: a case study with the domestic cat. Applied Animal Behaviour Science 94:117–131.

Watanabe, Y. Y., and A. Takahashi. 2013. Linking animal-borne video to accelerometers reveals prey capture variability. Proceedings of the National Academy of Sciences 110:2199–2204.

Watts, P., and C. Cuyler. 1988. Metabolism of the black bear under simulated denning conditions. Acta Physiologica Scandinavica 134:149–152.

Watts, P. D., K. L. Ferguson, and B. A. Draper. 1991. Energetic output of subadult polar bears (*Ursus maritimus*): resting, disturbance and locomotion. Comparative Biochemistry and Physiology -- Part A: Physiology 98:191–193.

Watts, P. D., and C. Jonkel. 1988. Energetic cost of winter dormancy in grizzly bear. Journal of Wildlife Management 52:654–656.

Watts, P. D., N. A. Øritsland, and R. J. Hurst. 1987. Standard metabolic rate of polar bears under simulated denning conditions. Physiological Zoology 60:687–691.

Whiteman, J. P. 2014. Physiological ecology of polar bears (*Ursus maritimus*) in

Alaska during summer. Thesis, University of Wyoming, Laramie, USA.

Whiteman, J. P., H. J. Harlow, G. M. Durner, R. Anderson-Sprecher, S. E. Albeke, E. V. Regehr, S. C. Amstrup, and M. Ben-David. 2015. Summer declines in activity and body temperature offer polar bears limited energy savings. Science 349:295–298.

Wickham, H. 2009. ggplot2: elegant graphics for data analysis. Springer-Verlag, New York, New York, USA.

Wikelski, M., and S. J. Cooke. 2006. Conservation physiology. Trends in Ecology and Evolution 21:38–46.

Williams, C. T., K. Wilsterman, V. Zhang, J. Moore, B. M. Barnes, and C. L. Buck. 2016. The secret life of ground squirrels: accelerometry reveals sex-dependent plasticity in above-ground activity. Royal Society Open Science 3:160404.

Williams, J. B., M. D. Anderson, and P. R. K. Richardson. 1997. Seasonal differences in field-metabolism, water requirements, and foraging behavior of free-living aardwolves. Ecology 78:2588–2602.

Williams, T. M. 1983. Locomotion in the North American mink, a semi-aquatic mammal. I. Swimming energetics and body drag. Journal of Experimental Biology 103:155–168.

Williams, T. M. 1989. Swimming by sea otters: adaptations for low energetic cost locomotion. Journal of Comparative Physiology A 164:815–824.

Williams, T. M. 1999. The evolution of cost efficient swimming in marine mammals: limits to energetic optimization. Philosophical Transactions of the Royal Society of London. Series B: Biological Sciences 354:193–201.

Williams, T. M., M. Ben-David, S. Noren, M. Rutishauser, K. McDonald, and W. Heyward. 2002. Running energetics of the North American river otter: do short legs necessarily reduce efficiency on land? Comparative Biochemistry and Physiology - A Molecular and Integrative Physiology 133:203–212.

Williams, T. M., W. A. Friedl, M. L. Fong, R. M. Yamada, P. Sedivy, and J. E. Haun. 1992. Travel at low energetic cost by swimming and wave-riding bottlenose dolphins. Nature 355:821–823.

Williams, T. M., J. Haun, R. W. Davis, L. A. Fuiman, and S. Kohin. 2001. A killer appetite: metabolic consequences of carnivory in marine mammals. Comparative Biochemistry and Physiology - A Molecular and Integrative Physiology 129:785–796.

Williams, T. M., T. L. Kendall, B. P. Richter, C. R. Ribeiro-french, J. S. John, K. L. Odell, B. A. Losch, D. A. Feuerbach, and M. A. Stamper. 2017. Swimming and diving energetics in dolphins: a stroke-by-stroke analysis for predicting the cost of flight responses in wild odontocetes. Journal of Experimental Biology 220:1135–1145.

Williams, T. M., L. Wolfe, T. Davis, T. Kendall, B. Richter, Y. Wang, C. Bryce, G. H. Elkaim, and C. C. Wilmers. 2014. Instantaneous energetics of cougar kills reveals advantage of felid sneak attacks. Science 346:81–85.

Wilmers, C. C., L. A. Isbell, J. P. Suraci, and T. M. Williams. 2017. Energetics-informed behavioral states reveal the drive to kill in African leopards. Ecosphere

8:e01850.

Wilmers, C. C., B. Nickel, C. M. Bryce, J. A. Smith, R. E. Wheat, and V. Yovovich. 2015. The golden age of bio-logging: how animal-borne sensors are advancing the frontiers of ecology. Ecology 96:1741–1753.

Wilson, R. P. 2011. Animal behaviour: the price tag. Nature 469:164–165.

Wilson, R. P., I. W. Griffiths, P. A. Legg, M. I. Friswell, O. R. Bidder, L. G. Halsey, S. A. Lambertucci, and E. L. C. Shepard. 2013. Turn costs change the value of animal search paths. Ecology Letters 16:1145–1150.

Wilson, R. P., F. Quintana, and V. J. Hobson. 2012. Construction of energy landscapes can clarify the movement and distribution of foraging animals. Proceeding of the Royal Society B 279:975–80.

Wilson, R. P., E. L. C. Shepard, and N. Liebsch. 2008. Prying into the intimate details of animal lives: use of a daily diary on animals. Endangered Species Research 4:123–137.

Wilson, R. P., C. R. White, F. Quintana, L. G. Halsey, N. Liebsch, G. R. Martin, and P. J. Butler. 2006. Moving towards acceleration for estimates of activity-specific metabolic rate in free-living animals: the case of the cormorant. Journal of Animal Ecology 75:1081–1090.

Wilson, R. R., J. S. Horne, K. D. Rode, E. V. Regehr, and G. M. Durner. 2014. Identifying polar bear resource selection patterns to inform offshore development in a dynamic and changing Arctic. Ecosphere 5:1–24.

Withers, P. C. 1977. Measurement of VO_2, VCO_2, and evaporative water loss with a flow-through mask. Journal of Applied Physiology 42:120–123.

Yoda, K., Y. Naito, K. Sato, A. Takahashi, J. Nishikawa, Y. Ropert-Coudert, M. Kurita, and Y. Le Maho. 2001. A new technique for monitoring the behaviour of free-ranging Adélie penguins. Journal of Experimental Biology 204:685–690.

Yoda, K., K. Sato, Y. Niizuma, M. Kurita, C.-A. Bost, Y. Le Maho, and Y. Naito. 1999. Precise monitoring of porpoising behaviour of Adélie penguins determined using acceleration data loggers. Journal of Experimental Biology 202:3121–3126.